Anna Makarewicz
Piotr Kowalczuk
Institute of Oceanology Polish Academy of Science
ul. Powstańców Warszawy 55
PL-81-712, Sopot, Poland

April 15, 2018

Prof. Dr. Oliver Zielinski,
Associate Editor Ocean Science
Head of Marine Sensor Systems
Vice Director Institute for Chemistry and Biology of the Marine Environment (ICBM)
University of Oldenburg, Germany
Cc/

Natascha Töpfer
Copernicus Publications
Editorial Support
Att. The response to review of manuscript by Makarewicz et al., 2017 submitted to Ocean Science and coded OS-2017-100 done by Reviewer#1, document reference OS-2017-100RC1

Dear Prof. Zielinski,

We thank the reviewers for their constructive comments. We have followed their guidance, and rewritten parts of the manuscript to place the work in better context. We have also gone through the text thoroughly to make any edits to the text to improve the flow and any grammatical errors we found that could be corrected. With this exercise we have also responded to all questions raised by Reviewer#1 and introduced necessary correction in revised manuscript.

The detailed comments to the Reviews are given below. After each of Reviewers single comments, our responses start with **Response:** (in bold)

Detailed Response to review by Reviewer #1:

General comments

The review submitted by Reviewer#1 concentrated mostly on methodological issues that we will explain in a point-by-point response below. The Reviewer#1 raised a concern about the main conclusion of our work that phytoplankton was the main source of the protein-like fraction of fluorescent dissolved organic matter, FDOM. We have come to this conclusion based on the simultaneous in situ measurements of protein-like FDOM fluorescence and chlorophyll *a* fluorescence performed with two different fluorometers integrated in one measurements system. The correlation coefficient R between those two variables was 0.804,

and the linear relationship between them explained 65% of variance (R^2 = 0.65). The regression analysis has been conducted on an extensive data set n = 24990 and results were very significant statistically ($p<0.0001$). The question put forward by Reviewer#1, that there was a very low determination coefficient values in the regression between protein-like FDOM fluorescence and chlorophyll *a* concentration concerned only analysis performed in case when chlorophyll *a* concentration was measured in discrete water samples. We admit that the relationship was weaker in this case, however it was statistically significant. This difference has been explained on Page 21 (lines 473 – 488) and can be attributed to time and space lag between instrumental measurements and water sample collection, reaching in some cases 1.5 hour and up to 3 nautical miles, respectively. This is caused by the "one instrument in water at a time" safety rule applied in almost all research vessels.

In addition, in both 2014 and 2015 we provided quantitative evidence of tight relationship between optical proxy for phytoplankton chlorophyll a concentration: the total absorption coefficient less due to water at 676 (atot-w(676)) and protein-like FDOM fluorescence (ICH3). The determination coefficient ranged between 0.423 and 0.860 depending on sampled water masses in a given year, see Figure S4 in supplement. We have also shown that there was a very tight coupling between total absorption coefficient less due to water at 676 nm, $a_{tot-w}(676)$ and chlorophyll *a* fluorescence intensity measured in different water masses in 2014 and 2015, Figure S3 in supplement. The determination coefficient between those variables ranged between 0.394 and 0.915 depending on sampled water masses in a given year. In addition to the quantitative analysis we have shown that there was a significant coupling in vertical distribution of protein-like FDOM fluorescence, ICH3 and $a_{tot-w}(676)$ and chlorophyll *a* fluorescence, see Figure 4, E, F, G, page 20.

Findings presented above have been thoroughly discussed in section 4.4 (Pages 31-34) where we have reviewed recent studies providing evidence based on in situ and mesocosm studies that protein-like FDOM fraction has been controlled by phytoplankton dynamics. Recent studies by Chen et al., (2017) (Science of The Total Environment, v:599–600, pp: 355-363) and Reteletti-Brogi et al, 2018 (Science of The Total Environment, 627, 802-811) presented new data linking high abundance of protein-like fluorescence with autochthonous production by phytoplankton and ice algae in the water of Amerasian Basin of Arctic Ocean, sea ice and under ice water in Canadian Archipelago. However, this evidence has been based on limited samples size collected in single surveys. Our data set is unprecedented in volume acquired in repeated surveys in the same area over several consecutive years, and acquired with a custom-made fluorescence sensor (excitation/emission pairs to detect different CDOM pools) simultaneously (the in situ 3 channel WetStar FDOM fluorometer by WetLabs). Therefore we are confident that our conclusion are based on sound arguments.

At the end of his/her review Reviewer#1 has asked questions (Question 13), why the CDOM absorption is not well correlated with DOC concentrations? Well, the weak but statistically significant relationship between $a_{CDOM}(350)$ and DOC concentrations in the North Atlantic is not necessarily unexpected in waters of Atlantic origin. In principle, the $a_{CDOM}(\lambda)$ and DOC is not correlated on oceanic basin scales (Siegel et al., 2002, Nelson and Siegel 2013). The empirical relationships between the $a_{CDOM}(\lambda)$ and DOC reported in literature (e.g.

Massicotte at al., 2017 and references therein) were driven by concentration gradient in DOC and $a_{CDOM}(\lambda)$ found between terrestrial, freshwater, marine and coastal ocean environments. Most of estimated empirical relationships between DOC and $a_{CDOM}(\lambda)$ were derived for coastal regions where there was a local point source of terrestrial DOC (river outlet). Such relationships published for Arctic were usually established for coastal regions in the vicinity of North American and Siberian Rivers (Amon et al., 2012; Matsuoka et al., 2012; 2013; Gonçalves–Araujo et al., 2015; Pavlov et al., 2016; Mann et al., 2016). The environment-specific determination coefficient in relationships between the $a_{CDOM}(\lambda)$ and DOC estimated by Massicotte at al., (2017) was lowest for pelagic ocean and reached 0.44. Our results are in line with statements from Siegel et al., 2002 and Nelson and Siegel, 2013 that the $a_{CDOM}(\lambda)$ and DOC is not correlated in pelagic ocean, as our study region in the Atlantic water inflow regions has very limited input from land runoff and the salinity range we have covered is very limited and high (with occasional freshening due to sea-ice melt rather than terrestrial runoff).

We have tried the Fichot and Benner (2011, 2012) approach to link spectral slope $S_{275\text{-}295}$ with carbon specific $a^*_{CDOM}(\lambda)$, but results were unsatisfactory. Rather we have presented similar non-linear relationship between the $S_{300\text{-}600}$ with carbon specific $a^*_{CDOM}(\lambda)$, which worked fairly well, and was consistent with non-linear relationship between those parameters presented by Norman et al., (2011) in Antarctica. Again, the Fichot and Benner approach to link spectral slope $S_{275\text{-}295}$ with carbon specific $a^*_{CDOM}(\lambda)$ was derived for Gulf of Mexico, where there were contrasting concentrations and compositional CDOM properties exists between the coast near the Mississippi River mouth and central oligotrophic part of Gulf of Mexico (Carder et al., 1999). In our opinion we have presented a thorough discussion comparing our results with existing literature, (Section 4.3).

We have tried to explain most critical points raised by Reviewer#1 in this section. Detailed responses to all individual questions are given below.

Detailed responses:

Abstract 1) page 2 line 45 why you concluded that phytoplankton is the main source of protein-like fluorescence based on a r2=0.36?

Response: This question has been addressed in General Comments section of our response letter, see above. We have deleted part of this sentence from the abstract: "~~and between the protein like fluorescence intensity and chlorophyll *a* concentration in discrete water samples (R_2=0.36, p<0.0001, n=299),~~"

2) page 3, line 51. how did you arrive to this conclusion? of the Arctic Ocean (Arrigo et al., 2008), which could potentially contribute to increased production of autochthonous (marine) dissolved organic matter (DOM). what about the ice algae? they will disappear and they also contribute to CDOM.

Response: We assume that Reviewer refers to line 61 in the Introduction. In fact, this remark does not refer to our results, and the Reviewer#1 likely wanted this sentence to be clarified. Similar remarks have been noted by Reviewer #1 in question 3, therefore we have decided to rewrite this paragraph in the Introduction. We agree with Reviewer #1 that ice algae can be considered as a potential source of autochthonous CDOM/DOM, (e.g. Granskog et al., 2015; Reteletti-Brogi et al, 2018) and this has been addressed in General Comments as well (see above). Above we have given points supporting our conclusion that phytoplankton is a dominant source of CDOM in the Nordic Seas influenced by Atlantic Waters - we have used the term "study area" to specify this (line 51). We would like to underline that we have been conducting field surveys in the ice-free waters, see section 2.1., as our research vessel is not classified as icebreaker. We neither did present any data nor written any conclusions about the sea ice.

We have changed the corresponding paragraph as follow:

The rapid reduction of summer sea ice in the Arctic Ocean in the past decades has various repercussions on the structure and functioning of the Arctic marine system: forcing changes in physics, biogeochemistry and ecology of this complex oceanic system (Meier et al., 2014). One of the most significant consequence of observed rapid Arctic Ocean transition is an increase in the primary productivity of the Arctic Ocean (Arrigo et al., 2008), which could potentially contribute to increased production of autochthonous (marine) dissolved organic matter (DOM) in ice free and under ice waters. The sea ice is also a source of autochthonous CDOM/DOM, (e.g. Granskog et al., 2015; Anderson and Amon, 2015 Reteletti-Brogi et al, 2018). However DOC produced by sympagic algae has limited effect on overall organic carbon mass balance in the Arctic Ocean, as melting of one meter of sea ice would negligibly change DOC concentration in top 50 m of water column, assuming an averaged DOC content in the ice of 100 μMol C, (Anderson and Amon, 2015). Simultaneously, response of terrestrial ecosystems to temperature increase will accelerate permafrost thaw and increase the riverine discharge, resulting in more allochthonous (terrestrial) DOM being released into the Arctic Ocean (Amon, 2004; Stedmon et al., 2011; Anderson and Amon, 2015; Prowse et al., 2015, and references therein). Terrestrial DOM presents a considerable role in the carbon budget of the Arctic Ocean (Findlay et al., 2015; Stein and Macdonald, 2004), especially in coastal waters and continental shelf with large inflow of terrestrial DOM, which constitutes 80% of total organic carbon delivered by Arctic rivers (Stedmon et al., 2011).

Following references have been added to text:

Amon, R.M.W. 2004. The Role of Dissolved Organic Matter for the Organic Carbon Cycle. the Arctic Ocean, [in:] The organic carbon cycle in the Arctic Ocean, Stein, R., and Macdonald, R. W. (Eds.) Springer, Berlin, Heidelberg Chapter 4, 82-99.

Anderson and Amon, 2015. DOM in the Arctic Ocean. [in:] Biogeochemistry of Marine Dissolved Organic Matter, D. A. Hansell, D. A., and Carlson, C. A. (eds), 609–633.

Granskog, M. A., Nomura, D., Müller, S., Krell, A., Toyota, T., & Hattori, H. (2015). Evidence for significant protein-like dissolved organic matter accumulation in Sea of Okhotsk sea ice. *Annals of Glaciology*, *56*(69), 1–8. https://doi.org/10.3189/2015AoG69A002

Retelletti-Brogi, S., S-Y. Ha, K. Kim, M. Derrien, Y.K. Lee, and J. Hur, 2018. Optical and molecular characterization of dissolved organic matter (DOM) in the Arctic ice core and the

underlying seawater (Cambridge Bay, Canada): Implication for increased autochthonous DOM during ice melting. Science of the Total Environment 627, 802–811

3) page 3 line 65, which percentage to carbon budget? DOM presents a considerable role in the carbon budget of...

Response: We agree with Reviewer#1 that this sentence wasn't clear. However, it is beyond the scope of this paper to place exact numbers on budget terms that have large margins of error even in the most up-to-date estimate of the carbon budget of the Arctic Ocean. We have changed it as follow:
Terrestrial DOM presents a considerable role in the carbon budget of the Arctic Ocean (Findlay et al., 2015; Stein and Macdonald, 2004), especially in coastal waters and continental shelf with large inflow of terrestrial DOM, which constitutes 80% of total organic carbon delivered by Arctic rivers (Stedmon et al., 2011).

4) line 71. please add Pegau reference to this list Hill, 2008; Granskog et al., 2007,

Response: Agree. The reference to:
Pegau,W. S. (2002), Inherent optical properties of the central Arctic surface waters, J.Geophys. Res., 107(C10), 8035, doi:10.1029/2000JC000382.
has been added to the revised manuscript text and reference list.

5) line 73 sorry this is not conclusive. UV can also produce radicals after interacting with CDOM resulting in more toxic and damaging effects! and preserves marine ecosystem from harmful ultraviolet radiation

Response: We agree with Reviewer suggestion. The sentence has been rewritten as follows:

Particularly in absence of sea ice, light absorbed by CDOM in visible part of the spectrum limits the light available for photosynthetic organisms (Arrigo and Brown, 1996), but also shields marine ecosystem from potentially harmful ultraviolet radiation strongly absorbing electromagnetic radiation in UVB and UVA (Erickson III et al., 2015). CDOM is also important substrate in photochemical reactions contributing to direct remineralization of organic carbon, production of bioavailable low molecular weight DOM but also formation of reactive oxygen species that could potentially be toxic to marine organisms (Mopper and Kieber, 2002, Kieber et al., 2003, Zepp, 2003).

Following references have been added to references list:

Arrigo K. and C. Brown, 1996. Impact of chromophoric dissolved organic matter on UV inhibition of primary productivity in the sea. Marine Ecology Progress Series, 140, 207-2016

Kieber, D.J., Peake, B.M., Scully, N.M., 2003. Reactive oxygen species in aquatic ecosystems. In: Helbling, E.W., Zagarese, H. (Eds.), UV Effects in Aquatic Organisms. Royal Society of Chemistry, Cambridge, pp. 251– 288.

Mopper, K., Kieber, D.J., 2002. Photochemistry and the cycling of carbon, sulfur, nitrogen and phosphorus. In: Hansell, D.A., Carlson, C.A. (Eds.), Biogeochemistry of Marine Dissolved Organic Matter. Academic Press, New York, pp. 455– 507.

Zepp, R.G., 2003. Solar ultraviolet radiation and aquatic biogeochemical cycles. In: Helbling, E.W., Zagarese, H. (Eds.), UV Effects in Aquatic Organisms and Ecosystems, vol. 1. The Royal Society of Chemistry, Cambridge UK, pp. 137– 184.

6)line 78, what fraction of DOM is CDOM? what fraction of CDOM is FCDOM?

Response: This is a good question, to which there is no consensus answer within the community working with DOM, and providing detailed answer to this question is beyond the scope of this paper. Stedmon and Nelson (2015) in their most recent book chapter presented only a qualitative schematic drawing of dissolved organic matter with subdivision for its chromophoric and fluorescent part with indication of elemental carbon, nitrogen, phosphorus, hydrogen and sulphur contribution. Unfortunately, no quantitative information is given (neither likely available). Similarly, the FDOM fraction has not been quantified as percent of CDOM or DOM (Stedmon and Nelson, 2015). Nelson and Siegel (2013) have defined CDOM as:

"Chromophoric dissolved organic matter (CDOM; also often referred to as gelbstoff or gilvin) is the fraction of DOM that interacts with solar radiation. CDOM compounds absorb light, and a fraction of them are also fluorescent. For the purposes of this review, we operationally define CDOM as material that passes through a submicron filter (usually 0.2–0.4 μm) and appreciably absorbs light in the solar radiation bands as found at the Earth's surface (e.g., UVB, UVA, and visible light; 280–700 nm). This definition practically excludes much of the DOM pool, which spectroscopically absorbs shortwave UV radiation but does not interact with light in the natural environment (Fichot & Benner 2011). We further operationally define the quantity of CDOM by its Naperian absorption coefficient at a reference wavelength. Quantification of CDOM in terms of mass or carbon content is not currently possible, so obviously optical characterization of any nature is relative to the exact composition of CDOM, which likely varies in both time and space."

Our definition, given in the Introduction comprise in a shorter form of definition given by Nelson and Siegel (2013). The research community has also consistently used optical properties to characterize CDOM in oceanic environments, following concepts developed by Jerlov (1968) over 50 years ago.

7) page 4 line 100, upstream you meant? changes associated with CDOM in the areas downstream of the Atlantic Water inflow region

Response: We agree with Reviewer#1. North Atlantic south of Nordic Seas, are upstream in the North Atlantic Current. Changed accordingly.

8) page 8 line 209, S between 300 and 600 nm line 218 why additional acdom375 and acdom443 when actually the range is 300 and 600 nm? line 224 why to use micron^{-1} use nm^{-1}

Response: We have calculated spectral slope coefficient in the spectral range 300 – 600 nm. We have included additional CDOM absorption coefficient values at 375 and 443 nm, $a_{CDOM}(375)$ and $a_{CDOM}(443)$, to enable direct comparison of results with presented in other relevant studies e.g. Stedmon and Markager, 2001, Matsuoka et al., 2011 2012, 2013, 2017; Granskog et al., 2012; Hancke et al., 2014; Gonçalves–Araujo et al., 2015; Pavlov et al., 2015. The values of the slope coefficient have been scaled by multiplying by 1000, and given

in units μm-1 for better visualization in tables and figures, which is consistent with Stedmon and Markager, 2001, 2003, Kowalczuk et al., 2006, Stedmon and Nelson, 2015 among others.

9) page 9 equation 3, why the use of spectrophometry for chl? this is an old technique that has a larger error and is less sensitive than fluorometry or HPLC. What is the error of this emthod? Did you compare this method with HPLC or fluorometry nonacidification technique?

Response: We agree with Reviewer#1 that the HPLC method is most accurate way for estimation of chlorophyll *a* concentration, however due to its high cost and time-consuming analysis, we have chosen the spectrophotometric method, because it is simple, fast, low-cost, and not dependent on external standards. The spectrophotometric method was the most convenient way for processing large number of collected samples. We worked in mesotrophic and eutrophic waters, where the chlorophyll *a* concentration varied between 0.1 to 15 mg m^{-3}. The spectrophotometric method for determination of chlorophyll *a* concentration originally developed by Lorentzen (1967) has been recommended for use in mesotrophic and eutrophic waters by "Guidelines for the Baltic monitoring program". Baltic Sea Environment Proceedings, 27D, Helsinki Commission, Publication BSEP27D, Helsinki, 1988. We agree that fluorometric method of chlorophyll *a* concentration is more sensitive, however it is also heavily dependent on the fluorescence quantum yield, that is different for various phytoplankton groups and the fluorometer must be routinely calibrated against the external standards. Recently, there has been observed a rapid and dramatic change in phytoplankton phenology in Nordic Seas, where dominant diatoms have been replaced by coccolithophores advancing northward with warm Atlantic Water (Oziel et al., 2017). So, in our opinion the fluorometric method of chlorophyll *a* concentration measurements could be biased by variable quantum yields. The spectrophotometric method based on extracted pigments absorption measurements is also much closer to measured optical Chl a proxies e.g. $a_{tot-w}(676)$.

The comparison between spectrophotometric method and HPLC method of chlorophyll *a* concentration measurements used in our lab has been previously presented by Darecki and Stramski, 2004, who found very good agreement between those two methods.

10) page 9 equation 4, I disagree. You cannot mix apples with bananas. DOC is not DOM unless you estimate DOM based on DOC with a curve or factor., same for equation 5

Response: We disagree. Specific DOC absorption (a* or SUVA) is a standard way adopted to examine CDOM properties in many studies measuring CDOM and DOC, and can provide insights about the quality of CDOM relative to DOC (Weishaar et al., 2003; Stedmon and Nelson , 2015; Massicotte et al., 2017). Principle goal of our study was to characterize the CDOM and FDOM optical properties and to identify their primary sources. As we mentioned in the answer to question 6, contributions of CDOM and FDOM to DOM (or DOC are generally unknown. Both CDOM and FDOM are characterized in aquatic environment through optical properties, Siegel and Nelson (2013). Optical properties normalized to DOC concentration are so called specific (in our case specific to carbon) optical properties and express the absorption crossection of the unit of mass of the substance. This specific optical crossection could be used as a measure of converting optical biogeochemical proxy into a concentration of substance (in this case carbon). Some of the specific optical properties have also biogeochemical meaning because they are related to diagenetic state of the substance, its chemical composition and molecular weight. Therefore, these variables were included in our manuscript. Stedmon and Nelson (2015) as well as Massicotte et al. (2017) advocated for

a use of those variables and ancillary parameters useful to characterize CDOM/FDOM and helpful in source identification. Therefore, we included those variables in our manuscript as they are relevant for the CDOM community, and would like to keep them.

11) line 305, how did you calculate the offset of wetstar-3 fluorescence measurements? reference with respect to nanopure? constant temperature?

Response: We have estimated a time drift of the fluorometer response, which was calculated by difference in raw counts values measured within similar pressure, salinity and temperature ranges (at ca. 200 m depth, temperature, 6.5 deg C. salinity >34.9) in the core of Atlantic Water, which we assume has not changed between years. The average difference in measured raw counts values in each channel in 2015 relative to 2014 was attributed to a drift of the optical detector, causing a deterioration of sensitivity and increase of raw counts. We calculated the average difference, and this was subtracted from all recorded raw counts in each channel measured during 2015 survey.

12) S slope without units?

Response: We could not identify the manuscript line where spectral slope unit was missing.

13) figure 3 is hard to interpret due to the vertical variability of properties

Response: We have foreseen this problem and Figure 3a presented a vertical distribution of sea water properties, giving a color scale of depth as third variable. An example of vertical distributions of ICH1 is shown in Figure 4.

14) many questions but fewer explanations or explanation attempts. beyond sampling aliasing, Why not acdom350 not well related to DOC? why not links between s275-295 and DOC? what is the linkage between particulate iron and absorption slopes?

Response: We have responded to this question in more detail in the General Response section (See above). In brief, we sampled a pelagic environment with narrow salinity range, and we believe that this in part explains why we cannot use CDOM as predictor of DOC. The area of study is not substantially influenced by riverine sources., therefore the we did expect that CDOM optical properties will predicts DOC in this environment with high accuracy.

At this point we can also address the last question concerning the iron. First of all, we have been analyzing properties of dissolved substances not particulate, therefore particulate iron did not affect our CDOM absorption measurements. At this point we could expresses how much useful was inclusion of SUVA254 variable in our analysis. Stedmon and Nelson (2015) in their book chapter has stated the variability of SUVA254 is between 0.5 – 5 m^2 $g^{-1}C$ in oceanic environment, and values over the 5 m^2 $g^{-1}C$ indicated the possible interference of dissolved iron on optical properties of CDOM. In this study SUVA254 was in the range of 0.56 – 2.54 m^2 $g^{-1}C$, with average value of ca. 1.7 m^2 $g^{-1}C$, which is a typical value for pelagic ocean (Massicotte et al., 2017). Based on this we can conclude that iron in dissolved and particulate phase had a negligible effect on CDOM/FDOM optical properties in our study area.

Anna Makarewicz
Piotr Kowalczuk
Institute of Oceanology Polish Academy of Science
ul. Powstańców Warszawy 55
PL-81-712, Sopot, Poland

April 15, 2018

Prof. Dr. Oliver Zielinski,
Associate Editor Ocean Science
Head of Marine Sensor Systems
Vice Director Institute for Chemistry and Biology of the Marine Environment (ICBM)
University of Oldenburg, Germany
Cc/

Natascha Töpfer
Copernicus Publications
Editorial Support
Att. The response to review of manuscript by Makarewicz et al., 2017 submitted to Ocean Science and coded OS-2017-100 done by Reviewer#2, document reference OS-2017-100RC2

Dear Prof. Zielinski,

We thank the reviewers for their constructive comments. We have followed their guidance, and rewritten parts of the manuscript to place the work in better context. We have also gone through the text thoroughly to make any edits to the text to improve the flow and any grammatical errors we found that could be corrected. With this exercise we have also responded to all questions raised by Reviewer#2 and introduced necessary corrections in the revised manuscript.

Response to general comments by Reviewer#2

The main critical point raised by Reviewer#2 was that we have failed to prove that observed interannual variability of CDOM optical properties was driven by large scale oceanic circulation. We have revised results section and we have added statistical analysis of variance requested by Reviewer#2 to highlight the statistical significance of observed interannual variability. We think that this information supports our statement. We know that definite proof could only be given if we knew the water masses history. Nordic Seas are a very complex and dynamic region and such analysis is very complex and beyond scope of this study. It should be underlined that numerous water masses that interface in Nordic Seas are in constant motion and their properties undergo continuous transformations due to thermodynamic phenomena in the polar zone (loss of heat content, freezing, and melting of ice cover) and dynamic phenomena driven by thermodynamics (loss of buoyancy and deep thermohaline convective mixing). Such complex physical processes and fluctuations of their intensity make interpretation of measurement of other physical parameters of oceanic waters

very difficult. Each of the identified water masses in the study area have had its history, which is beyond the scope of this study to analyze in detail. We were only capable to present a snapshot of current state of optical properties during the field campaigns. The main factor influencing the whole environment of Nordic Seas is an inflow of warm Atlantic waters. We have shown a co-incidence that the decrease of CDOM absorption occurred during intense inflow of Atlantic waters. We do admit that based on our data set we could not give a definitive proof of e.g. correlation with temperature or salinity anomalies, simply because the optical measurements time series were to scarce compared to number of hydrographic observations. Furthermore, temperature is not a conservative tracer of water masses.

Modification of DOM optical properties in a given water mass is superimposed on large scale circulation and dynamics. It is very important to underline that processes of in situ production, transformation and decomposition of DOM occur at different time scales and usually are delayed in phase (Nelson et al., 1998, Jorgensen et al, 2014). We have shown that a DOM fraction – protein-like substances - are produced by phytoplankton given the very strong correlation between fluorescence intensity of this fraction and chlorophyll *a* concentration. Simultaneously we did not observed any significant correlation between CDOM absorption at 350, $a_{CDOM}(350)$ with chlorophyll *a* concentration. This paradox can be explained by chemical properties of two different CDOM fractions, as FDOM is a sub-fraction of CDOM. The fluorescent amino acids have their excitation (absorption) band in UV-B between 260-275 nm, and belong to labile DOM. These compounds usually have a low number of aromatic rings built in their chemical structures. The absorption band of chromophoric dissolved organic compounds shift toward longer wavelengths and broadens its spectral width with increasing number of aromatic rings and increased number of conjugated bonds in delocalized molecular orbitals (Woźniak and Dera, 2007). Microbial transformation of DOM leads to creation of more condensed and more aromatic ("humic") DOM, that is characterized with absorption bands at longer wavelengths (in UV-C and visible part of the spectrum). The microbial transformation of labile and semi-labile DOM occurs on time scales ranging from three months (Nelson et al., 1998) to over a year (Jorgensen et al., 2014). During this time, in the Nordic Sea the given water mass where protein-like FDOM was produced have fair chance, to be transported further north to the Central Arctic Ocean basins, or be submerged into abyss during convective mixing events during winter. Therefore, likely due to temporal mismatch between in situ DOM production and its further transformation we could not observe correlation between, $a_{CDOM}(350)$ with chlorophyll *a* concentration. In our case $a_{CDOM}(350)$ represented past memory of DOM production and transformation process that occurred with variable intensity upstream in the North Atlantic Current, and the fluorescence intensity of protein-like DOM fraction represented a proxy of initial production processes. This interpretation does not contradict with the statement that phytoplankton growth is the main source of FDOM/CDOM in Nordic Seas.

The detailed comments to the Review#2 are given below. After each of Reviewer#2 single comments, our responses start with **Response:** (in bold)

Detailed response:

L. 83: what do the authors mean by efficient? Please, be more specific, otherwise the reader can read interpret it as the other methods are not efficient.

Response: We agree with Reviewer suggestion. The sentence has been rewritten as follows: "Use of in situ DOM fluorometers enables ~~efficient~~ low cost and high sample rate observations of distribution of FDOM and related biogeochemical proxies with greater temporal and spatial resolution (Belzile et al., 2006; Kowalczuk et al., 2010)"

L. 93-94: the contrasting optically properties of AW and PW are also with respect to the FDOM fraction (see Jørgensen et al 2014; Gonçalves-Araujo et al 2016). Additionally, such a contrast in CDOM properties is also highlighted in Stedmon et al 2015.

Response: We appreciate Reviewer suggestion and references have been added as follows:
"Optically these waters are contrasting especially with respect to CDOM (Granskog et al., 2012; Pavlov et al., 2015, Stedmon et al., 2015) and FDOM (Jørgensen et al., 2014; Gonçalves-Araujo et al., 2016)."

The reference to has been added to the revised manuscript text and reference list:
Jørgensen, L., Stedmon, C. A., Granskog, M. A. & Middelboe, M. Tracing the long-term microbial production of recalcitrant fluorescent dissolved organic matter in seawater. Geophys. Res. Lett. 41, 2481–2488, 2014.
Stedmon C. A., Granskog, M.A., and Dodd, P. A.: An approach to estimate the freshwater contribution from glacial melt and precipitation in East Greenland shelf waters using colored dissolved organic matter (CDOM). J. Geophys. Res.: Oceans, 120 (2), 1107-1117, doi.org/10.1002/2014JC010501, 2015b

L. 94-97: missing references

Response: We have added the following three references:

Skogen, M.D., Budgell, W.P. and Rey, F. Interannual variability in Nordic seas primary production. ICES Journal of Marine Science, 64(5), 889-898, 2007.

Olsen, E., Aanes, S., Mehl, S., Holst, J.C., Aglen, A. and Gjøsæter, H. Cod, haddock, saithe, herring, and capelin in the Barents Sea and adjacent waters: a review of the biological value of the area. ICES Journal of Marine Science, 67(1), pp.87-101, 2009.

Dalpadado, P., Arrigo, K.R., Hjøllo, S.S., Rey, F., Ingvaldsen, R.B., Sperfeld, E., van Dijken, G.L., Stige, L.C., Olsen, A. and Ottersen, G. Productivity in the Barents Sea-response to recent climate variability. PloS one, 9(5), p.e95273, 2014.

L. 100: would be interesting to shown how CDOM/FDOM measurements can be used as a proxy for tracing other parameters (e.g., freshwater, DOC, phytoplankton primary production, etc.).

Response: We agree with reviewer. This sentence has been revised as follows:.

"In context of ongoing and further anticipated intensification of Atlantic Ocean inflow to the Arctic Ocean, description of processes and factors controlling CDOM/FDOM properties and distribution could be used to better predict future changes associated with CDOM in the areas

downstream of the Atlantic Water inflow region inflow region, estimation of glacial melt water (Stedmon et. al.,2015) and tracing water masses (Gonçalves-Araujo et al., 2016).”

L. 102-118: There is a recent paper that may be useful for the authors: Gonçalves-Araujo et al 2018.

Response: According to the reviewer's suggestion, recent paper of Gonçalves-Araujo et al., 2018, has been included in the discussion section.

L. 110-113: please consider re-writing the sentence. It is missing a verb.

Response: Missing verb has been added to the sentence.
“Seasonal studies on CDOM contribution to overall variability of inherent optical properties (IOPs) were reported in sea ice (Kowalczuk et al., 2017) and in the water column during a spring under–ice phytoplankton bloom north of Svalbard (Pavlov et al., 2017).”

L. 139: consider adding the (Bjørnøya Current) BC to figure 1.

Response: Bjørnøya Current (BC) has been added to figure 1.

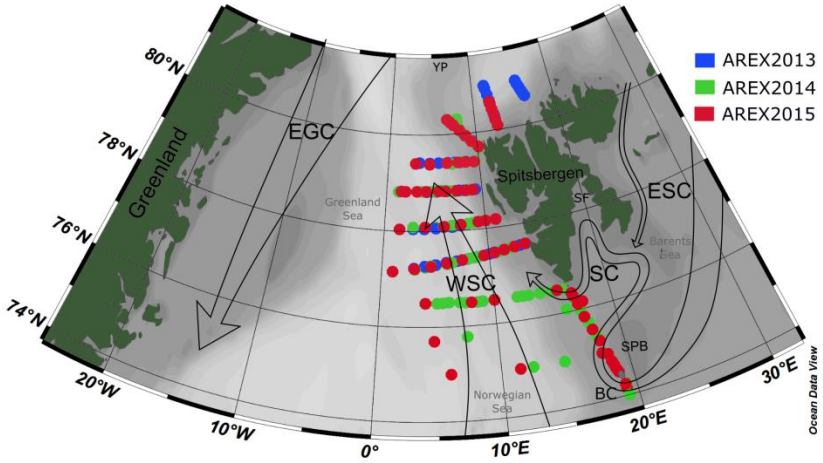

Figure 1: Map of the sampling stations during AREX2013 (blue circles), AREX2014 (green circles), AREX2015 (red circles) with general surface circulation patterns in the Nordic Seas. Atlantic Waters: WSC, West Spitsbergen Current. Polar waters: ESC, East Spitsbergen Current; SC, Sørkapp Current; EGC, East Greenland Current; BC, Bjørnøya Current; YP, Yermak Plateau; SF, Storfjorden; SPB, Spitsbergenbanken.

L. 171-172: the water sample collected below the Chl-a maximum. Authors can provide more information regarding it. Was it within the pycnocline? Or at the bottom of the deep Chla maximum layer? How was the sampling depth determined?

Response: The information concerning the range of depth of chlorophyll *a* samples has been described in detail in lines 169-173 and we feel this provides sufficient details:

“Samples were collected at three depths: near the surface, ca. 2 m depth, at chlorophyll *a* maximum, that was usually located between 15 and 25 m depth, and below chlorophyll *a*

maximum, between 50 and 70 m. The exact position of chlorophyll *a* maximum depth was estimated from vertical profile of chlorophyll *a* fluorescence during CTD downcast."

The sampling depth below the chlorophyll *a* maximum depth was determined visually based on the vertical profile of chlorophyll *a* fluorescence during CTD downcast. The vertical salinity profiles in core of AW water do not have detectable pycnocline within top 200 m, see Figure 4. The pycnocline associated with melt water overlying AW was observed in the frontal zone within marginal ice zone, Figure 4. The phytoplankton bloom associated with the marginal ice zone has its subsurface maximum within the pycnocline at 15-25 m, as shown on vertical profiles of chlorophyll *a* fluorescence, Figure 4. The subsurface chlorophyll *a* maximum in the marginal ice zone and core of AW waters was located in a similar depth range.

L. 178-189: have the authors performed any test to check whether the differences in storage affected their results?

Response: We did not perform any test to check how storage can influence the results. However, according to Stedmon and Markager, 2001 a few months of storage has little or no effect on CDOM absorption spectrum compared to the possibility of spectra disturbances onboard due to vibration, pitch and roll of the ship. Given the delays were similar between cruises the data are still comparable. We also prefer this over freezing samples, which modify the optical properties of DOM even more.

L. 250: was is the meaning of CRM?

Response: CRM is the abbreviation for consensus reference material. CRM is used as quality control of DOC measurements internationally. The explanation of the abbreviation has been added to the manuscript as follows:

"Consensus reference material (CRM) supplied by Hansell Laboratory from University of Miami was performed as quality control of DOC concentrations. The methodology provided sufficient accuracy(average recovery 95%; n = 5; CRM = 44 - 46 μM C; our results = 42 - 43 μM C) and precision represented by a relative standard deviation (RSD) of 2%."

L. 303: Sagan et al 2017. Authors should avoid citing unpublished work.

Response: We agree with Reviewer suggestion. Citation has been changed to: "(Sagan S., *personal communication, 2017*)".

L. 315-317: It is worth to mention that the referred water masses are found within the "upper layer", given that no water mass from deep layers was presented.

Response: The sentence has been rewritten as follows: "The epipelagic layer of the Nordic Seas is dominated by AW and PSW, and waters formed in the mixing process and local modifications (precipitation, sea–ice melt, riverine run–off, and surface heating or cooling) of these two water masses."

L. 324: the meaning of the PSWw (as well as its thermohaline characteristic intervals) was not presented. Additionally, and for consistency the PSWw is mostly referred in the literature as ASW (e.g. Pavlov et al 2015 and Gonçalves-Araujo et al 2016).

Response: We appreciate Reviewer suggestion and explanation of the PSWw abbreviation has been added to the revised manuscript as follows:
"Part of AW (except Polar Surface Water warm, PSWw) included waters with density below $\sigma\theta$=27.7 kgm-3 (marked on Figure 3 with dashed isopycnal line) used by Rudels et al (2005) as a threshold value between AW and PW."
Thermohaline characteristics for all water masses defined by Rudels et al. (2005) were presented in Table S1 in Supplement. Additionally detailed description and thermohaline characteristics of PSWw were presented in lines 330-334. Furthermore, a note about ASW has been added to the revised manuscript:
"Warmer PSWw has been considered here with the same $\sigma\theta \leq 27.7$ kg m-3 criterion and $\Theta > 0°C$ (Rudels et al., 2005), due to summer season measurements and higher temperatures of low salinity surface waters in the eastern Fram Strait. Furthermore PWSw was also limited to the uppermost 50 m of the water column with $S \leq 34.9$. The water mass with similar TS characteristics to PSWw but slightly different limits was referred in the literature as Arctic Surface Water, ASW (e.g. Pavlov et al 2015 and Gonçalves-Araujo et al 2016) but due to the dominance in the area of water originating from Atlantic Ocean the name PSWw from Rudels et al., (2005) classification is used."

L. 339: I suggest the authors to add some specific words to the title that would better reflect the results presented in this sub-section: spatial variability and hydrography.

Response: Thank you. According to Reviewer suggestion and the title of sub-section 3.1. has been changed as follows:
"*3.1. Interannual and spatial variability of CDOM absorption in Nordic Seas surface waters in relation to hydrography."*

L. 340-357: please consider including the standard deviation or standard error to the averaged values presented through the text.

Response: Done accordingly. The required information has been added in the revised manuscript.

L. 353: 200 m water layer. The indication for meter is missing.

Response: The unit has been added to the revised manuscript: "(…) and salinity time series in the top 200 m water layer (Walczowski et al., 2017)." Thank you.

L. 358: what do the authors mean by distinct? Please be more specific.

Response: We agree with Reviewer suggestion that the word "distinct" has been used in a non-clear context. The sentence has been rewritten as follows:

„In 2015, SC and ESC branches originating from the Barents Sea were pronounced, as indicated by lower temperature and salinity, Figure 2c, ~~were distinct~~ leading to elevated $a_{CDOM}(350)$ values on the West Spitsbergen Shelf and along the section from Sørkapp down to 74°N and near Bjørnøya Island."

L. 371-372: How do the authors explain the higher CDOM in PSWw compared to PSW? Shouldn't the DOM signal in PSWw be diluted by sea-ice melt waters and therefore, lower

than the DOM observed in the core of PSW as highlighted in Pavlov et al 2015, Stedmon et al 2015, Granskog et al 2012, Gonçalves-Araujo et al 2016, etc.?

Response: According to Rudels classification PSWw originates from AW water during its cooling during winter and mixing with PW in the Barents Sea and Nansen Basin and distinguished from PSW by higher temperature in the similar salinity range, see Figure 3. Pavlov et al., (2017) and Kowalczuk et al., (2017) and also Gonçalves-Araujo et al 2018, have provided data that PSWw north of Svalbard and in Nansen Basin do not differ very much from AW in terms of inherent optical properties. We agree that in general, CDOM absorption in PSWw should be lower compared to CDOM absorption in PSW, however in our study PSW was represented by very low samples number and those variations between PSW and PSWw were not statistically significant in 2013 (p=0.631005, T-Test).

L. 378-379: highest aCDOM(350) found within PSW and AAW in 2015...are those values for each water mass significantly similar? How do the authors explain such a high CDOM content associated to the AAW?

Response: In 2015, most of averaged values of $a_{CDOM}(350)$ between classified water masses show significant differences (Table r1). Only PSW and AAW are not significantly different ($p>0.05$) and shows high similarity between each other. This may be due to the low number of samples in a given class. Additionally, AAW in 2015 has a wide range of depths between 5-257 m with mean depth 76±76m.

Table r1: P-values obtained as a result of the T-test between classified water masses in 2015. Red numbers mean p>0.05.

Year	Water masses	t-value	df	p	significance
2015	AW vs. PSW	-4.44626	160	0.000016	S
	AW vs. PSWw	-4.06548	227	0.000066	S
	AW vs. AAW	-4.78185	163	0.000004	S
	AW vs. IW/DW	3.248989	173	0.001392	S
	PSW vs. PSWw	2.620125	77	0.010584	S
	PSW vs. AAW	0.295868	13	0.772004	NS
	PSW vs. IW/DW	4.306062	23	0.000263	S
	PSWw vs. AAW	-2.64463	80	0.009840	S
	PSWw vs. IW/DW	4.851875	90	0.000005	S
	AAW vs. IW/DW	5.090324	26	0.000026	S

L. 380-382: Could this represent a consistency in the DOM content (fingerprint) with respect to each water mass?

Response: The similarity of the variability ranges of the optical characteristics for 2013 and 2015 is not consistent within each water mass, except in PSW (p=0.806317) based on T-test. Variability range in 2013 is much wider towards higher values than in 2015. Each year represented a different optical and hydrographic situation. The year 2013 and 2015 are similar through higher CDOM values in comparison to 2014 and the visible effect of low salinity water from SC current on the West Spitsbergen Shelf. This sentence may confuse readers and therefore have been removed from the manuscript:

~~"There were similarities between 2013 and 2015 regarding variability ranges of CDOM optical characteristics in the water masses and distribution of low saline waters from ESC and SC."~~

L. 386-391: Since SUVA254 and a350* are both normalized by the same value (DOC concentration), what do the differences between the two parameters mean?

Response: Both spectral carbon specific absorption coefficients were normalized to the same DOC concentration values. They have the same physical meaning, and represent absorption cross section of a mass unit of element at different wavelengths. However those specific absorption coefficients have different meaning from biogeochemical point of view. The $SUVA_{254}$ is related to saturation of DOM mixture with aromatic rings (Weishaar et al 2003), and $a^*_{CDOM}(350)$ has been frequently used for remote sensing application for DOC determination with use satellite imagery (Fichot and Benner, 2011). This paragraph was not intended to reveal the differences between $a^*_{CDOM}(350)$ and $SUVA_{254}$ but to report the existing state of various optical parameters in the Nordic Seas and to indicate differences or similarities between years. Both of the parameters ($a^*_{CDOM}(350)$ and $SUVA_{254}$) were useful in discussion on CDOM origin in section 4.3 and 4.2, respectively.

L. 396-397: is that decrease significant?

Response: The interannual changes in DOC describe a significant decrease between 2013 and 2015 ($p<0.000001$, T-Test) and 2014 and 2015 ($p<0.000001$, T-Test). The difference in DOC concentration between 2013 and 2014 is not significant ($p=0.314$, T-Test). The sentence has been modified as follows:
"The average DOC concentration in the study area was highest in 2013 (80.69 μmol/L) and decreased significantly ($p<0.000001$) year by year (Table 3) to 67.64 μmol/L in 2015."

L. 396-399: what was the correlation between a350 and Chla? If autochthonous DOM is dominant in the sampling region, there should be a good correlation between the two parameters, right? (or at least for AW, with little continental/Arctic influence)

Response: There are studies that reported the correlation between $a_{CDOM}(\lambda)$ and chlorophyll *a* concentrations e.g. Meler et al., 2017; Dall'Olmo et al., 2017, but in the current study we did not observe correlation between $a_{CDOM}(350)$ and chlorophyll *a* concentration in the Nordic Sea during study period. In the General Response we have explained why such a statistical relationship has not been observed in the Nordic Seas. Simply the time scales of water transport mixing, convection and water properties transformations due to loss of heat content are shorter than time scales required for transformation of labile and semi-labile DOM into more condensed and aromatic refractory DOM by bacteria.

Fig 3b: It is clear that the Ich1 had the highest fluorescence intensity values in R.C., but, since the results of this MS are more focused on the Ich3 (autochthonous), I suggest the authors to present the Ich3 in this figure as well.

Response: Thank you. The figure for I_{CH3} has been transferred from the supplement to the manuscript together with description:

"In case of protein-like FDOM the highest values were observed in PSW, PSWw mid depth (15-50m,what can be associated with chlorophyll a maximum) and in part of AW, which was

separated from PSWw (upper part: T>0, σθ≤27.7, S>34.9). The lowest protein-like FDOM values were observed in AW (lower part: 27.7<σθ≤27.97) and in PSWw where σθ≤26.5 (Figure S2b)."

L. 469-470: "The relationship was more significant in 2014...". It looks like that the significance is the same for both years. Did the authors want to say that the relationship was stronger (given differences in r2)?

Response: We agree with Reviewer and the sentence has been rewritten as follows:
"The relationship was ~~more significant~~ stronger in 2014 (R^2 = 0.75, p<0.0001, n = 17700, blue line in Figure 5a, Table 4) when broader ~~stronger~~ influence of AW water was observed (Walczowski et al., 2017), than in 2015 (R^2 = 0.45, p<0.0001, n = 7290, red line in Figure 5a)."

Fig 5a: Looking at the legend it is not clear what the black line means. Is it the regression curve for the combined dataset from 2014 and 2015 or was it the difference between them? I also think that the information displayed in Table 4 can be easily incorporated to Fig 5.

Response: According to the Reviewer's advice the legend in Figure 5 has been modified. The Black line corresponds to a regression line for combined datasets from 2014 and 2015. The information displayed in Table 4 has been combined with the Figure 5.

L. 508: At what salinity did Grankog et al 2007 found acdom(355) greater than 15m-1? It would make it easier to establish comparison to the other studies.

Response: The required information about salinity has been added in the revised manuscript as follows:

"Exceptionally high CDOM absorption has been also observed in the southern part of Hudson Bay near river outlets with *a*CDOM(355)> 15 m^{-1}, at salinity close to 0 (Granskog et al., 2007)."

L. 502-518: There is a recent paper from Gonçalves-Araujo et al 2018 that shows aCDOM values for the central Arctic and surroundings that the authors may want to look at.

Response: We have used the information presented in the paper by Gonçalves-Araujo et al 2018 in the Discussion section. We have updated the discussion to include this as follows:

The highest CDOM absorption in the Arctic Ocean has been observed in coastal margins along Siberian Shelf in Laptev Seas, close to Lena River delta; $a_{CDOM}(440)$ = 2.97 m^{-1}, salinity close to 0, (Gonçalves–Araujo et al., 2015) and in Laptev Sea Shelf Water at the surface; a_{CDOM} (443)>1m^{-1}, salinity <28, (Gonçalves–Araujo et al., 2018) and at the coast of Chukchi Sea and Southern Beaufort Sea influenced by riverine inputs of Yukon and Mackenzie Rivers; aCDOM(440) > 1 m^{-1}, salinity <28, (Matsuoka et al., 2011, 2012; Bélanger et al., 2013). Exceptionally high CDOM absorption has been also observed in the coastal Hudson Bay near rivers outlets with $a_{CDOM}(355)$> 15 m^{-1}, salinity close to 0 (Granskog et al., 2007). Pavlov et al. (2016) reported $a_{CDOM}(350)$ of up to 10 m^{-1} at salinity of 21 in surface waters of the White Sea. Terrestrial CDOM from Siberian Shelf has been diluted and $a_{CDOM}(440)$ decreased to ca. 0.12 m^{-1}, at salinities 32.6 (Gonçalves–Araujo et al., 2015) and transported further toward the Fram Strait by the Transpolar Drift being gradually diluted or removed (Stedmon et al., 2011;

Granskog et al., 2012). In the Transpolar Drift and the central AO, CDOM absorption in surface waters was dominated by terrestrial sources with observed $a_{CDOM}(443)$ values varied between ~0.15 m^{-1}, at salinities close to +/-27 (Lund–Hansen et al., 2015) and ~0.5 m^{-1} at salinity range from 26.5 to 29.5 (Gonçalves-Araujo et al., 2018). Dilution also effectively decreased CDOM absorption in western Arctic Ocean, and average CDOM absorption in the Chukchi Sea and Beaufort Seas was $a_{CDOM}(440) = 0.046\ m^{-1}$, at salinities > 32.3 (Matsuoka et al., 2011, 2012; Bélanger et al., 2013).

Also we have added the sentence at the end of mentioned paragraph:

"The influence of transformed Atlantic Water generated in the Barents and Norwegian Sea had impacted on $a_{CDOM}(443)$ values in the Beaufort Gyre and Amundsen and Nansen basins, causing its decrease below 0.2 m^{-1} as reported by Gonçalves–Araujo et al., (2018).

L. 521: do the values also agree with results published in Stedmon et al 2015?

Response: The $a_{CDOM}(350)$ values range (~0.1- 0.2 m^{-1}) from the western part of Fram Strait section reported by Stedmon et al. 2015 also agree with our results from AREX2014. The citation has been added to the revised manuscript.

"The reported lower range of $a_{CDOM}(350)$ observed in AW during AREX2014 (2014: 0.14±0.06 m^{-1}) is in good agreement with data from eastern part of Fram Strait at 79°N section reported by Granskog et al. (2012), Stedmon et al., (2015) and Pavlov et al. (2015) and with data reported by Hancke et al. (2014) south of the Polar Front in the Barents Sea."

L. 541: "...and similar features of CDOM properties were..." - What do you mean by similar features of CDOM properties?

Response: We have used wrong phrase for description of similar variability ranges of CDOM absorption coefficient and spectral slope coefficient. Pavlov at el. (2017) mentioned the lack of differences in optical properties (absorption coefficient values) for water with lower salinity and lower temperature and Atlantic water. A similar relationship was observed in our study. This sentence has been rewritten as follows:

"Despite lower salinity and lower temperature, CDOM optical properties in PSW in this study did not differ significantly from AW in 2013 and 2015, and similar variability ranges of CDOM absorption coefficient and spectral slope coefficient were reported by Pavlov at el. (2017) north of Svalbard. "

L. 549: What do the authors mean by "Statistical distribution"?

Response: Indeed, "statistical distribution" is not an appropriate expression in this sentence. The authors mean the average values and ranges of values listed in the Table 2. The sentence has been rewritten as follows:

"Average values of *a*CDOM(350) in 2014 in PSW (Table 2) were similar with Arctic Waters north of the Polar Front in Barents Sea described by Hancke et al. (2014) and slightly higher than observed in this study in 2013 (0.32±0.16 m^{-1}) and 2015 (0.26±0.09 m^{-1})."

L. 553: How did the authors infer that the waters are from different origins based on their dataset?

Response: This discussion sentence was not based our data set but on data presented in the literature. The DOM composition in the western part of Fram Strait in EGC transporting the PW southward is compositionally different from AW in the eastern part of Fram Strait. According to results presented by Jorgensen et al., (2014) and Gonçalves-Araujo et al 2016, humic substances dominated the composition of DOM in EGC, and the fluorescence intensity of humic-like substances was 3 to 5 times higher in these waters than in the AW in eastern part of Fram Strait. As the values coefficient describing CDOM optical properties in waters north of Svalbard were similar to those in Nordic Sea, we could speculate that water masses classified by hydrographic properties as PW north of Svalbard could have different DOM composition. This is consistent with findings by Gonçalves-Araujo et al 2018 who found very low CDOM absorption in the Amundsen and Nansen basins.

To avoid speculations we had deleted this sentence.
" PW in the ESC in eastern part of Fram Strait was optically different from PW in EGC in western part of Fram Strait and thus likely of different origin"

L. 556: Gonçalves-Araujo et al 2016 has studied FDOM and not CDOM as mentioned in the text.

Response: Corrected accordingly, the reference has been deleted.
"According to Hancke et al. (2014) the CDOM pool in the Barents Sea was predominantly of marine origin, while several studies show terrestrial CDOM in the PW of EGC (Granskog et al., 2012, Pavlov et al., 2015; ~~Gonçalves-Araujo et al., 2016~~) and *a*CDOM(350) reported for PW in the EGC was significantly higher, by factor 2, than values reported in this study around Svalbard."

L. 565-566: Have the authors tried to look for the a350 vs. temperature correlations?

Response: We have been analyzing the correlations the $a_{CDOM}350$ vs. temperature. The results showed very week, negative correlation between $a_{CDOM}(350)$ vs. temperature, especially in 2014 and 2015 data sets however due to low values of determination coefficient we decided not to present these results.

L. 571-572: where did the authors take this information from?? Was it from the literature (then it is missing a citation) or from their dataset (then I would like to know how the data supports such an affirmation)?

Response: This speculative sentence has been deleted from the revised manuscript.

L. 573: "S300-600 varied little between water masses in a given season..." Have you tested it for significance?

Response: According to the Reviewer's suggestion, we have checked the significance between water masses in a given season with use of T test. The results are presented in the Table r2. The only statistically significant difference is IW / DW vs. other water masses in 2015.

Table r2: Results of T test of S300-600 grouped by year and water masses. Table list results of t-test that measure significance in differences in mean value. The difference between variable averages in selected layer are significant if significance level $p<0.05$. NS - not significant, S – signify cant differences.

Year	Variable	Layer	t-value	df	p	Significance
2013	S300-600	AW vs.PSW	0.524860	44	0.602315	NS
		AW vs.PSWw	1.118054	74	0.267160	NS
		PSW vs. PSWw	0.064696	34	0.948795	NS
2014	S300-600	AW vs.PSW	-0.405673	176	0.685476	NS
		AW vs.PSWw	0.874175	200	0.383071	NS
		AW vs.AAW	0.240337	176	0.810348	NS
		AW vs.IW/DW	1.881482	183	0.061494	NS/close
		PSW vs. PSWw	0.811732	30	0.423340	NS
		PSW vs.AAW	0.713604	6	0.502273	NS
		PSW vs.IW/DW	1.561149	13	0.142494	NS
		PSWw vs.AAW	-0.123383	30	0.902627	NS
		PSWw vs.IW/DW	1.316258	37	0.196184	NS
		AAW vs.IW/DW	1.058590	13	0.309061	NS
2015	S300-600	AW vs.PSW	0.455974	160	0.649027	NS
		AW vs.PSWw	1.928425	227	0.055050	NS/close
		AW vs.AAW	2.012286	163	0.045837	S
		AW vs.IW/DW	-2.89410	173	0.004292	S
		PSW vs. PSWw	0.193909	77	0.846757	NS
		PSW vs.AAW	0.752780	13	0.464996	NS
		PSW vs.IW/DW	-1.49834	23	0.147646	NS
		PSWw vs.AAW	0.900161	80	0.370736	NS
		PSWw vs.IW/DW	-3.14968	90	0.002219	S
		AAW vs.IW/DW	-2.86486	26	0.008150	S

L. 612: "...could indicate freshly produced CDOM." . At what depth was this found? Have you looked at the correlation between S300-600 and Chla? Is there any correlation for the high Chla samples?

Response: We have not observed any correlation between $S_{300\text{-}600}$ and chlorophyll *a* concentration even for high Chla samples. The lower values of $S_{300–600}$ (<18 μm^{-1}) with higher absorption (>0.15 m^{-1}) were found at an average depth 30.81±33.26 m (min- max:: 0 - 129 m)

L. 611-614: This is an important discussion of the main results and could be discussed more in deep

Response: We appreciate Reviewer#2 comments, however, we have been discussing CDOM origin and its potential source in the Discussion, subsection 4.2, where in several paragraphs we have provided arguments that lead us to conclusion that CDOM is predominantly of autochthonous origin in the Nordic Seas.

L. 617-620: Not clear whether the authors have checked that or it is only an assumption.

Response: We have checked the location of points outside the model. The points were scattered and did not have one precise location, most of them were in places that could indicate the contribution from land: for example, points located at the mouth of the fjords or under the influence of low saline PW. Especially in 2015, all points outside the model limits were placed in cold and low saline water.

L. 623-625: Not clear what the authors wanted to state in that sentence.

Response: It is a statement taken from the cited reference. It leads to a discussion about $SUVA_{254}$, with very low values potentially associated with very low aromaticity of DOM in Nordic Seas**.**

L. 654: Authors may want to look at the results from Walker et al 2013 for comparison.

Response: We have added citation to Walker et al., 2013. In context of the first paragraphs of subsection 4.3, we have thought about that paper by Fichot et al, 2013, Scientific Reports, 3 : 1053 | DOI: 10.1038/srep01053, which presents use of remote sensing methods for tracing terrigenous organic matter in the Arctic Ocean.

"The riverine input can be monitored by optical methods with absorption, fluorescence or remote sensing measurements (Spencer et al., 2012; Walker et al., 2013; Fichot et al., 2013; Mann et al., 2016)."

Reference to [papers by Fichot et al., 2013 and Walker et al., 2013 have been added to reference list.

Fichot, C. G., K. Kaiser, S. B. Hooker, R. M. W. Amon, M. Babi, S. Bélanger, S. A. Walker, and R. Benner. Pan-Arctic distributions of continental runoff in the Arctic Ocean. , Scientific Reports, 3: 1053, DOI: 10.1038/srep01053, 2013.

Walker, S. A., R. M. W. Amon, and C. A. Stedmon (2013), Variations in high-latitude riverine fluorescent dissolved organic matter: A comparison of large Arctic rivers, Journal of Geophysical Research Biogeoscience, 118, 1689–1702, doi:10.1002/2013JG002320

L. 682-683: Why do the authors think the a350* vs. S300-600 behaves like this? Was the correlation also strong (and significant) for each year analyzed separately? It does not look like that (specially for 2013) when looking at Fig. 8.

Response: The non-linear, hyperbolic type of relationship between spectral slope and spectral values of specific (and also bulk) absorption coefficient are commonly reported in many papers (e.g. Fichot and Benner 2011, 2012, Fichot et al, 2013, Norman et al., 2011). This effect is similar to effect of mixing of two water bodies with contrasting CDOM optical

properties, explained theoretically by Stedmon and Markager (2003). One should note that distribution of values of specific absorption coefficient across of variety of aquatic environments is similar to CDOM absorption coefficient distribution pattern. The highest a_{CDOM}*(□) values were associated in fresh water environments: swamps rivers, humic lakes, and the smallest were reported in oligotrophic subtropical oceanic gyres – the same global pattern applied to a_{CDOM}(□) (see Massicotte et al., 2017). Secondly, this kind of relationship is regulated by DOM chemical structures – more humic, more aromatic DOM is characterized by higher values of a_{CDOM}*(□), compared to autochthonous, marine DOM that has lower saturation with aromatic rings and has more aliphatic structures. The only difference between ours and by Fichot and Benner results, is the choice of spectral range used for spectral slope calculations. However, our results were consistent with the a_{CDOM}*(375) vs $S_{300\text{-}650}$ relationship presented by Norman et al., 2011. It seems that in an environment influenced by terrigenous DOM a hyperbolic relationship works better for spectral slope calculated over 275-295 nm spectral range, while in oceanic environments it is better to use a longer spectral range for slope calculations. We have used whole data set to derive our relationship. Of course, the use of smaller data sets for specific years will produce different results with lower values of determination coefficient.

L. 695-696: significant differences for humic-like and PTN-like FDOM...With respect to what were these differences?

Response: This was misfortunate phrase. We referred to global pattern of distribution of humic-like and protein-like fluorescence intensities values presented in cited references. The sentence has been rewritten for clarity as follows.

"The pattern distribution of fluorescence intensities of main FDOM components with depth in the global oceans' biogeochemical provinces is significantly different for humic–like and protein–like FDOM (Stedmon and Nelson, 2015, Catalá et al., 2016)."

L. 699-701: How do the authors explain such behavior?

Response: It is beyond the scope of this study to explain the global distribution pattern of main fluorophores in the ocean. This has been presented by e.g. Jorgensen et al., 2011, Kowalczuk et al., 2013, and Stedmon and Nelson, 2015, Catalá et al., 2016 and Yamashita et al., 2017. This behavior is the complex result of photobleaching, in situ production and microbial processing and vertical mixing. All those processes have different time scales and intensity in a given biogeochemical ocean province and produce specific type of vertical distribution of fluorescence intensity of given fluorophore types. Reviewer#2 may find detailed information in provided reference examples. We have cited them because we have also presented examples of distribution of ICH1 and ICH3 with depth, comparing our results to global patterns.

L. 702-705: not clear if the authors are presenting their own results or results from other studies.

Response: Citations indicated that we have been referring to published results from other studies. We have rewritten this sentence for clarity.

"The global pattern of fluorescence intensity of protein–like FDOM distribution across the oceanic biogeochemical provinces and with depths was opposite compared to humic–like

FDOM. Protein–like FDOM fluorescence intensity usually increased toward the open ocean and the highest intensity was observed in the surface waters, rapidly decreasing with depth, reaching constant low level below the epipelagic layer (Jørgensen et al., 2011; Kowalczuk et al., 2013; Catalá et al., 2016).”

L. 722-723: It is not completely clear based on the results presented here. The authors may want to rephrase that sentence. The authors state that the PTN-like FDOM is the dominant fraction at high salinity. However, studies have shown that the humic-like (visible fluorescence) can be the dominant signal at sal>34 in the Arctic Ocean.

Response: We partially agree with the Reviewer’s suggestion. The humic-like FDOM may be significant in some Arctic Ocean Basins, but not in the Nordic Seas, where influenced by warm Atlantic Water as we shown in our results. There is hardly any sources of terrigenous origin to be found in these Atlantic dominated waters. We have rewritten this sentence for clarity,
“
“The distribution of fluorescence intensity of main FDOM components in the Nordic Seas, dominated by warm water of Atlantic origin followed the general trends observed globally.”

L. 732-734: This sentence does not help the discussion and could be easily removed.

Response: According to the reviewer's suggestion, the sentence:
“The PW flowing through the Canadian Arctic Archipelago was enriched with humic–like component compared to Labrador Sea (Guéguen, et al., 2014).” has been deleted from the discussion section.

L. 742: The paper from Gonçalves-Araujo et al 2016 does not show CDOM results.

Response: Corrected accordingly.

“This was also in a good agreement with CDOM distribution in the Fram Strait (Granskog et al., 2012; Pavlov et al.; 2015~~, Gonçalves–Araujo et al., 2016~~) and FDOM humic–like fraction 743 (Ex/Em = 280/450 nm) distribution presented by (Granskog et al., 2015).”

L. 756: "...and same dominant factor controlling these parameters in time and space." How do your results support that statement?

Response: It is broad and well established consensus in ocean optics community that following optical parameters: chlorophyll *a* fluorescence intensity, I_{FChla} and total non–water absorption coefficient at 676 nm, *a*tot–w(676) are regarded as optical proxies for phytoplankton biomass. In the main body of this manuscript and supplementary materials we have shown that both: I_{FChla} and *a*tot–w(676) were strongly and significantly correlated with I_{CH3}. Therefore a tight coupling between those parameters and overlapping distribution with depth, justified our statement and is fully supported by our data set..

L. 762-763: Could the authors identify what FDOM fractions are produced through each of the mentioned processes (e.g. phytoplkt extracellular release, phytoplkt degradation or lysis)??

Response: Based on information provided in the literature we just name the processed known to lead to release of DOM by phytoplankton into adjacent waters, without specifying which process produce specific FDOM fraction. It would be a subject of further studies. For clarity we have deleted this sentence and we have removed citations from reference list.

~~"Our findings are in agreement with studies that proposed FDOM/CDOM production is tightly coupled with to phytoplankton extracellular release (Romera-Castillo et al., 2010) or by phytoplankton degradation or lysis (Hur et al., 2006; Organelli et al., 2014)."~~

Characteristics of Chromophoric and Fluorescent Dissolved Organic Matter in the Nordic Seas

Anna Makarewicz[1], Piotr Kowalczuk[1], Sławomir Sagan[1], Mats A. Granskog[2], Alexey K. Pavlov[2], Agnieszka Zdun[1], Karolina Borzycka[1], Monika Zabłocka[1]

[1]Institute of Oceanology, Polish Academy of Sciences, ul. Powstańców Warszawy 55, 81–712 Sopot, Poland

[2]Norwegian Polar Institute, Fram Centre, 9296 Tromsø, Norway

Correspondence to: Anna Makarewicz (araczkowska@iopan.gda.pl)
phone: +48 58 7311804,
fax: +48 58 5512130,

~~Manuscript draft~~Revised manuscript: ~~7~~ 4 ~~December~~May, 201~~7~~8

Abstract

Optical properties of Chromophoric (CDOM) and Fluorescent Dissolved Organic Matter (FDOM) were characterized in the Nordic Seas including the West Spitsbergen Shelf during June–July of 2013, 2014 and 2015. The CDOM absorption coefficient at 350 nm, $a_{CDOM}(350)$ showed significant interannual variation (T test, $p<0.00001$). In 2013, the highest average $a_{CDOM}(350)$ values ($a_{CDOM}(350) = 0.30\pm0.12$ m^{-1}) were observed due to the influence of cold and low–saline water from the Sørkapp Current in the southern part of West Spitsbergen Shelf. In 2014, $a_{CDOM}(350)$ values were significantly lower (T test, $p<0.00001$) than in 2013 (av. $a_{CDOM}(350) = 0.14\pm0.06$ m^{-1}), which was associated with the dominance of warm and saline Atlantic Water (AW) in the region, while in 2015 intermediate CDOM absorption (av. $a_{CDOM}(350) = 0.19\pm0.05$ m^{-1}) was observed. *In situ* measurements of three FDOM components revealed that fluorescence intensity of protein–like FDOM dominated in surface layer Nordic Seas. ~~, while the and concentrations~~ Concentrations of marine and terrestrial humic–like DOM were very low and ~~its~~ distribution of those components ~~waserewere~~ generally vertically homogenous in the upper ocean (0–100 m). Fluorescence of terrestrial and marine humic–like ~~F~~DOM decreased in surface waters (0–15 m) near the sea–ice edge by dilution of oceanic waters by sea–ice melt water. The vertical distribution of protein–like FDOM was characterized by a prominent sub–surface maximum that matched the subsurface chlorophyll *a* maximum and was observed ~~all~~ across the study area. The highest protein–like FDOM fluorescence was observed in the Norwegian Sea in the core of warm AW. There was a significant relationship between the protein–like fluorescence and chlorophyll *a* fluorescence ($R^2=0.65$, $p<0.0001$, $n=24490$)~~ and between the protein–like fluorescence intensity and chlorophyll *a* concentration in discrete water samples ($R^2=0.36$, $p<0.0001$, $n=299$)~~, which suggests that phytoplankton was the primary source of protein–like DOM in the Nordic Seas and West Spitsbergen Shelf waters. Observed variability ~~range~~ of selected spectral indices (spectral slope coefficient, $S_{300–600}$, carbon–~~–~~specific CDOM absorption coefficient at 254 and 350 nm, $SUVA_{254}$, a^*_{CDOM}~~*~~(350)) and non–linear relationship between CDOM absorption and spectral slope coefficient also indicate a dominant marine (autochthonous) source of CDOM and FDOM in the study area. Further, our data suggest that ~~while~~ $a_{CDOM}(350)$ cannot be used to predict dissolved organic carbon (DOC) concentrations in the study region, ~~and~~ however the slope coefficient ($S_{300–600}$) shows some promise to be used.

1. Introduction

The rapid reduction of summer sea ice in the Arctic Ocean in the past decades has various repercussions on the structure and functioning of the Arctic marine system: forcing changes in physics, biogeochemistry and ecology of this complex oceanic system (Meier et al., 2014). One of the most significant consequences of observed rapid Arctic Ocean transition is an increase in the primary productivity of the Arctic Ocean (Arrigo et al., 2008), which could potentially contribute to increased production of autochthonous (marine) dissolved organic matter (DOM). in ice free and under ice waters. The sea ice is also a source of autochthonous CDOM/DOM, (e.g. Granskog et al., 2015a; Anderson and Amon, 2015; Reteletti-Brogi et al, 2018). However, DOC produced by sympagiicec algae has limited effect on overall organic carbon mass balance in the Arctic Ocean, as melting of one meter of sea ice would negligibly change DOC concentration in top 50 m of water column, assuming an averaged DOC content in the ice of 100 µMol C, (Anderson and Amon, 2015). Simultaneously, response of terrestrial ecosystems to temperature increase will accelerate permafrost thaw and, increase the riverine discharge, potentially resulting in more allochthonous (terrestrial) DOM being released into the Arctic Ocean (Amon, 2004; Stedmon et al., 2011; Anderson and Amon, 2015; Prowse et al., 2015, and references therein). Both Tterrestrial and marine DOM presents a considerable role in the carbon budget of the Arctic Ocean (Findlay et al., 2015; Stein and Macdonald, 2004), especially in coastal waters and continental shelf with large inflow of terrestrial DOM, which constitutes 80% of total organic carbon delivered by Arctic rivers (Stedmon et al., 2011).

The optically active DOM fraction called chromophoric or colored dissolved organic matter (CDOM) represents the light absorbing molecules (Coble, 2007; Nelson and Siegel, 2013; Stedmon and Nelson, 2015). Once entered or produced in surface waters of the Arctic Ocean, CDOM has a significant influence on heating of the uppermost ocean layer and its stratification (Pegau, 2002; Hill, 2008; Granskog et al., 2007, 2015b). Particularly in absence of sea ice, light absorbed by CDOM in visible part of the spectrum limits the light available for photosynthetic organisms (Arrigo and Brown, 1996), but also shields has impact on available spectrum of light for photosynthetic organisms and preserves marine ecosystem from potentially harmful ultraviolet radiation strongly absorbing electromagnetic radiation in UVB and UVA bands (Erickson III et al., 2015). CDOM is also important substrate in photochemical reactions contributing to direct remineralization of organic carbon, production of bioavailable low molecular weight DOM but also formation of reactive oxygen species that

could potentially be toxic to marine organisms (Mopper and Kieber, 2002, Kieber et al., 2003, Zepp, 2003). The mineralization by photochemical reactions or microbes of DOM both terrestrial and marine is a crucial but still insufficiently quantified mechanism in the Arctic carbon cycle (e.g. Osburn et al., 2009). Despite the importance of CDOM, studies on its distribution, properties and transformation in the Arctic Ocean and its marginal seas are still limited, partly by their remoteness and seasonal accessibility.

A sub–fraction of CDOM fluoresces and is called fluorescent dissolved organic matter (FDOM). Recent advances in fluorescence spectroscopy (Coble, 1996) and data analyses techniques has provided a more comprehensive overview of FDOM characteristics. Based on excitation/emission spectra fluorescence spectroscopy it is possible to distinguish~~ed~~ amidst different origin groups of fluorophores e.g. terrestrial, marine and anthropogenic (Stedmon et al., 2003, Murphy et al., 2013; Murphy et al., 2014). Use of *in situ* DOM fluorometers enables ~~efficient~~ low cost and high sample rate observations of distribution of FDOM and related biogeochemical proxies with greater temporal and spatial resolution (Belzile et al., 2006; Kowalczuk et al., 2010).

North Atlantic sector of the Arctic Ocean is a region with complex interaction of inflowing warm and highly productive Atlantic Waters entering the Arctic and cold and fresh Polar Surface Waters exiting the Arctic Ocean. Recent studies have reported intensification of Atlantic Water (AW) inflow into Arctic Ocean (Walczowski 2014; Polyakov et al., 2017; Walczowski et al., 2017) further highlighting the importance of the European sector of the Arctic Ocean to better understand the complex interactions between inflowing AW and Polar Waters. Optically these waters are contrasting, especially with respect to CDOM (Granskog et al., 2012; Pavlov et al., 2015, Stedmon et al., 2015) and FDOM (Jørgensen et al., 2014; Gonçalves-Araujo et al., 2016). ~~Optically, and especially with respect to CDOM, these waters are contrasting (Granskog et al., 2012; Pavlov et al., 2015).~~ In absence of sea ice, favorable vertical mixing conditions and sufficient levels of solar radiation makes it a very productive and important region from an ecosystem and socio–economic standpoint, thus ensuring motivation for ongoing studies of the complex marine system in the area (Skogen et al., 2007; Olsen et al., 2009; Dalpadado et al., 2014). In context of ongoing and further anticipated intensification of Atlantic Ocean inflow to the Arctic Ocean, description of processes and factors controlling CDOM/FDOM properties and distribution could be used to better predict future changes associated with CDOM in the areas up~~down~~stream of the

Atlantic Water inflow region, to estimate~~ion~~ of glacial melt water (Stedmon et. al.,2015) and to trace~~ing~~ water masses (Gonçalves-Araujo et al., 2016).~~.~~

A number of occasional synoptic surveys of CDOM and optical properties have been conducted in the different regions of the European Arctic Ocean and concentrated on the western part of the Fram Strait influenced by Polar Water outflow with EGC (Granskog et al., 2012; Pavlov et al., 2015; Gonçalves–Araujo et al., 2016). The CDOM distribution in the area influenced by AW were reported by Stedmon and Markager (2001) in the central part of the Greenland Sea, and by Granskog et al. (2012) and Pavlov et al. (2015) who presented CDOM and particulate absorption distribution along transect across Fram Strait at 79°N. Hancke et al. (2014) studied seasonal distribution of CDOM absorption coefficient ($a_{CDOM}(\lambda)$) in an area across the Polar Front in the central part of the Barents Sea. Seasonal studies on CDOM contribution to overall variability of inherent optical properties (IOPs) were reported in sea ice (Kowalczuk et al., 2017) and in the water column during a spring under–ice phytoplankton bloom north of Svalbard (Pavlov et al., 2017). In this study we aimed to present variability of CDOM and FDOM optical properties in a large area spanning parts of the Barents, Norwegian and Greenland Seas (particularly focusing on West Spitsbergen Shelf) over a period of three consecutive years (2013–2015) and understand the role of *i*) large scale ocean circulation patterns~~, *ii*) regional~~ and water mass distribution and *iii*~~*i*~~) phytoplankton productivity as controlling factors on CDOM and FDOM distribution.

2. Material and Methods

2.1. Study area

Observations were done in the framework of long term observational program AREX, conducted since 1987 by Institute of Oceanology Polish Academy of Science, Sopot, Poland and covered the area of water masses exchange between the North Atlantic Ocean and the Arctic Ocean (Figure 1). The Norwegian, Barents and Greenland Seas, called Nordic Seas, represents a crucial component of the Northern Hemisphere climate system due to two contrasting water masses and their contribution to the heat and salt exchanges between the North Atlantic and the Arctic Ocean (Walczowski, 2014; Schlichtholz and Houssais, 1999a, b). The warm and salty Atlantic Waters (AW) carried northward by the North Atlantic Current (NAC), which further splits into two major branches. Norwegian Current (NC) flows into the Barents Sea as the Barents Sea Branch, while the West Spitsbergen Current (WSC) heads north along the eastern flank of the Fram Strait. The East Greenland Current (EGC)

flows south along the western side of Fram Strait, and carries cold and low saline Polar Surface Waters (PSW) and sea ice (Figure 1) (e.g. Schlichtholz and Houssais, 2002). East Spitsbergen Current (ESC) could also affect the region with transformed Polar Water originating from north–east Barents Sea (Sternal at al., 2014). Main ESC branch flows southward along the coast of Spitsbergen and its extension is the Sørkapp Current that influences the West Spitsbergen Shelf. Remaining part of Polar Water from the Barents Sea flows southwestward along the eastern slope of the Spitsbergenbanken (SPB) towards Bear Island as the Bjørnøya Current (BC) (Loeng, 1991) in the Norwegian Sea and the Barents Sea border. Presence and extensiveness of Polar Water from the Barents Sea depends on favorable wind conditions affecting the magnitude and the exchange with the AW inflow (Nilsen et al., 2015; Walczowski, 2014).

Optical measurements and water sampling were conducted during three summer Arctic expeditions (AREX) onboard r/v Oceania in 2013, 2014 and 2015 (AREX2013, AREX2014, and AREX2015, respectively) (Table 1). *In situ* FDOM fluorescence measurements were conducted in 2014 and 2015. AREX expeditions covered the Norwegian Sea with a main section along the border between the Norwegian Sea and the Barents Sea (sampled in late June to early July in 2014 and 2015). The area of the western and northern Spitsbergen shelf was investigated in July of 2013–2015 (Figure 1), along sections spanning from shelf towards the sea–ice edge. The westernmost and northernmost sampling stations north of 76°N, shown on Figure 1, corresponds to the sea ice edge position in July in the given year.

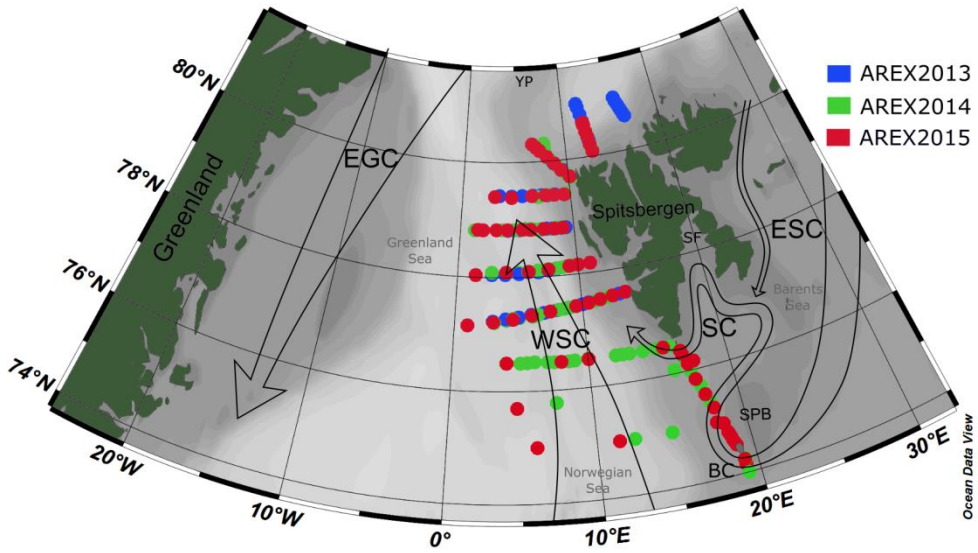

Figure 1: Map of the sampling stations during AREX2013 (blue circles), AREX2014 (green circles), AREX2015 (red circles) with general surface circulation patterns in the Nordic Seas. Atlantic Waters: WSC, West Spitsbergen Current. Polar waters: ESC, East Spitsbergen Current; SC, Sørkapp Current; EGC, East Greenland Current; BC, Bjørnøya Current; YP, Yermak Plateau; SF, Storfjorden; SPB, Spitsbergenbanken.

Table 1. Dates of AREX expeditions, and number of samples or number of *in situ* vertical profiles of CDOM, DOC, chlorophyll *a*, *Chla*, inherent optical properties, (IOP), chlorophyll a fluorescence, (I_{FChla}), and FDOM fluorescence collected.

Cruise	Date	Water samples		Instrumental measurements	
		CDOM / DOC	*Chla*	IOP ac 9, and I_{FChla}	FDOM
		N samples		N profiles	N profiles
AREX2013	13.07–24.07.2013	79	78	57	0
AREX2014	20.06–23.07.2014	221	138	100	100
AREX2015	19.06–24.07.2015	263	142	68	68

2.2. Sample collection and processing

Water samples for determination of CDOM absorption, chlorophyll *a* and DOC were collected with SeaBird SBE32 Carousel Water Sampler equipped with Niskin bottles, the SBE 911 *plus* CTD probe (SBE 9plus CTD Unit and SBE 11plus Deck Unit) and Wetlabs ECO Chlorophyll fluorometer. Samples were collected at three depths: near the surface, ca. 2 m depth, at chlorophyll *a* maximum, that was usually located between 15 and 25 m depth, and below chlorophyll *a* maximum, between 50 and 70 m. The exact position of chlorophyll *a* maximum depth was estimated from vertical profile of chlorophyll *a* fluorescence during CTD downcast. During AREX2013 water samples for CDOM absorption measurements were immediately filtered in two steps: firstly through acid–washed GF/F filters, and secondly through acid–washed Sartorius 0.2 μm pore size cellulose membrane filters to remove finer particles. In 2014 and 2015 CDOM samples were filtered directly from rosette Niskin bottles through a Millipore Opticap XL4 Durapore filter cartridge with nominal pore size 0.2 μm into acid washed 200 ml amber glass bottles. The cartridge filter was kept in 10% HCl solution and was rinsed with ultrapure MilliQ and sample water before collecting CDOM samples. In 2013 and 2015 collected unpreserved water samples for determination of CDOM absorption

were stored on board r/v Oceania in dark, at temperature of 4°C, and were transferred after the cruise to land–based laboratory for spectroscopic measurements. In 2014, all spectroscopic measurements for determination of CDOM absorption ~~and~~ were done in the laboratory onboard r/v Oceania, immediately after collection. Samples for determination of DOC concentration were collected the same way as CDOM samples. Water that passed through 0.2 µm filters was collected into pre–cleaned 40 ml glass vials (certified pre–cleaned sample vials, Sigma–Aldrich) and acidified with drop of concentrated 38% HCl. Acidified samples were stored on board ship in dark, at temperature of 4°C, and were transferred after the cruise to land–based laboratory for measurements.

Water samples for determination of chlorophyll *a* concentration were filtered immediately after collection under low vacuum on Whatman (GE Healthcare, Little Chalfont, UK) 25 mm GF/F filters. Filter pads with particulate material retained on them, were immediately deep frozen in a freezer and thereafter stored at -80°C prior to analyses.

2.3. CDOM absorption

Before spectroscopic scans were conducted, the temperature of the CDOM absorption samples was increased to room temperature. CDOM absorption of AREX2013 and AREX2015 was measured using a double–beam Perkin Elmer Lambda 650 spectrophotometer in ~~a~~the spectral range~~s~~ 240 ~~– and~~ 700 nm, in the laboratory at the Institute of Oceanology Polish Academy of Sciences in Sopot, Poland. Measurements of the CDOM absorption samples collected during AREX2014 were done on board of research vessel, using a double–beam Perkins Elmer Lambda 35 spectrophotometer in the same spectral range as in 2013 and 2015. The 10–cm quartz cuvette was chosen for all measurements and the reference was fresh ultrapure water. Absorbance $A(\lambda)$ spectra were transformed to the CDOM absorption coefficients, $a_{CDOM}(\lambda)$ [m^{-1}], according to:

$$a_{CDOM}(\lambda) = 2.303 \cdot A(\lambda)/L \quad (1)$$

where, 2.303 is the natural logarithm of 10, A(λ) is the corrected spectrophotometer absorbance reading at a specific wavelength (λ) and L is the path length of optical cell in meters (here 0.1 m).

Slope coefficient of the CDOM absorption spectrum, S, between 300 and 600 nm was derived ~~from~~ using Equation (2) and was implemented in Matlab R2011b by adopting a nonlinear least squares fit with a Trust–Region algorithm (Stedmon et al., 2000, Kowalczuk et al., 2006):

$$a_{CDOM}(\lambda) = a_{CDOM}(\lambda_0)e^{-S(\lambda_0 - \lambda)} + K \qquad (2)$$

where: λ_0 is a reference wavelength (here 350 nm), and K is a background constant representing any possible baseline shifts not due to CDOM absorption. Simultaneous calculation of three parameters~~.~~: $a_{CDOM}(350)$, S, and K were done according to Equation (2) in the spectral range between 300 and 600 nm by non–linear regression. CDOM absorption coefficient values ~~were~~ are also included at two other wavelengths: $a_{CDOM}(375)$~~,~~ and $a_{CDOM}(443)$ to enable direct comparison of our results with previously published studies. In 2014 the range of spectral slope coefficient had to be reduced to 300–500 nm due to spectra disturbances over 500 nm in data set from the western and northern Spitsbergen shelf. To assess the effect of the narrower spectral range on spectral slope coefficient calculations we calculated slopes for both spectral ranges in 2013 and 2015. On average, spectral slope coefficient in the spectral range 300–500 nm was higher by 1.76 μm^{-1} relative to $S_{300–600}$. Calculated average bias was deduced from $S_{300–500}$ calculated in 2014 to comply with 2013 and 2015 data set. Linear regression model was used on log–transformed CDOM absorption spectra for spectral slope coefficient calculations at spectral range 275–295 nm, $S_{275–295}$.

2.4. Chlorophyll a concentration.

Filters pads containing suspended particles (including pigments) were used for determination of the chlorophyll *a* concentration for all AREX cruises. Pigments were extracted at room temperature in 96% ethanol for 24 hours. Spectrophotometric determination of chlorophyll *a* concentration, *Chla* [mg m^{-3}], was done with two spectrophotometers: UV4–100 (Unicam, Ltd) and with a Perkin Elmer Lambda 650 in 2013 and 2014–2015, respectively. The optical density (absorbance) of pigment extract in ethanol was measured at 665 nm. Background signal was corrected in the near infrared (750 nm): $\Delta OD = OD(665nm) - OD(750nm)$. Subsequently, conversion of absorbance to chlorophyll *a* was done according to following equation (Strickland and Parsons, 1972; Stramska et al., 2003)~~.~~:

$$Chla = (10^3 \cdot \Delta OD \cdot V_{EtOH})/(83 \cdot V_w \cdot l). \qquad (3)$$

where: 83 [dm^3 $(g\ cm)^{-1}$], is chlorophyll *a* specific absorption coefficient in 96% ethanol, V_w [dm^3] is the volume of filtered water , V_{EtOH} [dm^3] is ethanol extract volume, and the l is path length of cuvette (here 2 cm).

2.5. DOC concentration

DOC measurements were done with a 'HyPer+TOC' analyzer (Thermo Electron Corp., The Netherlands) using UV persulphate oxidation and non–dispersive infrared detection (Sharp, 2002). Potassium hydrogen phthalate was used as standard addition measurements method for each sample in triplicate. Consensus rReference material (CRM) supplied by Hansell Laboratory from University of Miami was performed analyzed as a quality control of DOC concentrations. The methodology provided sufficient accuracy (average recovery 95%; n = 5; CRM = 44 − 46 µM C; our results = 42 − 43 µM C) and precision represented by a relative standard deviation (RSD) of 2%.

The carbon–specific CDOM absorption coefficient at 350 nm, $a^*_{CDOM}(350)$ [$m^2 g^{-1}$], was determined as the ratio of the CDOM absorption coefficient at a given wavelength $a_{CDOM}(350)$ to the DOC concentration (Equation 4):

$$a^*_{CDOM}(350) = \frac{a_{CDOM}(350)}{DOC} \qquad (4),$$

where DOC is expressed in mg l^{-1}.

The carbon–specific UV absorption coefficient (SUVA) is defined as the UV absorbance of water sample at specific wavelength normalized for DOC [mg l^{-1}] concentration (Weishaar et al., 2003). SUVA [m^2 gC^{-1}] at 254 nm ($SUVA_{254}$, Equation 5) is an indicator of aromaticity of aquatic humic substances and was calculated as:

$$SUVA_{254} = \frac{a_{CDOM}(254)}{DOC} \qquad (5).$$

2.6. Instrumental in situ measurements of inherent optical properties, FDOM and chlorophyll a fluorescence

Vertical profiles of inherent optical properties (IOP), FDOM and chlorophyll *a* fluorescence together with conductivity, temperature and pressure were measured at all stations from the surface down to 200 m depth with use ofusing an integrated instrument package consisting of an ac–9 *plus* attenuation and absorption meter (WET Labs Inc., USA), a WetStar CDOM fluorometer (WET Labs Inc., USA), a MicroFlu–Chl chlorophyll *a* fluorometer (TrioS GmbH, Germany), and a Seabird SBE 49 FastCAT Conductivity–Temperature–Depth probe (Seabird Electronics, USA).

Spectral light absorption, $a(\lambda)$ and beam attenuation, $c(\lambda)$, coefficients were measured at nine wavelengths (412, 440, 488, 510, 532, 555, 650, 676, and 715 nm). The ac–9 *plus* calibrations were performed regularly., Aafter cleaning, using with ultrapure water, and stability instruments readings were inspected with in-air measurements. The required correction of absorption signal for scattering was performed with so–called proportional method where zero absorption is estimated at 715 nm (Zaneveld et al., 1994). Subtraction of absorption coefficients from attenuation coefficients determined volume scattering coefficient, $b(\lambda)$. Excitation channel and the maximum emission of light detector of the MicroFlu–Chl chlorophyll *a* fluorometer were set at 470 nm and at 686 nm, respectively. Recorded chlorophyll *a* fluorescence intensity signals, I_{FChla} were reported as analog voltage output in the range 0–5 V DC. The instrument setup is described in detail in Granskog et al. (2015b).

FDOM was measured using a 3–channel WETLabs WetStar fluorometer equipped with two laser LEDs that excited the water sample inside the flow–through quartz cell at 280 and 310 nm, and two detectors to measure emission intensity at 350 and 450 nm. Such construction allowed for combinations of three channels with distinct excitation/emission features in specific peak areas as given in Coble (1996): Channel 1 (CH1), ex./em. 310/450 nm, represents marine ultraviolet humic–like peak C and marine humic–like peak M; Channel 2 (CH2), ex./em. 280/450 nm, represents UVC terrestrial humic–like peak A; and Channel 3 (CH3), ex./em. 280/350 nm, represents the protein–like tryptophane peak T (Figure S1). I_{CHn} is the fluorescence intensity at particular channel where *n* denotes the channel number from 1 to 3. Recorded I_{CHn} could be transformed from raw instrument counts into either the quinine sulfate equivalent (QSE) units, or particular compounds concentration with factory calibration curves. Application of the factory calibration curves, especially the blank ultrapure water readings offset resulted in negative values for I_{CH1} and I_{CH2}. Therefore, we reported fluorescence intensities acquired from the WetStar fluorometer in raw counts, (R.C.) corrected for a noticeable but small drift. This offset was determined as the difference in any I_{CHn}, between initial measurements in July 2014 in the depth range 100–150 m, at salinity >34.9 and temperature T >0°C and measurements repeated in the same salinity and temperature range during field campaign in 2015. The water salinity and temperature characteristics at the chosen depth range was typical for core of Atlantic water inflow, which is characterized with stable values of spectral absorption (measured with ac–9 *plus* attenuation and absorption meter), negligible chlorophyll *a*, and very low background CDOM absorption

level (Sagan S.,~~et al.,~~*personal communication,* 2017). Therefore, we assume that any differences in raw WETLabs WetStar 3–channel fluorometer readings between measurements in 2014 and 2015 resulted from instrument drift, and the offset between the years has been subtracted from florescence intensity values at each channel measured in 2015.

2.7. Classification of water masses

Water masses were classified according to Rudels at al. (2005) based on potential temperature (Θ), potential density (σ_θ) and salinity (S). The original classification definitions are derived for Fram Strait (Rudels et al., 1999) and categorization used in Rudels et al. (2002, 2005) considers mainly the EGC, the area of Yermak Plateau and Storfjorden located on the east coast of Spitsbergen. To adjust the classification to the broader area of Nordic Seas including Atlantic part (Norwegian and Barents Sea) some modifications have been introduced (see Table S1).

The epipelagic layer of the Nordic Seas is~~are~~ dominated by AW and PSW, and waters formed in the mixing process and local modifications (precipitation, sea–ice melt, riverine run–off, and surface heating or cooling) of these two water masses. AW masses were usually characterized by potential temperature and density thresholds defined by Rudels et al. (2005) (Table S1). To better distinguish AW from PSW, we added a third criterion: any water mass classified as PSW (Rudels et al., 2005) with salinity higher than S>34.9, has been considered as AW. The salinity criterion equal to 34.9 is widely used in the literature (Swift and Aagaard 1981; Schlichtholz and Houssais 2002; Walczowski 2014) and eliminates Rudels' et al. (2005) classification ambiguity caused by modification of AW by local sources of fresh water. Part of AW (except Polar Surface Water warm, PSWw) included waters with density below σ_θ=27.7 kgm^{-3} (marked on Figure 3~~2~~ with dashed isopycnal line) used by Rudels et al (2005) as a threshold value between AW and PW. Lower density of waters of Atlantic domain with high salinity (>34.9) is predominantly caused by high temperatures and cannot be referred to as PSW, which lower density is attributed to lower salinity. Polar Surface Water (PSW) is defined as Θ≤0°C and σ_θ≤27.7 kgm^{-3}. The temperature of PSW is usually negative, however, positive temperatures (3–5°C) can be observed during summer (Swift and Aagaard 1981). Warmer PSWw has been considered here with the same σ_θ≤27.7 kg m^{-3} criterion and Θ>0°C (Rudels et al., 2005), due to summer season measurements and higher temperatures of low salinity surface waters in the eastern Fram Strait. Furthermore PWSw was also limited to the uppermost 50 m of the water column with S≤34.9. The water mass with similar TS

characteristics to PSWw but slightly different ranges ~~limits was~~were referred to in the literature ~~as~~for Arctic Surface Water, ASW (e.g. Pavlov et al., 2015 and Gonçalves-Araujo et al., 2016), but due to the dominance in the area of water originating from Atlantic Ocean the name PSWw from Rudels et al.~~,~~ (2005) classification is used. We could find Arctic Atlantic Water (AAW) in our data set as a result of mixing process of AW and PW, in the range of $0<\Theta\leq2$°C and $27.7<\sigma_\theta\leq27.97$ (Rudels et al., 2005). Arctic Intermediate Waters (AIW) was defined as $\Theta\leq0.3$°C, $27.97<\sigma_\theta$, $\sigma_{0.5}\leq30.44$ (Rudels et al., 2005) and included measurements taken at greatest depth in this study.

3. Results

3.1. Interannual and spatial variability of CDOM properties in surface waters ~~in~~with relation to hydrography.

Spatial distribution of temperature, salinity and $a_{CDOM}(350)$ in surface waters of West Spitsbergen Shelf and Norwegian Sea shows considerable variation between years (Figure 2). In 2013, the ~~western~~ West Spitsbergen S~~s~~helf was under the influence of cold and low saline waters from SC. The impact of this current together with possible terrestrial runoff (highest $a_{CDOM}(350)$ values were observed at Spitsbergen fjords entrances) was reflected in high $a_{CDOM}(350)$ (av. 0.47±0.26 m^{-1}) for coastal waters on the West Spitsbergen Shelf. Lower values of $a_{CDOM}(350)$ ~~was~~ were observed in the PSWw (av. 0.33±0.17 m^{-1}) from coastal areas and in the warm and salty AW from the WSC (av. 0.28±0.07 m^{-1}). The lowest CDOM absorption (av. 0.25~~6~~±0.05 m^{-1}) in 2013 was observed at the northernmost and northeastmost stations influenced by low saline PSW affected by sea–ice melt water.

A quite different situation was observed in 2014 (Figure 2b). The spatial extent of AW was distinctly wider, as shown by temperature and salinity distributions. The higher proportion of AW over the West Spitsbergen Shelf in 2014 was confirmed by the temperature and salinity time series in the top 200 m water layer (Walczowski et al., 2017). This large volume of AW influenced CDOM absorption, which was lowered to half of the values (av. $a_{CDOM}(350) = 0.15$±0.06 m^{-1}) compared to 2013. Besides, mean $a_{CDOM}(350)$ values around 0.1±0.03 m^{-1} ~~-~~were observed in the northern Spitsbergen shelf in the area affected by sea ice melting (within the salinity range of 31.4–33.9).

In 2015, SC and ESC branches originating from the Barents Sea were pronounced, as indicated by lower temperature and salinity, Figure 2c, ~~leading to~~resulting in elevated

$a_{CDOM}(350)$ values ~~distinct~~ on the West Spitsbergen Shelf and along the section from Sørkapp down to 74°N and near Bjørnøya Island. In 2015 AW was characterized by low CDOM concentration ($a_{CDOM}(350)$ av. 0.17~~9~~±0.02 m^{-1}) in contrast to PSW observed north of Svalbard (av. $a_{CDOM}(350)$ = 0.27~~5~~±0.05 m^{-1}).

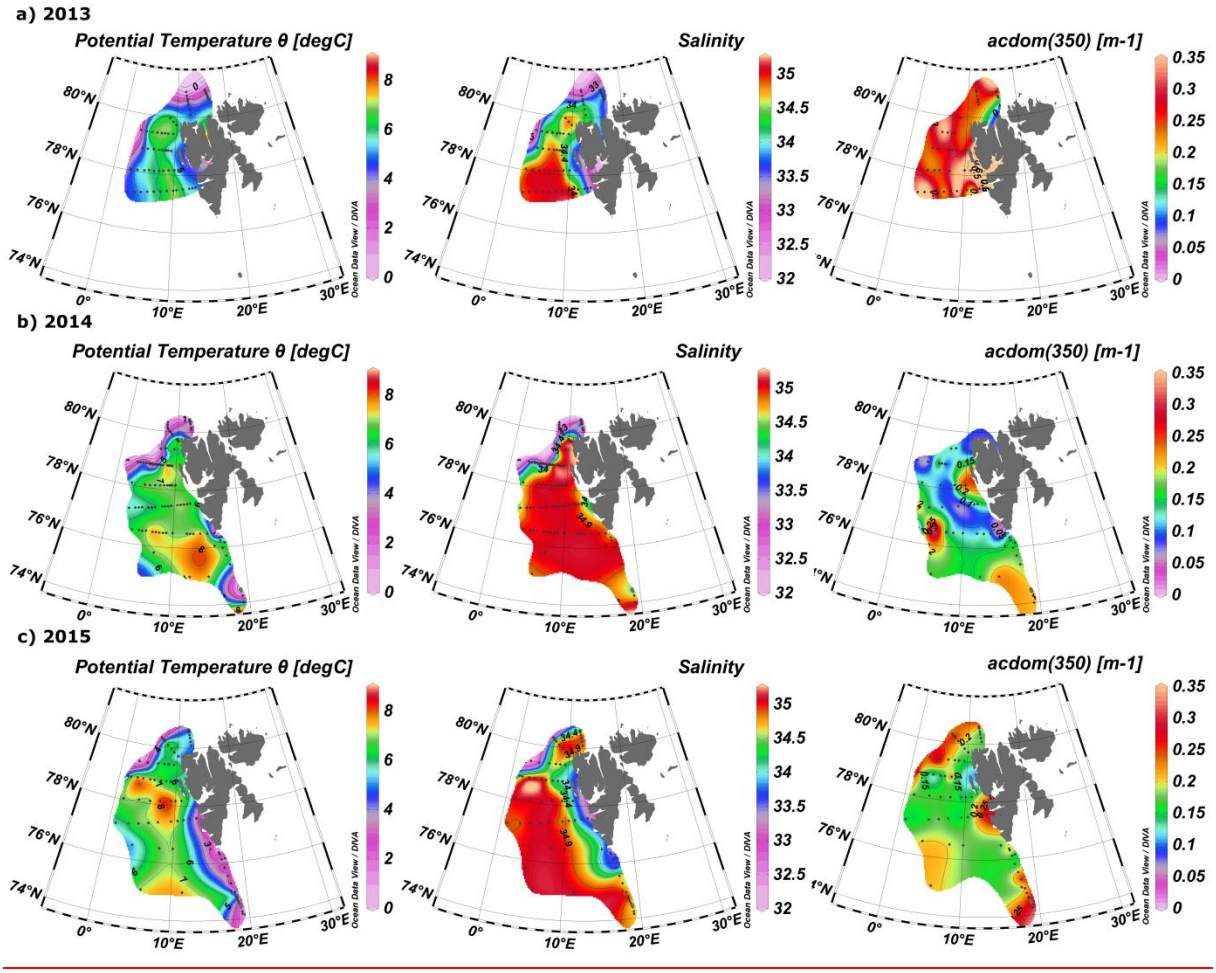

Figure 2: Surface distribution of temperature, salinity and $a_{CDOM}(350)$ in 2013–2015 (~~a~~A ~~–c~~ C respectively). Plots were created with use of Ocean Data View (Schlitzer, R., Ocean Data View, http://odv.awi.de, 2016.)

Summary statistics of the variability of $a_{CDOM}(350)$, $a_{CDOM}(443)$, $S_{275–295}$, $S_{300–600}$, $a^*_{CDOM}(350)$ and $SUVA_{254}$ in different water masses in a given year is provided in Table 2. The highest $a_{CDOM}(350)$ was observed in 2013 (Table 2) when CDOM absorption in AW and PSW were similar (av. $a_{CDOM}(350)$ = 0.28±0.07 m^{-1}). CDOM absorption in PSWw

was higher and was characterized by the greatest variability (av. $a_{CDOM}(350)$ = 0.32±0.16 m^{-1}; min–max: 0.15–0.9 m^{-1} C.V. = 50%). In 2014 $a_{CDOM}(350)$ values were almost 2 times lower compared to other summer seasons (Table 2). In 2014 79% of all samples were classified as AW (av. $a_{CDOM}(350)$ = 0.14±005 m^{-1}) which corresponded to the highest temperature, widespread AW distribution and lack of apparent influence by SC waters. Less than 15% samples represented PSWw (av. $a_{CDOM}(350)$ = 0.14±0.05 m^{-1}) (Table 2). In 2015 we observed intermediate $a_{CDOM}(350)$ values in AW and PSWw (Table 2) with the highest values in PSW and AAW (PSW: $a_{CDOM}(350)$ = 0.26±0.09 m^{-1}, AAW: $a_{CDOM}(350)$ = 0.25±0.06 m^{-1}). ~~There were similarities between 2013 and 2015 regarding variability ranges of CDOM optical characteristics in the water masses and distribution of low saline waters from ESC and SC.~~

The spectral slope coefficient is often inversely non–linearly related to CDOM absorption coefficient (Stedmon and Markager 2001; Stedmon et al., 2003, Kowalczuk et al., 2006, Meler et al., 2016). $S_{275–295}$ and $S_{300–600}$ was lowest in 2013 and highest in 2014, with intermediate values in 2015 (Table 2). The carbon–specific CDOM absorption coefficient $a^*_{CDOM}(350)$ was significantly lower (p<0.000001, T test) in 2014 compared to 2013 and 2015. While the values of $SUVA_{254}$ were most diverse in 2013 whereas the greatest variability in AW (min–max: 0.64–9.23 m^2 gC^{-1}) was observed in 2014. In 2014 and 2013~~5~~ average values of $SUVA_{254}$ for whole season were similar, around 1.7 m^2 gC^{-1} (Table 3), however average values in AW and PSWw were higher in 2013 and 2014, respectively (Table 2). In 2015 average $SUVA_{254}$ values were similar within identified water masses and low variation (± 0.15 m^2 gC^{-1}) between different waters was observed. The interannual variability of $SUVA_{254}$ was insignificant (p=0.89, T test) between 2013 and 2014, however the average $SUVA_{254}$ values observed in 2015 were significantly different (p<0.002, T test) than in 2013 and 2014 (Table 2).

The average DOC concentration in the study area was highest in 2013 (80.69 µmol/L) and decreased significantly (p<0.000001, T test) year by year (Table 3) to 67.64 µmol/L in 2015. The average chlorophyll *a* concentration was lowest in 2013 (0.87 mg/m^3), almost doubled in 2014 (1.58 mg/m^3), and decreased by 12% in 2015 (1.39 mg/m^3), relative to previous year.

Table 2. Descriptive statistics of selected parameters from AREX 2013–2015. Average and standard deviation, range of variability in depth, potential temperature (Θ), salinity (S), absorption coefficient at 350 nm ($a_{CDOM}(350)$), absorption coefficient at 443 nm ($a_{CDOM}(443)$), spectral slope coefficient in range 275–295 nm ($S_{275–295}$), spectral slope coefficient in range 300–600 nm ($S_{300–600}$). Water masses were classified according to Rudels et al. (2005) with minor modifications (see Table S1).

WM/N	Depth [m]	Θ [°C]	S	σ_θ [kg*m^{-3}]	$a_{CDOM}(350)$ [m^{-1}]	$a_{CDOM}(443)$ [m^{-1}]	$S_{275–295}$ [µm^{-1}]	$S_{300–600}$ [µm^{-1}]	a^*_{CDOM}(350) [m^2 g^{-1}]	SUVA$_{254}$ [m^2 gC^{-1}]
AREX 2013										
AW n=43	**31 ±23**	**4.94 ±1.3**	**35.01 ±0.06**	**27.68 ±0.15**	**0.28 ±0.07**	**0.05 ±0.02**	**15.36 ±3.40**	**18.25 ±1.78**	**0.35 ±0.12**	**1.95 ±0.60**
	0 80	2.15 7.48	34.82 35.10	27.34 27.95	0.19 0.55	0.03 0.14	10.53 25.38	13.64 20.79	0.15 0.60	1.01 3.16
PSW n=3	**23 ±25**	**-0.86 ±0.7**	**33.62 ±1.00**	**27.04 ±0.84**	**0.28 ±0.03**	**0.05 ±0.00**	**16.02 ±2.35**	**17.69 ±2.15**	**0.24 ±0.02**	**1.31 ±0.28**
	0 50	-1.35 -0.02	32.50 34.42	26.09 27.70	0.24 0.30	0.05 0.06	14.26 18.69	15.21 19.07	0.22 0.25	1.00 1.55
PSWw n=33	**4 ±9**	**4.87 ±1.6**	**34.21 ±0.66**	**27.05 ±0.45**	**0.32 ±0.16**	**0.07 ±0.07**	**15.37 ±3.16**	**17.55 ±3.58**	**0.29 ±0.11**	**1.64 ±0.72**
	0 30	0.15 7.30	32.21 34.89	25.83 27.66	0.15 0.90	0.01 0.32	11.61 28.32	9.95 30.06	0.15 0.58	0.95 3.80
AREX 2014										
AW n=174	**39 ±39**	**5.57 ±1.2**	**35.03 ±0.05**	**27.62 ±0.14**	**0.14 ±0.06**	**0.02 ±0.02**	**14.66 ±2.19**	**20.98 ±5.42**	**0.16 ±0.08**	**1.79 ±1.33**
	0 200	2.05 7.45	34.86 35.09	27.36 27.94	0.04 0.34	0.00 0.09	11.20 24.52	10.83 42.26	0.05 0.59	0.64 9.23
PSW n=4	**15 ±12**	**-0.62 ±0.4**	**32.59 ±1.33**	**26.19 ±1.09**	**0.11 ±0.04**	**0.01 ±0.01**	**12.20 ±0.40**	**22.08 ±4.91**	**0.15 ±0.05**	**1.96 ±0.63**
	5 25	-0.91 -0.01	31.29 33.88	25.14 27.25	0.08 0.16	0.01 0.02	11.80 12.71	17.03 28.35	0.09 0.20	1.26 2.76
PSWw n=28	**18 ±15**	**2.82 ±1.9**	**34.14 ±0.73**	**27.19 ±0.54**	**0.14 ±0.05**	**0.02 ±0.01**	**13.89 ±2.42**	**20.03 ±4.72**	**0.17 ±0.07**	**1.62 ±0.78**
	5 50	0.34 5.83	32.41 34.88	25.94 27.70	0.05 0.29	0.00 0.07	10.51 21.40	13.18 33.79	0.05 0.38	0.76 3.81
AAW n=4	**80 ±24**	**1.36 ±0.5**	**34.86 ±0.05**	**27.91 ±0.05**	**0.15 ±0.05**	**0.02 ±0.01**	**16.56 ±5.58**	**20.32 ±0.46**	**0.15 ±0.08**	**1.44 ±0.81**
	50 100	0.59 1.89	34.83 34.94	27.86 27.97	0.10 0.20	0.01 0.02	12.45 24.28	19.77 20.87	0.08 0.26	0.67 2.31
IW/DW n=11	**1627 ±979**	**-0.66 ±0.3**	**34.94 ±0.04**	**28.09 ±0.02**	**0.17 ±0.08**	**0.03 ±0.03**	**16.46 ±5.85**	**17.83 ±4.58**	**0.17 ±0.09**	**1.07 ±0.26**
	301 2823	-0.86 -0.07	34.91 35.01	28.08 28.15	0.06 0.32	0.00 0.10	10.66 26.04	11.13 28.35	0.05 0.37	0.56 1.38
AREX 2015										
AW n=156	**61 ±65**	**4.89 ±1.5**	**35.00 ±0.06**	**27.68 ±0.15**	**0.18 ±0.04**	**0.03 ±0.01**	**19.42 ±2.55**	**19.77 ±2.15**	**0.21 ±0.05**	**1.41 ±0.24**
	5 470	2.23 8.15	34.78 35.09	27.26 27.97	0.11 0.34	0.01 0.10	10.94 25.51	13.08 25.48	0.14 0.39	0.86 2.19
PSW n=6	**32 ±11**	**-0.58 ±0.6**	**34.14 ±0.22**	**27.44 ±0.16**	**0.26 ±0.09**	**0.05 ±0.03**	**18.34 ±3.93**	**19.35 ±3.12**	**0.32 ±0.11**	**1.99 ±0.30**
	25 50	-1.38 -0.01	33.93 34.45	27.28 27.69	0.20 0.42	0.02 0.12	12.28 22.19	13.92 22.32	0.23 0.50	1.65 2.54

PSWw n=73	**17 ±15** 1 50	**4.13 ±1.9** 0.37 8.14	**34.33 ±0.61** 32.17 34.89	**27.22 ±0.44** 25.80 27.70	**0.20 ±0.05** 0.12 0.34	**0.04 ±0.02** 0.01 0.09	**18.69 ±3.15** 11.51 24.96	**19.13 ±2.70** 13.56 24.87	**0.25 ±0.06** 0.15 0.40	**1.54 ±0.28** 0.96 2.63
AAW n=9	**76 ±76** 5 257	**1.69 ±0.2** 1.49 1.96	**34.72 ±0.09** 34.64 34.88	**27.77 ±0.08** 27.71 27.91	**0.25 ±0.06** 0.15 0.33	**0.05 ±0.02** 0.02 0.08	**17.72 ±2.81** 13.90 23.42	**18.28 ±2.42** 15.06 23.40	**0.28 ±0.07** 0.19 0.37	**1.64 ±0.38** 1.18 2.26
IW/DW n=19	**2175 ±604** 794 2872	**-0.70 ±0.1** -0.79 -0.15	**34.92 ±0.01** 34.91 34.93	**28.08 ±0.01** 28.06 28.10	**0.14 ±0.05** 0.09 0.27	**0.02 ±0.01** 0.01 0.06	**21.22 ±3.58** 13.32 27.90	**21.32 ±2.71** 15.57 26.59	**0.19 ±0.07** 0.12 0.44	**1.49 ±0.46** 1.03 2.46

437 Table 3. Yearly averaged descriptive statistics of selected CDOM optical properties from AREX 2013–2015.

Year N	**Θ [°C]**	**S**	$a_{CDOM}(350)$ [m^{-1}]	$a_{CDOM}(443)$ [m^{-1}]	$S_{275–295}$ [μm^{-1}]	$S_{300–600}$ [μm^{-1}]	$a^*_{CDOM}(350)$ [$m^2 g^{-1}$]	$SUVA_{254}$ [m^2 gC^{-1}]	DOC [µmol/l]	N	*Chla* [mg/m^3]
2013 79	**4.69 ±1.77** -1.35 7.48	**34.62 ±0.63** 32.21 35.10	**0.30 ±0.12** 0.15 0.90	**0.06 ±0.05** 0.01 0.32	**15.39 ±3.24** 10.53 28.32	**17.94 ±2.68** 9.95 30.06	**0.32 ±0.11** 0.15 0.60	**1.79 ±0.66** 0.95 3.80	**80.69 ±24.46** 40.46 127.45	**71**	**0.87 ±1.13** 0.07 8.83
2014 221	**4.72 ±2.18** -0.91 7.45	**34.86 ±0.52** 31.29 35.09	**0.14 ±0.06** 0.04 0.34	**0.02 ±0.00** 0.10 0.02	**14.65 ±2.63** 10.51 26.04	**20.71 ±5.26** 10.83 42.26	**0.17 ±0.08** 0.05 0.59	**1.73 ±1.23** 0.56 9.23	**77.57 ±22.10** 40.28 131.70	**138**	**1.58 ±1.38** 0.12 10.42
2015 263	**4.04 ±2.23** -1.38 8.15	**34.78 ±0.45** 32.17 35.09	**0.19 ±0.05** 0.09 0.42	**0.03 ±0.02** 0.01 0.12	**19.26 ±2.91** 10.94 27.90	**19.64 ±2.44** 13.08 26.59	**0.23 ±0.06** 0.12 0.50	**1.47 ±0.30** 0.86 2.63	**67.64 ±6.50** 51.12 121.83	**142**	**1.39 ±0.83** 0.14 3.70

438

3.2. Optical properties of different water masses

All measured salinity and temperature values are presented in the temperature–salinity (TS) diagram as a function of depth (Figure 3a) to visualize water masses sampled during AREX2013, AREX2014 and AREX2015 campaigns. Majority of measurement represented characteristics of AW that covered all depth ranges. The second water mass represented in our data set was low density PSWw ($\sigma_\theta \leq 27.7$ kg m^{-3}), which was observed above 50 m depth. The smallest fraction of data points belonged to PSW, which was aggregated in subsurface, 20–70 m depth range and AAW which was encountered within 50–100 m depth range (Figure 3a). To visualize the distribution of DOM properties within classified water masses we have chosen the fluorescence intensity of the marine humic–like DOM (I_{CH1}), fluorescence intensity of the protein–like DOM (I_{CH3}), and CDOM absorption $a_{CDOM}(350)$. The highest I_{CH1} values were observed in PSW and lowest in PSWw (Figure 3b). Humic–like FDOM in AW was characterized with large dynamic range and both low (320 R.C.) and high values (>360 R.C.), were observed (Figure 3b). In case of I_{CH3} the highest values were observed in PSW, PSWw mid depth (15-50m, what can be associated with chlorophyll a maximum) and in part of AW, which was separated from PSWw (upper part: $T>0$, $\sigma_\theta \leq 27.7$, $S>34.9$). The lowest I_{CH3} values were observed in AW (lower part: $27.7<\sigma_\theta \leq 27.97$) and in PSWw where $\sigma_\theta \leq 26.5$ (Figure 3c). There was a large variability and no consistent trends in distribution of $a_{CDOM}(350)$ values in different water masses in the study area, as shown in the TS diagram (Figure 3d~~e~~). The distribution of fluorescence intensity of the terrestrial humic–like DOM (I_{CH2})~~,~~ ~~protein–like DOM (I_{CH3})~~ and $SUVA_{254}$ in the TS diagram i~~was~~ shown in the supplementary information (Figure S2).

a)

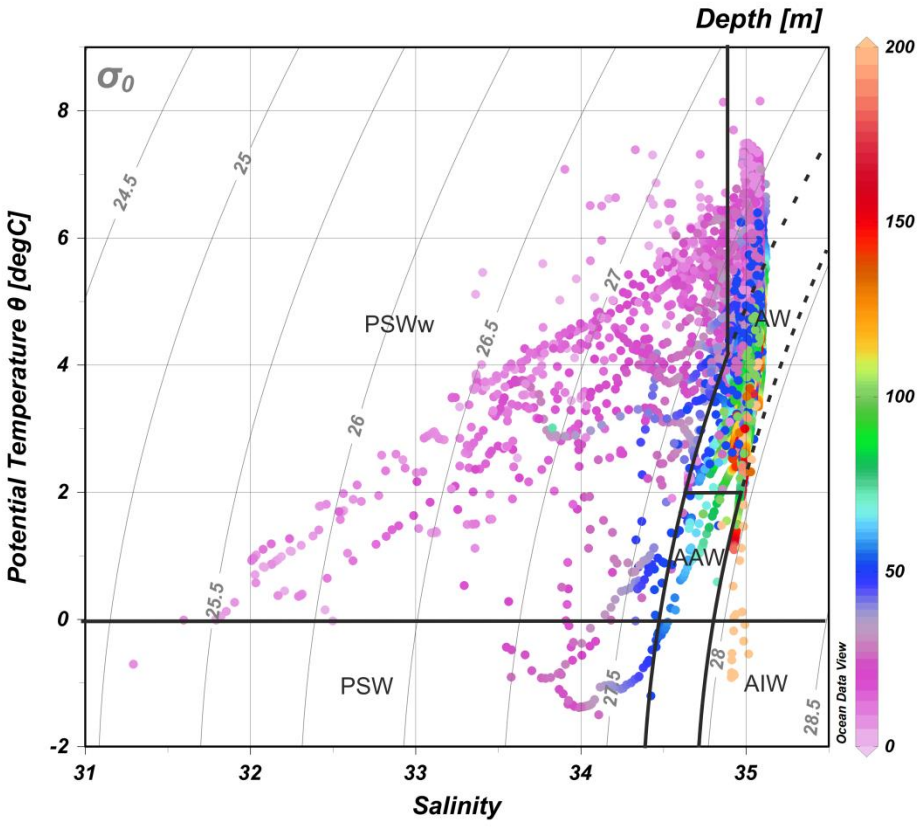
Depth [m]
σ0
Potential Temperature θ [degC]
Salinity
PSWw
AW
AAW
PSW
AIW
Ocean Data View

b)

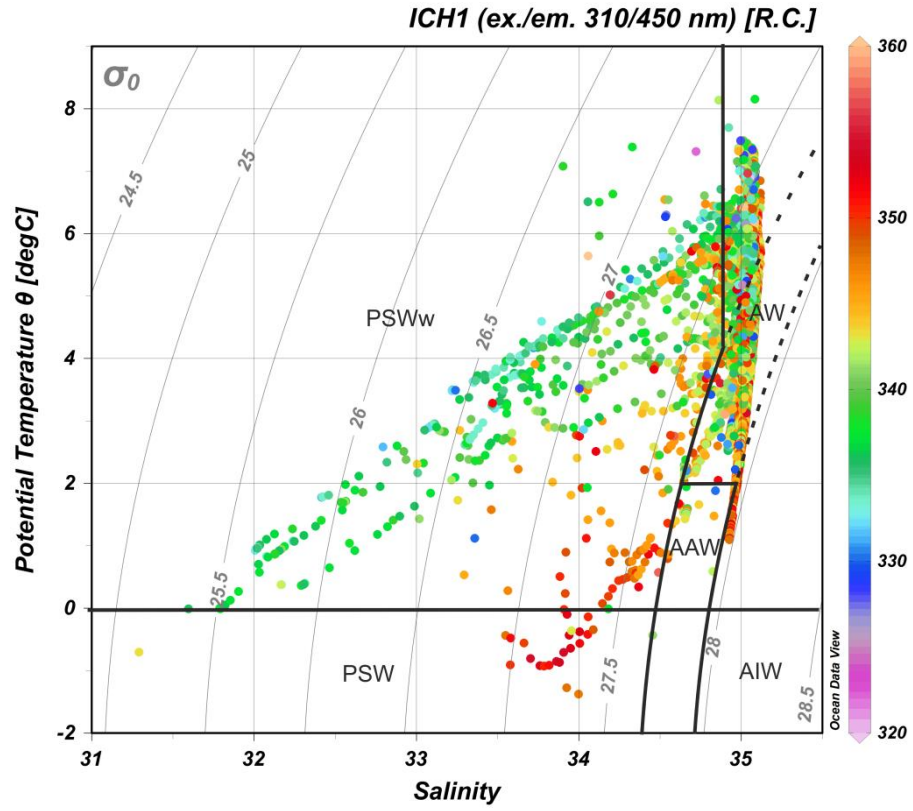
ICH1 (ex./em. 310/450 nm) [R.C.]
σ0
Potential Temperature θ [degC]
Salinity
PSWw
AW
AAW
PSW
AIW
Ocean Data View

c)

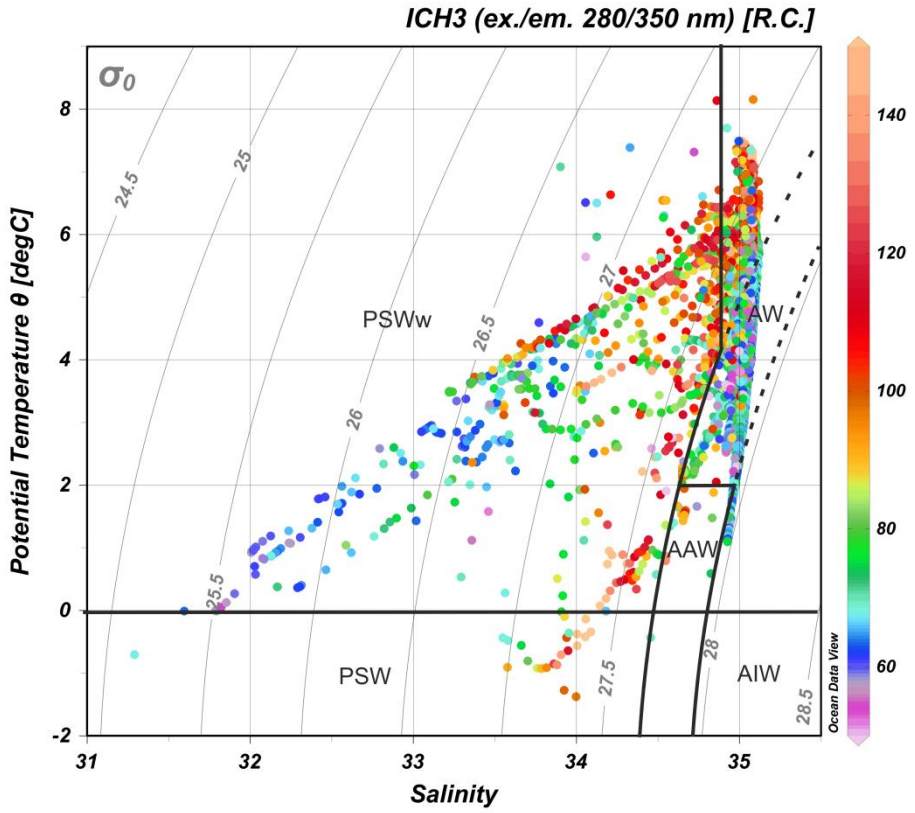
ICH3 (ex./em. 280/350 nm) [R.C.]
σ0
24.5
25
25.5
26
26.5
27
27.5
28
28.5
PSWw
AW
AAW
PSW
AIW
Potential Temperature θ [degC]
Salinity
Ocean Data View
140
120
100
80
60

d)

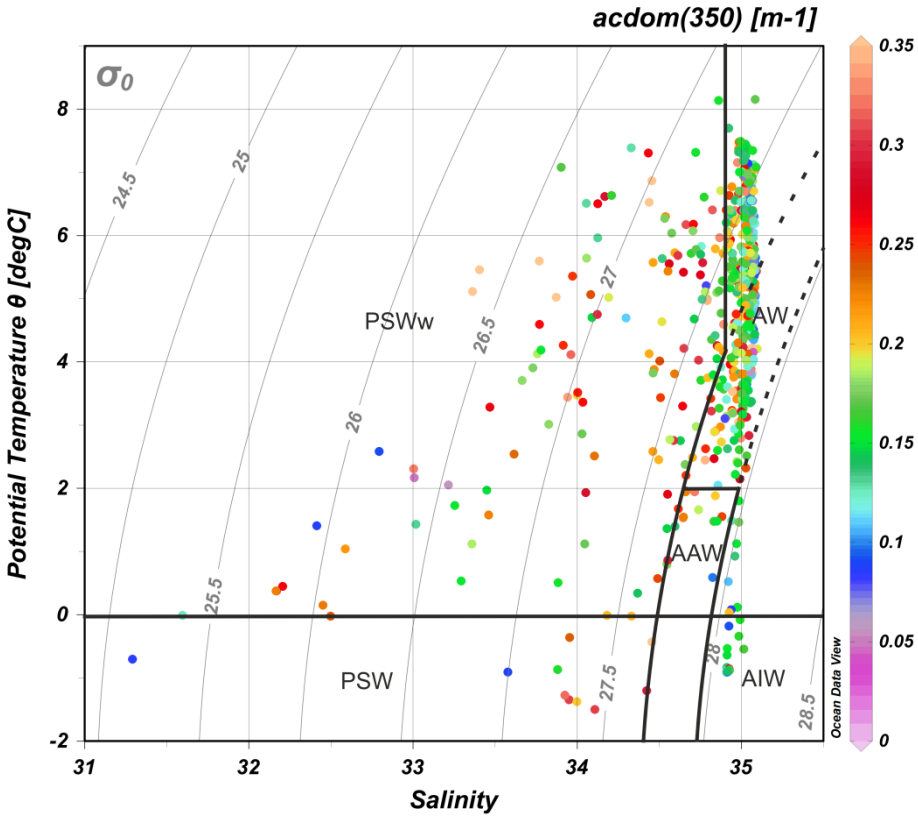
acdom(350) [m-1]
σ0
24.5
25
25.5
26
26.5
27
27.5
28
28.5
PSWw
AW
AAW
PSW
AIW
Potential Temperature θ [degC]
Salinity
Ocean Data View
0.35
0.3
0.25
0.2
0.15
0.1
0.05
0

Figure 3: TS diagram of water mass distribution in~~on~~ the study area in 2013–2015. A) colorbar represents depth [m]. B) colorbar represents humic–like fraction fluorescence intensity I_{CH1}, (–ex./em. 310/450 nm, [R.C.]). C) colorbar represents protein–like fraction fluorescence intensity I_{CH1}, (ex./em. 310/450 nm, [R.C.]). D~~C~~) colorbar represents values of absorption coefficient at 350 nm, $a_{CDOM}(350)$ [m^{-1}]. The lower number of points in D~~c~~) resulted from fewer number of discrete water samples for determination of CDOM. Water masses: AW (Atlantic Water), AAW (Arctic Atlantic Water), AIW (Arctic Intermediate Water), PSW (Polar Surface Water), PSWw (Polar Surface Water warm). Three areas noted as AW follow the three sets of conditions that define AW (see Table S1).

3.3. Vertical distribution of FDOM components

The instrumental *in situ* synchronous IOP measurements enabled to resolve FDOM distribution with better resolution, compared to coarser discrete water sampling of CDOM. Representative vertical profiles of temperature, salinity, FDOM and chlorophyll *a* fluorescence are shown in Figure 4. Differences in the vertical distribution of salinity and temperature (Figure 4a,b) were observed in sampling stations located near the sea ice edge (black stars), where a cold and fresher surface layer (typically 5–10 m deep; classified as PSWw) was present. The salinity at stations located in the core of Atlantic waters (green circles) and at the south–western Spitsbergen shelf (red circles) was~~ere~~ uniform in the upper 100 m (Figure 4a,b). There was very little spatial and vertical variation in humic–like FDOM (I_{CH1} and I_{CH2}). The only exception was the slightly higher, but still vertically homogenous distribution, of humic–like FDOM observed at stations near the Spitsbergen coast in 2014. (red dots; Figure 4c,d).

The vertical distribution of protein–like FDOM (I_{CH3}, Figure 4e) was very similar to distribution of chlorophyll *a* fluorescence (I_{FChla}, Figure 4f) and total non–water absorption coefficient at 676 nm ($a_{tot-w}(676)$, Figure 4g). All three parameters had a strong subsurface maximum at the depth range between 10 and 30–40 m and similar spatial distribution. The surface values for these three parameters were higher than values below the maximum (40 m) for profiles in the AW (green and red symbols). Near the ice edge, however, stations were characterized by lower values in the surface layer, comparable to the values below 40 m, likely due to dilution of FDOM and *Chla* by sea–ice melt water at the very surface. The

$a_{tot-w}(676)$ vertical profiles in AW were different, with elevated values throughout the whole upper layer (0–30 m depth), which dropped sharply to a background level below the subsurface chlorophyll *a* maximum.

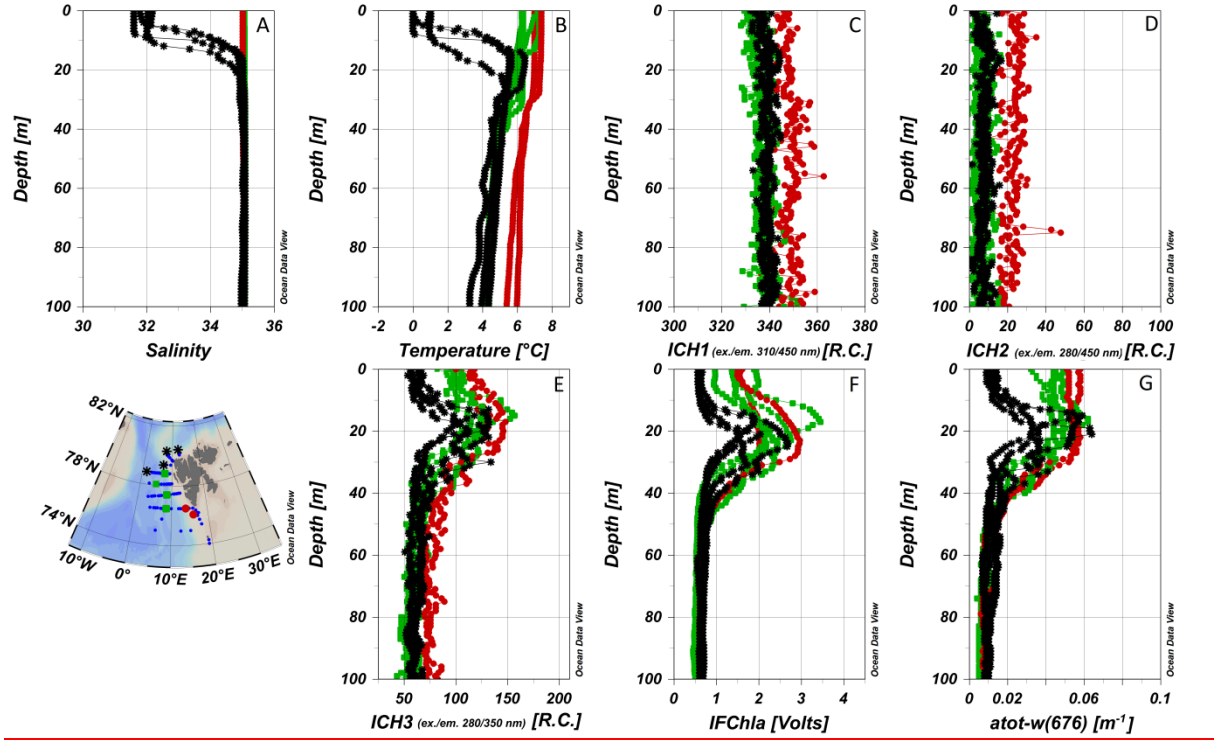

Figure 4: Vertical profiles of: salinity (A), temperature (B), different ~~fluorescent~~ FDOM components: marine humic–like FDOM (I_{CH1}, C), terrestrial humic–like fraction of DOM (I_{CH2}, D), protein–like FDOM (I_{CH3}, E), chlorophyll *a* fluorescence (I_{FChla}, F) and total non–water absorption coefficient at 676 nm ($a_{tot-w}(676)$, G) in 2014. Red dot, green square, black star symbols correspond to vertical profiles obtained over the West Spitsbergen Shelf (influenced by SC), in the core of the WSC, and near the ice edge (with a presence of PSWw in the surface 0–20 m layer), respectively.

3.4. Relationship between chlorophyll a and protein–like FDOM

The qualitative correspondence between fluorescence of protein–like FDOM and chlorophyll *a* fluorescence intensity (Figure 4) has been quantitatively confirmed by regression analysis. A significant positive relationship between I_{CH3} and I_{FChla} was found in both 2014 and 2015 ($R^2 = 0.65$, $p<0.0001$, $n = 24490$; Figure 5a~~, Table 4~~). The relationship was ~~more significant~~ stronger in 2014 ($R^2 = 0.75$, $p<0.0001$, $n = 17700$, blue line in Figure 5a~~,~~

~~Table 4~~) when ~~stronger~~ broader influence of AW water was observed (Walczowski et al., 2017), than in 2015 (R^2 = 0.45, p<0.0001, n = 7290, red line in Figure 5a).

The same relationship was confirmed using data from discrete water samples. A statistically significant relationship between I_{CH3} and *Chla* values was found in both years, and the determination coefficient for combined data set was R^2 = 0.36 (p<0.0001) (Figure 5b~~,~~ ~~Table 4~~). There was higher correlation observed between I_{CH3} and *Chla* values in 2015 compared to 2014 (Figure 5b~~Table 4~~). Higher dispersion between FDOM fluorescence intensity measured *in situ* and chlorophyll *a* measured in water samples could be a result of the time lag between instrumental measurements and water collection that reached up to 1.5 hours. The IOP instruments deployment were usually done simultaneously with CTD down cast, while water sample collection was~~ere~~ performed during CTD rosette up cast, that was significantly delayed especially at deep water stations (at sampling stations location with water depth >1000 m). Observed higher protein–like FDOM values per chlorophyll *a* concentration unit could be explained by phytoplankton physiological response due to higher water temperature observed in 2014 and consequent more efficient extracellular DOM release. This physiological effect is evident in relationships between chlorophyll a fluorescence and $a_{tot-w}(676)$. In 2014 ~~the~~ phytoplankton were more fluorescent at the same absorption level (Figure S3).

a)

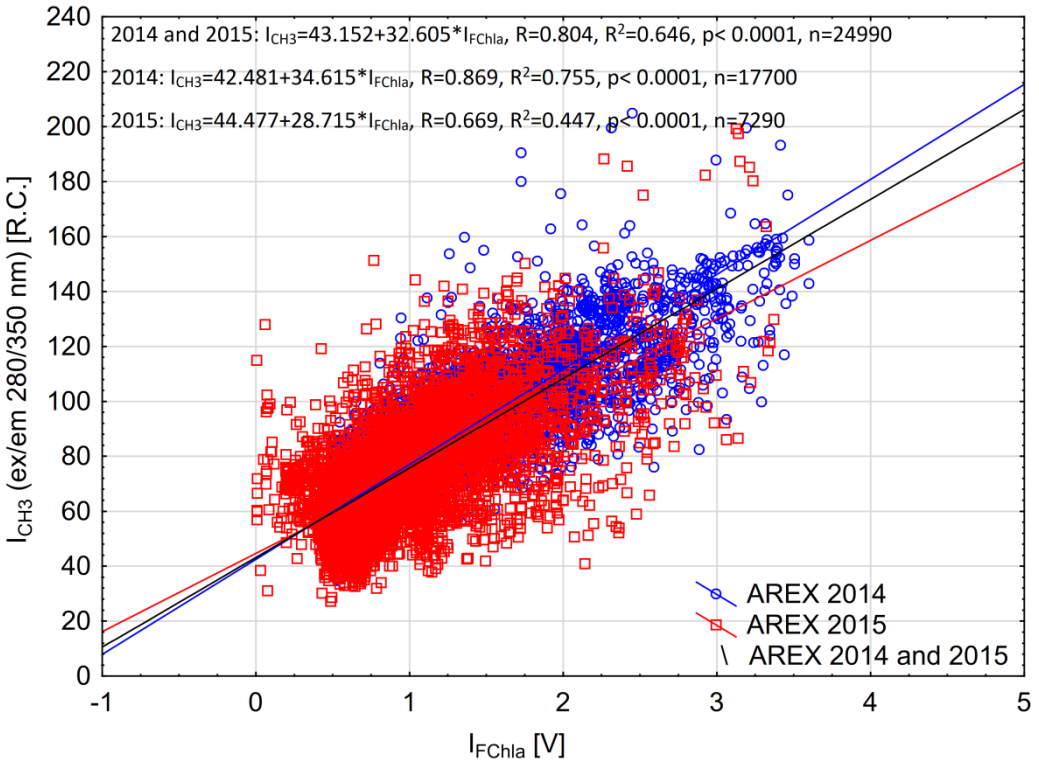

b)

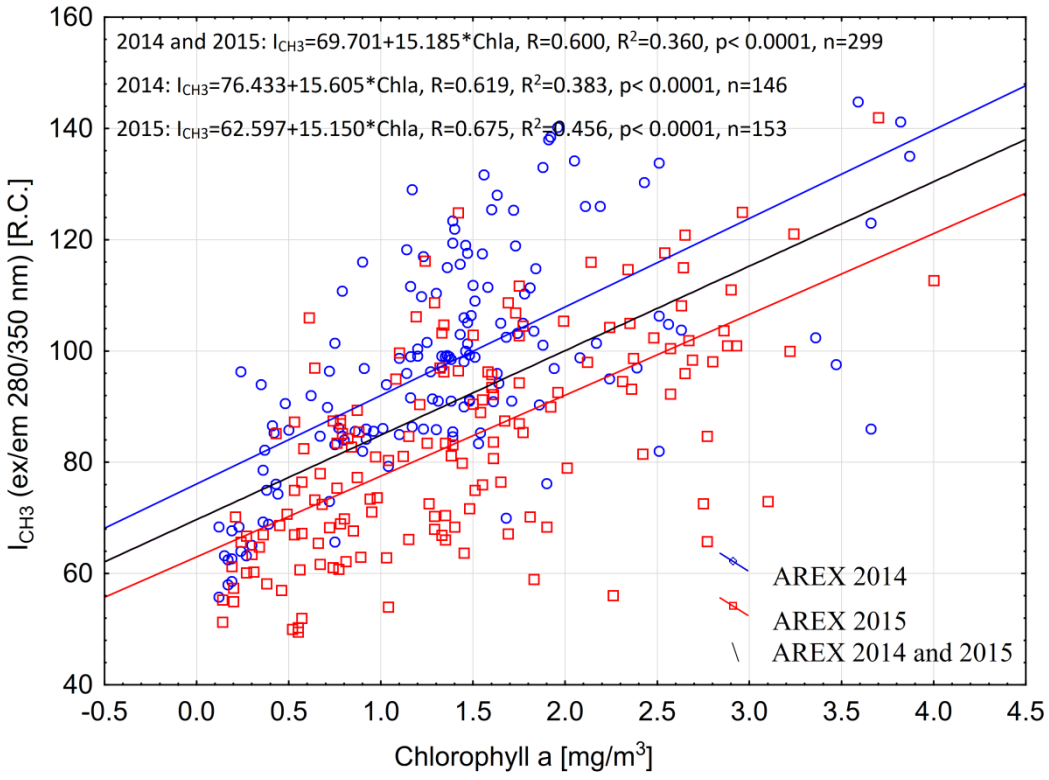

529 Figure 5. Relationship between chlorophyll a fluorescence (I_{FChla}) and fluorescence of
530 the protein–like component (I_{CH3}) (a) and relationship between fluorescence

of the protein–like component (I_{CH3}) and chlorophyll a concentration from discrete water samples (b) in the upper 200m of water column in 2014 and 2015. ~~For regression details see Table 4.~~

~~Table 4.~~ Set of linear regression functions, correlation coefficient (R), coefficient of determination (R^2), p–value and number of samples (n) ~~for~~ ~~were~~are presented ~~relationship between: Y=I_{CH3} and X= I_{FChla} presented o~~in Figure 5~~a and Y = I_{CH3} and X = Chla shown in~~on Figure 5~~b in 2014 and 2015~~. ~~Symbol colors correspond to linear regression colors for the given years marked at Figure 5a and 5b.~~

~~Data Set Year (Figure No., color)~~	~~Equation~~	~~R~~	~~p~~	~~R^2~~	~~n~~
~~2014 (**5a,** \)~~	~~I_{CH3}=42.481+34.615*I_{FChla}~~	~~0.869~~	~~p<0.0001~~	~~0.755~~	~~17700~~
~~2015 (**5a,** \)~~	~~I_{CH3}=44.477+28.715*I_{FChla}~~	~~0.669~~	~~p<0.0001~~	~~0.447~~	~~7290~~
~~2014–2015 (**5a,** \)~~	~~I_{CH3}=43.152+32.605*I_{FChla}~~	~~0.804~~	~~p<0.0001~~	~~0.646~~	~~24990~~
~~2014 (**5b,** \)~~	~~I_{CH3}=76.433+15.605*Chla~~	~~0.619~~	~~p<0.0001~~	~~0.383~~	~~146~~
~~2015 (**5b,** \)~~	~~I_{CH3}=62.597+15.150*Chla~~	~~0.675~~	~~p<0.0001~~	~~0.456~~	~~153~~
~~2014–2015 (**5b,** \)~~	~~I_{CH3}=69.701+15.185*Chla~~	~~0.600~~	~~p<0.0001~~	~~0.360~~	~~299~~

4. Discussion

4.1. Variability and spectral properties of CDOM in the Nordic Seas

The highest CDOM absorption in the Arctic has been observed in coastal margins along Siberian Shelf in Laptev Seas, close to Lena River delta; $a_{CDOM}(440)$ = 2.97 m^{-1}, salinity close to 0; (Gonçalves–Araujo et al., 2015) and in Laptev Sea Shelf Water at the surface; a_{CDOM} (443) > 1 m^{-1}, salinity <28, (Gonçalves–Araujo et al., 2018) and at the coast of Chukchi Sea and Southern Beaufort Sea influenced by riverine inputs of Yukon and Mackenzie Rivers; $a_{CDOM}(440)$ > 1 m^{-1}, salinity <28, (Matsuoka et al., 2011, 2012; Bélanger et al., 2013). Exceptionally high CDOM absorption has been also observed in the ~~coastal~~ southern part of Hudson Bay near rivers outlets with $a_{CDOM}(355)$ > 15 m^{-1}, at salinity close to 0 (Granskog et al., 2007). Pavlov et al. (2016) reported $a_{CDOM}(350)$ of up to 10 m^{-1} at salinity

554 of 21 in surface waters of the White Sea. Terrestrial CDOM from Siberian Shelf has been
555 diluted and $a_{CDOM}(440)$ decreased to ca. 0.12 m^{-1}, at salinities 32.6 (Gonçalves–Araujo et al.,
556 2015) and transported further toward the Fram Strait by the Transpolar Drift being gradually
557 diluted or removed (Stedmon et al., 2011; Granskog et al., 2012). In the Transpolar Drift and
558 the central ~~AO~~Arctic Ocean, CDOM absorption in surface waters was dominated by
559 terrestrial sources with ~~average~~ observed $a_{CDOM}(443)$ values varied between ~0.15 m^{-1}, at
560 salinities close to +/-27 (Lund–Hansen et al., 2015) and ~0.5 m^{-1} at salinity range from 26.5 to
561 29.5 (Gonçalves-Araujo et al., 2018). Dilution also effectively decreased CDOM absorption
562 in western Arctic Ocean, and average CDOM absorption in the Chukchi Sea and Beaufort
563 Seas was $a_{CDOM}(440)$ = 0.046 m^{-1}, at salinities > 32.3 (Matsuoka et al., 2011, 2012; Bélanger
564 et al., 2013). The influence of transformed Atlantic Water generated in the Barents and
565 Norwegian Sea had impacted on $a_{CDOM}(443)$ values in the Beaufort Gyre and Amundsen and
566 Nansen basins, causing its decrease below 0.2 m^{-1} as reported by Gonçalves–Araujo et al.
567 (2018).

568 The reported lower range of $a_{CDOM}(350)$ observed in AW during AREX2014 (2014:
569 0.14±0.06 m^{-1}) is in good agreement with data from eastern part of Fram Strait at
570 79°N section reported by Granskog et al. (2012), Stedmon et al. (2015) and Pavlov et al.
571 (2015) and with data reported by Hancke et al. (2014) south of the Polar Front in the Barents
572 Sea. ~~While~~ Kowalczuk et al. (2017) observed similar $a_{CDOM}(350)$ north of Svalbard. Higher
573 values of CDOM absorption in AW observed in 2015 were within published variability range
574 (Pavlov et al., 2015; Hancke et al., 2014; Kowalczuk et. al, 2017). Highest $a_{CDOM}(350)$ values
575 in AW in 2013, 0.28±0.07 m^{-1} (Table 2) were similar to Hancke et al. (2014) north of the
576 Polar Front in the Barents Sea. Very low values of $a_{CDOM}(443)$ aligned with previous
577 reports~~reported record~~: in the core Atlantic waters in Greenland Sea measured during TARA
578 Expedition in 2013 (Matsuoka et al., 2017), in the eastern Fram Strait (Pavlov et al., 2015)
579 and in the Barents Sea (Hancke et al., 2014) and north of Svalbard (Kowalczuk et al., 2017).
580 It should be underlined that data comparison could be biased by number of observations, as
581 this study documented $a_{CDOM}(350)$ and $a_{CDOM}(443)$ statistics based on significantly higher
582 number of samples and wider spatial coverage compared to the sources cited above.

583 The AW inflow with the WSC is an extension of NAC originating from the Atlantic
584 Ocean and CDOM absorption presented in this study were comparable with values found in
585 the North Atlantic Ocean (Kowalczuk et al., 2013; Kitidis et al., 2006). In contrast, values of

absorption coefficients were two times higher in Norwegian Coastal Waters which are influenced by Lofoten Gyre, and presumably by terrestrial runoff as reported by Nima et al. (2016).

Despite lower salinity and lower temperature CDOM optical properties in PSW in this study did not differ significantly from AW in 2013 and 2015, and similar ~~features~~ variability ranges of CDOM properties were mention by Pavlov at el. (2017) north of Svalbard. Therefore, PW in the eastern Fram Strait has not been advected from the central Arctic Ocean, as in the EGC (Granskog et al., 2012; Pavlov et al., 2015), but rather it is a modified AW, strongly affected by heat loss and diluted by sea–ice melt in the Barents Sea. Similar processes occur also on North Spitsbergen Shelf, where PW was also found near the ice edge in surface waters diluted and cooled by sea–ice melt.

According to Aas and Hokedal (1996) freshwater run–off from different sources influence Svalbard waters and there is no universal relation between salinity and CDOM in this area. ~~Statistical distribution~~Average values of $a_{CDOM}(350)$ in 2014 in PSW (Table 2) were similar with Arctic Waters north of the Polar Front in Barents Sea described by Hancke et al. (2014) and slightly higher than observed in this study in 2013 (0.32±0.16 m^{-1}) and 2015 (0.26±0.09 m^{-1}). ~~PW in the ESC in eastern part of Fram Strait was optically different from PW in EGC in western part of Fram Strait and thus likely of different origin. .~~ According to Hancke et al. (2014) the CDOM pool in the Barents Sea was predominantly of marine origin, while several studies show terrestrial CDOM in the PW of EGC (Granskog et al., 2012; Pavlov et al., 2015) ~~; Gonçalves–Araujo et al., 2016)~~ and $a_{CDOM}(350)$ reported for PW in the EGC was significantly higher, by factor 2, than values reported in this study around Svalbard.

CDOM absorption in WSC reported by Pavlov et al. (2015) and our observations enabled to observe significant interannual variability of $a_{CDOM}(350)$ since 2009 until 2015. The year to year changes in average $a_{CDOM}(350)$ may differ in AW as much as 200% (Table 2). We link these changes with intensity of AW transport to the West Spitsbergen Shelf presented as spatially and vertically average salinity and temperature time series (Walczowski et al., 2017). According to this study the average temperature north of 74°N was higher in 2009 than in 2010 that corresponded to ~~observed~~ lower $a_{CDOM}(350)$ ~~observed~~ in 2009 relative to 2010 (Pavlov et al., 2015). Similarly in 2013, with highest CDOM absorption in our observations, the temperature was lower than in 2014 and 2015~~, and that corresponded to highest $a_{CDOM}(350)$ in our data set~~(Walczowski et al., 2017). The average salinity of 35.05

reported in 2014 by Walczowski et al. (2017) was close to record high of 35.08 measured in the period 2000–2016. In 2014 we ~~have~~ observed the lowest $a_{CDOM}(350)$ reported since 2009. ~~The advection of AW into Nordic Seas could effectively lower the CDOM absorption via two mechanisms: firstly the CDOM absorption level in AW is lower than in PW (Granskog et al., 2012), secondly a large volume of AW in WSC blocked the extent of ESC and SC, which lowered the mixing rate between PW and AW, further reducing the CDOM absorption.~~

$S_{300–600}$ varied very little between water masses in a given season (Table 2), thus we assume that average seasonal values are representative for all water masses (Table 3). The largest variation of $S_{300–600}$ (Figure 6, Table 3) was observed in 2014, while the lowest variation of this parameter and a shift towards lower values was observed in 2013 and 2015. Spectral slope coefficient values (19.0±2.7 μm^{-1}) reported by ~~(~~Granskog et al.~~,~~ (2012)~~) were reported~~ for AW across a section in eastern Fram Strait were very similar to those found during AREX2013 and AREX2015 (Table 2). Spectral slopes presented by Granskog et al. (2012), however, were calculated in broader spectral range 300–650 nm, while Hancke et al. (2014) calculated spectral slope coefficient in narrower spectral range of 350–550 nm. Recalculation of the spectral slope coefficient for our data set in the spectral range 300–650 nm, resulted in an average increase of S by <1 μm^{-1} relative to $S_{300–600}$. The spectral slope reported by Hancke et al. (2014) varied between seasons; values in May 2008 (16±4 μm^{-1}) were higher than those observed in~~ in~~ August 2007 (14±4 μm^{-1}) but both were similar with values reported in this study. Although Hancke et al. (2014) calculated spectral slope coefficient for a narrower spectral range resulted consistently in lower spectral slope values by ~2 μm^{-1} their values were within the range of $S_{300–600}$ in the current dataset. In the WSC the $S_{300–600}$ values were higher than those for surface waters north of Svalbard in winter–spring reported by Kowalczuk et al. (2017). Observations reported by Kowalczuk et al. (2017) were conducted earlier in the season and samples were collected below sea ice, so CDOM was less exposed to solar radiation and was potentially less affected by photobleaching. The highest $S_{300–600}$ were found during AREX2014 (20.71±5.26 μm^{-1}), when over 79% samples were classified as AW, what could be associated with photomineralization of DOM in aging sea water (Obernosterer and Benner, 2004).

4.2. Identification of CDOM sources

According to Stedmon and Markager (2001) the non–linear relationship between spectral slope $S_{300–600}$ and $a_{CDOM}(375)$ allows to differentiate between terrestrial (allochthonous) and marine (autochthonous) CDOM pools as well as assess changes in ~~its~~ CDOM composition. This approach was validated by Granskog et al. (2012), who found that CDOM samples taken in PW with high fractions of meteoric water (i.e. river water) in the western part of Fram Strait were outside the Stedmon and Markager (2001) model limits for marine CDOM. Increasing spectral slopes and decreasing CDOM absorption provides information about degradation of autochthonous CDOM originated from marine environment (Stedmon and Markager, 2001; Whitehead and Vernet, 2000). We found decreasing $S_{300–600}$ values with increasing CDOM absorption in all three years (Figure 6). This is similar to that presented by Kowalczuk et al. (2006) in the Baltic Sea and Pavlov et al. (2014~~6~~) in Kongsfjorden, West Spitsbergen.~~the White Sea~~. In our study almost all data points are within the Stedmon and Markager (2001) model limits (Figure 6), and suggests a dominant marine (autochthonous) source of CDOM. The highest $S_{300–600}$ (>25 μm^{-1}) with very low CDOM absorption (<0.075 m^{-1}) suggest a highly degraded CDOM pool in 2014. In contrast, lower values of $S_{300–600}$ (<18 μm^{-1}) with higher absorption (>0.15 m^{-1}) could indicate freshly produced CDOM. Lack of correlation between salinity and $a_{CDOM}(\lambda)$ was found here (not shown) as by Hancke et al. (2014), which further suggests a marine origin of organic matter in the study area.

There were some data points, measured in 2013 characterized by absorption (>0.25 m^{-1}) and spectral slope ~18 μm^{-1} that were outside the upper Stedmon and Markager (2001) model limits. These points could bias the $S_{300–600}$ and $a_{CDOM}(375)$ relationship derived for present data set, and suggest either more terrestrial contribution at high $a_{CDOM}(375)$ from local sources or influence of the Polar Water in the western part of the Fram Strait or recirculating modified AW. Slight increase of humic–like DOM fluorescence (I_{CH1} and I_{CH2}), observed near the south–western Spitsbergen shelf (Figure 4), could indicate a small local contribution from a terrestrial CDOM source.

The presumed molecular structure of marine autochthonous DOM is composed mainly with low molecular weight aliphatic organic compound characterized with low saturation with aromatic rings (Harvey et al., 1983). $SUVA_{254}$ ~~(Eq. 5)~~ defined by Weishaar et al. (2003) is

related ~~with~~ to aromatic ring content within the mixture of water soluble organic DOM. Massicotte et al. (2017) presented the global distribution of $SUVA_{254}$, and found that $SUVA_{254}$ decreased sharply in the aquatic continuum from fresh (4.8 $m^2\ gC^{-1}$) to oceanic waters (1.68 $m^2\ gC^{-1}$). $SUVA_{254}$ also decreases with increasing salinity, rapidly in the salinity range 0–8.7, remained stable in salinity 8.7–26.8 and decreased slowly until salinity reached oceanic values, and further remained at stable level of ca. 1.7 $m^2\ gC^{-1}$ (Massicotte et al., 2017). $SUVA_{254}$ values presented in this study (Table 2) were at the lower end of the global range, close to the oceanic end member values. The highest average $SUVA_{254}$ values were found in PSWw in 2013 (1.95±0.60 $m^2\ gC^{-1}$) and PSW in 2014 and 2015 (1.96±0.63 $m^2\ gC^{-1}$ and 1.99±0.30 $m^2\ gC^{-1}$, respectively) and lowest in PSW (1.31±0.28 $m^2\ gC^{-1}$) and AW (1.41±0.24 $m^2\ gC^{-1}$) in 2013 and 2015, respectively. Pavlov et al. (2016) reported $SUVA_{254}$ values at salinity >34.3 in the southern Barents Sea waters in the range 1.3–1.8 $m^2\ gC^{-1}$, which agree well with our findings. The $SUVA_{254}$ values observed in the Siberian Shelf at salinity >30 varied between 1.25–2.3 $m^2\ gC^{-1}$, (Gonçalves–Araujo et al., 2015). Low $SUVA_{254}$ values suggested, overall low saturation of CDOM with aromatic rings, which supports hypothesis on predominantly autochthonous CDOM origin and minor influence by terrestrial DOM in the Nordic Seas ~~and where~~ , with hydrography dominated by ~~Atlantic waters dominate~~AW inflow.

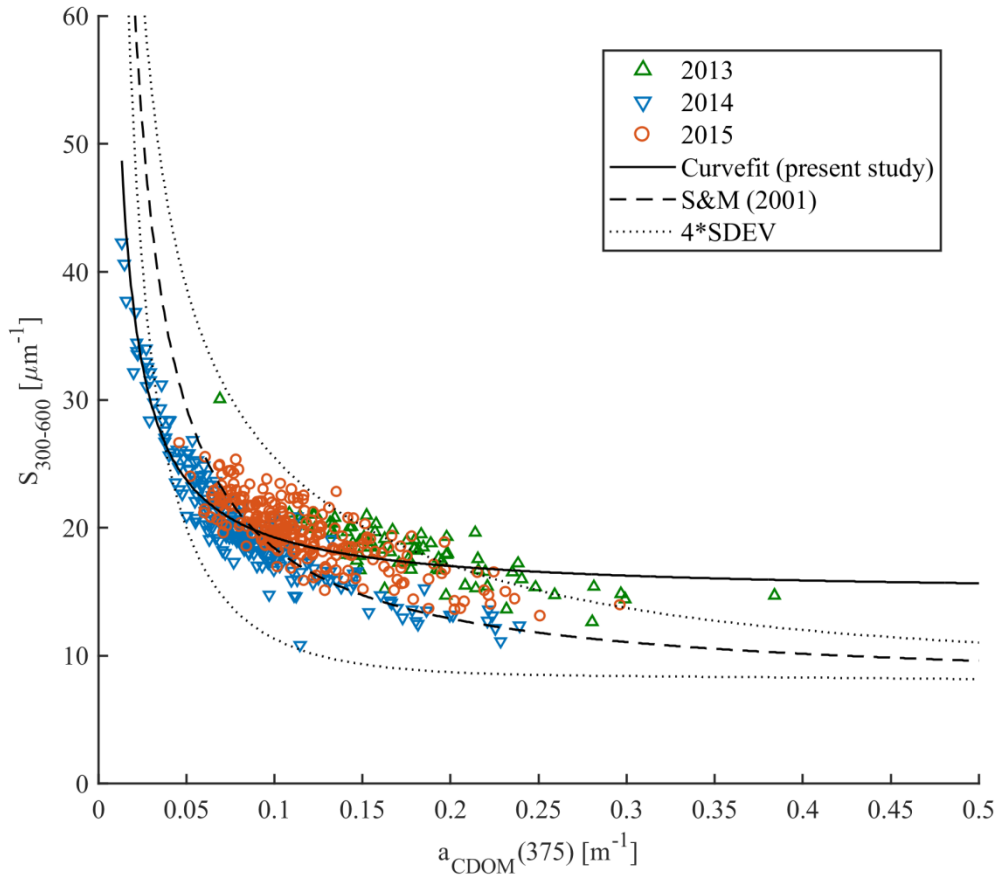

Figure 6: Spectral slope $S_{300–600}$ vs. $a_{CDOM}(375)$ in samples from 2013 (green triangles), 2014 (blue reversed triangles), 2015 (red circles). Stedmon and Markager (2001) model (dashed line) with model limits (±4 standard deviation times the precision of the S–estimate; dotted line) adopted from equation: S=7.4+11/ $a_{CDOM}(375)$. Solid line represents the modeled nonlinear fit for the present study data set.

4.3 Relationship between CDOM absorption and DOC

The significant amount of DOC in the Arctic Ocean ~~is largely~~mainly originates from riverine inflow and permafrost thaw (Stedmon et al., 2011; Amon et al., 2012; Spencer et al., 2015). The riverine input can ~~easily~~ be monitored by optical methods with absorption ~~or,~~ fluorescence or remote sensing measurements (Spencer et al., 2012; Walker et al., 2013; Fichot et al., 2013; Mann et al., 2016). The largest DOC concentrations were found in Siberian rivers: e.g. Lena – 1300 µmol/l, Yenisey – 842 µmol/l, Ob – 950 µmol/l, and was lower in North American Rivers: Yukon – 816 µmol/l and McKenzie – 648 µmol/l (Amon et al., 2012; Mann et al., 2016). Both CDOM and DOC in coastal areas in the Arctic Ocean

show an inverse relationship with salinity (Amon et al., 2012) and very good correlation between CDOM absorption and DOC has been reported for regions influenced by riverine input (Matsuoka et al., 2012; 2013; Gonçalves–Araujo et al., 2015; Pavlov et al., 2016; Mann et al., 2016). The DOC concentration observed by Amon et al. (2003) in the EGC in the western part of Fram Strait and in Denmark Strait was considerably lower and ranged from 76 µmol/l in PSW to 55 µmol/l in AW. Amon et al. (2003) found a weak inverse relationship between DOC and salinity in the Nordic Seas and a weak correlation between DOC and CDOM fluorescence. The DOC concentration reported in this study in AW dominated eastern part of Fram Strait was similar to that reported by Amon et al. (2003) in the EGC, but lower than found in Barents Sea waters entering the White Sea at salinities close to 34.9 (Pavlov et al., 2016). The DOC concentration in open Laptev Sea was over 100 µmol/l as reported by Gonçalves–Araujo et al. (2015). We observed a very weak correlation between DOC concentration and $a_{CDOM}(350)$ (Figure 7). That could be explained ~~that we have had~~by ~~very~~ low ~~representation~~ number of samples influenced by terrestrial humic substances ~~rich in DOC~~ in our data, that have elevated $a_{CDOM}(350)$, DOC and lower salinity. Additionally our data were at the lower range of globally observed distribution of DOC and $a_{CDOM}(350)$, where the relationship is characterized by large uncertainty (Massicotte et al., 2017).

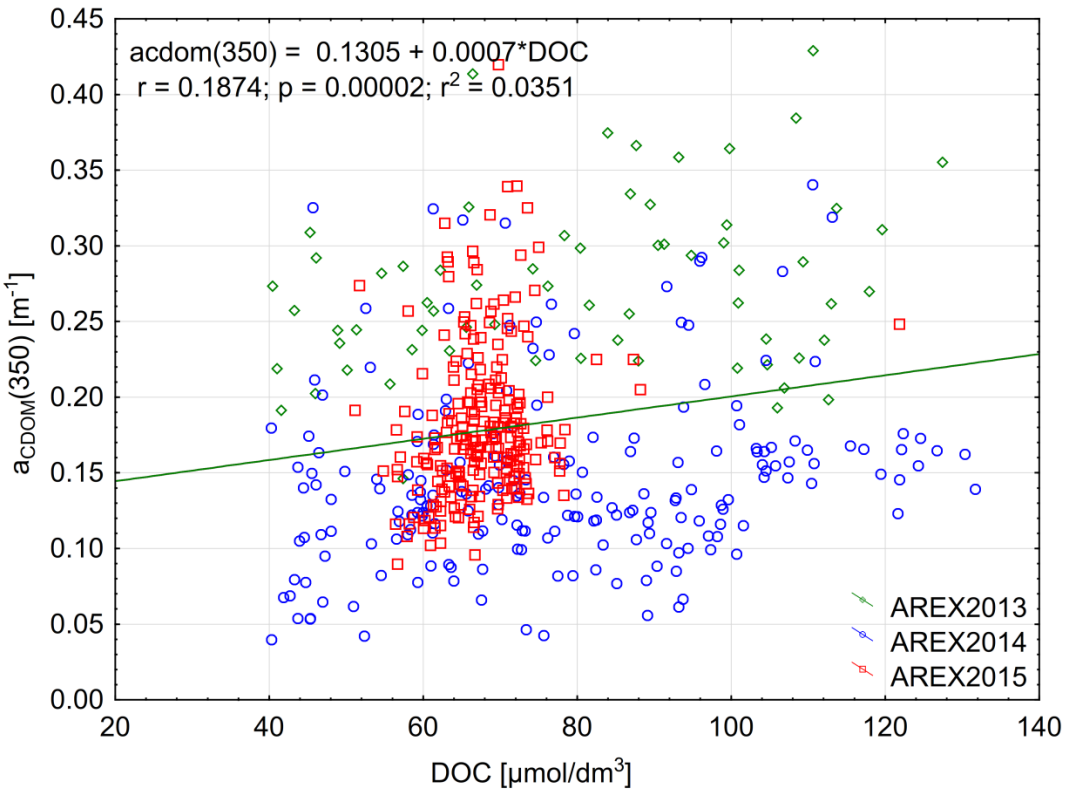

Figure 7. Relationship between $a_{CDOM}(350)$ and DOC and linear relationship between those parameters in 2013–2015.

The relationship between the carbon-specific CDOM absorption coefficient $a^*_{CDOM}(350)$ and $S_{275–295}$ was another approach derived suggested by Fichot and Benner (2011, 2012) in the Gulf of Mexico to recognize trace the influence of terrigenous dissolved organic carbon DOC in coastal margins, and to estimate DOC from optical measurements. We did not observe a significant relationship between $a^*_{CDOM}(350)$ and $S_{275–295}$ (not shown). However, $a^*_{CDOM}(350)$ as a function of $S_{300–600}$ showed much more promise (Figure 8). This could be potentially applied for DOC estimations from CDOM absorption measurements in Nordic Seas.

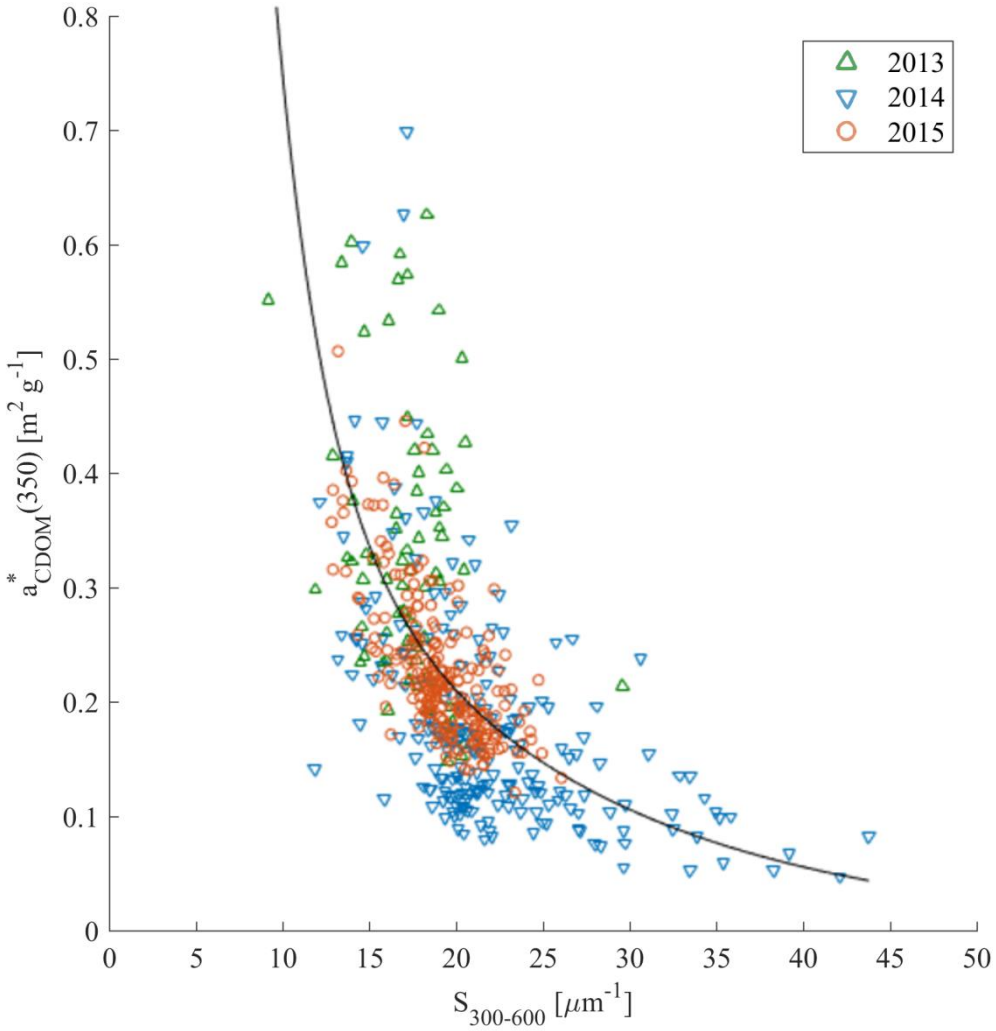

Figure 8. $a^*_{CDOM}(350)$ against $S_{300–600}$ in samples from 2013 (green triangles), 2014 (blue reversed triangles), 2015 (red circles). Non–linear fitting function between those parameters was adopted from Fichot and Benner (2012): $y = e^{(b_1 - b_2 x)} + e^{(b_3 - b_4 x)}$; regression coefficients $b_1 = 0.0027$; $b_2 = 73.31$, $b_3 = 1.29$; $b_4 = -91.39$, were estimated with Matlab curve fitting toolbox, with determination coefficient $R^2 = 0.38$, $n = 525$.

4.4. Distribution of FDOM components in the ocean and their dependence from allochthonous and autochthonous sources

The ~~pattern~~ distribution pattern ~~of fluorescence intensities~~ of main FDOM components with depth in the global oceans' biogeochemical provinces is significantly different ~~The global distribution of different FDOM components identified in water samples revealed significant differences~~ for humic–like and protein–like FDOM (Stedmon and Nelson, 2015, Catalá et al., 2016). The intensity of humic–like FDOM fraction ~~was~~ is usually higher close to continental margins and significantly depleted in the centers of subtropical gyres (Murphy et al., 2008; Jørgensen et al., 2011; Kowalczuk et al., 2013). The fluorescence of humic–like DOM fractions ~~were~~ is low in the surface layer and~~,~~ is rapidly ~~increased~~ increasing with depth reaching a constant high level below 200 m depth. ~~The global pattern of fluorescence intensity of protein–like FDOM distribution across the oceanic biogeochemical provinces and with depths The general trends of fluorescence of protein–like FDOM was opposite compared to humic–like FDOM.~~ Protein–like FDOM fluorescence intensity usually ~~increased~~ increases toward the open ocean and the highest intensity is~~wa~~s observed in the surface waters, rapidly decreasing with depth, reaching constant low level below epipelagic layer (Jørgensen et al., 2011; Kowalczuk et al., 2013; Catalá et al., 2016). Such profiles indicate that amino acid–like DOM is linked to surface water production. Catalá et al. (2016) demonstrated that the global depth distribution tryptophan–like FDOM component has a local maximum associated with a chlorophyll *a* maximum. The linkage between protein–like components with chlorophyll *a* concentration shown qualitatively in the global ocean by Stedmon and Nelson (2015) and Catalá et al. (2016) was ~~usually~~ previously confirmed quantitatively in the mesocosm studies e.g. Romera–Castillo et al. (2010), which ~~documented~~ inicated that phytoplankton ~~–~~ excreted tryptophan like fluorophores, and tryptophan–like components ~~concertation~~ concentration has been related to primary production (Brym et al., 2014). *In situ* quantitative correlation between chlorophyll *a* concentrations and fluorescence intensity of protein–like FDOM fraction has been observed and documented recently. Yamashita et al. (2017) reported

significant positive correlation of tryptophan–like component and *Chla* (r = 0.53, p<0.001) in the surface waters of the Pacific Ocean. Yamashita et al. (2017) found also spatial coupling between the tryptophan–like component and chlorophyll *a* concentration which was strongest in Bering Sea. Study by Loginova et al. (2016) from Peruwian upwelling system also reported positively correlated chlorophyll *a* concentration and protein–like component (R^2 =0 .40, p<0.001).

The distribution of fluorescence intensity of main FDOM components in the Nordic Seas, dominated by warm water of Atlantic origin ~~FDOM in the Arctic Ocean~~ followed the general trends observed globally. The highest FDOM intensity, especially of humic–like components ~~were~~ was observed close to continental margins, in~~at~~ the vicinity of major rivers outflows. Para et al. (2013) observed significant inverse trends of humic–like FDOM components with salinity in the Canadian shelf of the Beaufort Sea close to McKenzie River outflow. Similar observations were documented by Gonçalves–Araujo et al. (2015) in the Lena River delta at Siberian Shelf and by Pavlov at. al. (2016) near the Northern Dvina River outlet in the White Sea. The impact of humic–like FDOM component on DOM composition decreased with increased distance from fresh water sources and increased salinity, where the protein–like FDOM fraction became dominant e.g. outside of McKenzie River plume in Beaufort Sea (Para et al., 2013) and in the White Sea (Pavlov et al., 2016). ~~The PW flowing through the Canadian Arctic Archipelago was enriched with humic–like component compared to Labrador Sea (Guéguen, et al., 2014).~~ In the Fram Strait the distribution of humic–like fluorescence (Ex/Em = 340/420 nm) observed by Amon et al. (2003) in the Fram and Denmark Strait was related to large scale water masses distribution in Nordic Seas and was characterized with elevated values of FDOM intensity in the western part of Fram Strait that was under influence of EGC, and low FDOM intensity and uniformly distributed with depth FDOM intensity in the core of AW in its eastern part. The FDOM distribution in AW shown by Amon et al. (2003) corresponded well ~~with~~ to vertical profiles of I_{CH1} and I_{CH2} in AW, shown on Figure 4. This was also in a good agreement with CDOM distribution in the Fram Strait (Granskog et al., 2012; Pavlov et al., 2015~~; Gonçalves–Araujo et al., 2016~~) and FDOM humic–like fraction (Ex/Em = 280/450 nm) distribution presented by (Granskog et al., 2015b). Humic–like fraction of DOM in the Eastern Fram Strait is more than 10 times lower compared to PW in EGC (Granskog et al., 2015b). A layer of 20 m deep of less saline water diluted by sea–ice melt characterized by significantly lower humic–like FDOM intensity was overlying the PW water with high FDOM intensity in EGC (Granskog et al., 2015b).

In situ fluorometry provided an opportunity to study FDOM distribution in greater detail and commercially available FDOM fluorometers are usually built to detect humic substances (Amon et al., 2003; Belzile et al., 2006; Kowalczuk et al., 2010; Aiken et al., 2011; Loginova et al., 2016). In this study we measured simultaneously three different FDOM components, and the most interesting feature observed with use of this new instrument was very significant spatial coupling between I_{CH3} and I_{FChla}. Similarities in vertical distribution of protein–like FDOM, I_{CH3} and stimulated chlorophyll *a* fluorescence intensity, I_{FChla} and total non–water absorption coefficient at 676 nm, $a_{tot-w}(676)$ implied quantitative interrelation between those parameters and same dominant factor controlling these parameters in time and space. We found a significant positive correlation ($R^2 = 0.65$, $p<0.0001$) between I_{CH3} and I_{FChla} (Figure 5a) which suggests that production of protein–like FDOM is closely related with spatial and temporal phytoplankton dynamics. Additionally a statistically significant dependence of I_{CH3} and *Chla* concentration from water samples indicated that phytoplankton biomass is an important source of protein–like FDOM. ~~Our findings are in agreement with studies that proposed FDOM/CDOM production is tightly coupled with to phytoplankton extracellular release (Romera–Castillo et al., 2010) or by phytoplankton degradation or lysis (Hur et al., 2006; Organelli et al., 2014).~~

5. Conclusions

We observed significant interannual variation of CDOM optical properties in the Nordic Seas. It is likely that ~~those~~ these year to year changes in CDOM absorption coefficient and spectral slope coefficient were related to intensity of AW inflow to Nordic Seas. According to Walczowski et al. (2017) there was very strong interannual variability in AW inflow overlaid on the long–term increasing trend. CDOM absorption decreased and spectral slope coefficient increased during years when increase of temperature was observed for Atlantic Waters (AW) (Walczowski et al., 2017), e.g. in 2009 (Pavlov et al., 2015) and in 2014 (this study). Decrease of AW temperature was accompanied by mutual increase of $a_{CDOM}(350)$ and decrease of $S_{300–600}$, e.g.: in 2010 (Pavlov et al., 2015) and in 2013 and 2015 (this study). We surmise that during less intense inflow of AW to Nordic Seas a higher proportion of PW is transported with ESC and SC to eastern part of Fram Strait contributing to increase of CDOM in West Spitsbergen Shelf waters.

In situ observations with use of a 3–channel fluorometer coupled with other optical instruments enabled to show a significant correlation between protein–like FDOM and

chlorophyll *a* in the Nordic Seas. ~~*In situ* fluorometric measurements also showed very tight spatial coupling between phytoplankton distribution and increased concentrations of protein–like FDOM fractions.~~ Quantitative dependence between protein–like FDOM (I_{CH3}) and chlorophyll *a* fluorescence (I_{FChla}) and between protein–like FDOM (I_{CH3}) and total non–water absorption coefficient at 676 nm ($a_{tot-w}(676)$) based on direct *in situ* observations clearly indicated that phytoplankton biomass is the primary source of low molecular weight DOM fraction in Nordic Seas influenced by warm Atlantic waters. ~~That~~ This ~~highlighted~~ highlights the role of phytoplankton dynamics ~~as~~ as an important factor controlling FDOM/CDOM ~~controlling factor~~. Freshly produced protein–like FDOM fraction did not contribute to CDOM/FDOM optical properties observed in visible spectral range as its fluorescence excitation (absorption) and emission characteristics were located in the ultraviolet spectral range. Observed variability of spectral indices ($a^*_{CDOM}(350)$, $SUVA_{254}$, $S_{300-600}$) values ~~supported conclusions~~suggest that CDOM/FDOM in the Nordic Seas has an autochthonous origin. Yet, further investigation of the DOM transformations processes from labile freshly produced protein–like DOM fractions to more complex organic molecules ~~remained~~ is needed to better understand the CDOM/FDOM dynamics in the Nordic Seas. ~~In general~~Typically humic–like FDOM was found in low concentrations in the study area, showcasing the limited terrestrial influence, in contrast to e.g. the East Greenland Current (Gonçalves–Araujo et al., 2016).

Dissolved organic carbon (DOC) was weakly correlated with $a_{CDOM}(350)$ in the study area, likely due to limited terrestrial influence, and $a_{CDOM}(350)$ shows no promise to be used as a tool to predict DOC. The same was the case for spectral slope at short wavelengths ($S_{275-295}$), proven earlier to work for near–shore environs (Fichot and Benner, 2011, 2012). On the other hand there was a significant inverse non–linear relationship of CDOM specific DOC absorption ($a^*_{CDOM}(350)$) with spectral slope at a broader spectral range ($S_{300-600}$). This relationship provides a potential for indirect estimates of DOC with use of optical measurements in this region.

Acknowledgements: We thank the crew of RV Oceania and colleagues for the help onboard. This work was supported by the Polish–Norwegian Research Programme operated by the National Centre for Research and Development under the Norwegian Financial Mechanism 2009–2014 in the frame of Project Contract Pol–Nor/197511/40/2013, CDOM–HEAT. This work was partially financed from the funds of the Leading National Research Centre

(KNOW) received by the Centre for Polar Studies for the period 2014–2018. MAG was supported by the Centre for Ice, Climate and Ecosystems (ICE) at the Norwegian Polar Institute, and AKP by the Research Council of Norway through the STASIS project (221961/F20).

References

Aas, E. and Høkedal, J.: Penetration of ultraviolet B, blue and quanta irradiance into Svalbard waters, Polar Research, 15(2), 127–138, doi:10.1111/j.1751-8369.1996.tb00464.x, 1996.

Aiken, C. R. M., Petersen, W., Schroeder, F., Gehrung, M., and Ramirez von Holle, P. A.: Ship–of–Opportunity Monitoring of the Chilean Fjords Using the Pocket FerryBox, Journal of Atmospheric and Oceanic Technology, 28, 1338–1350, 2011.

Amon, R. M. W., Budéus, G., and Meon, B.: Dissolved organic carbon distribution and origin in the Nordic Seas: Exchanges with the Arctic Ocean and the North Atlantic, J. Geophys. Res., 108(C7), 3221, doi:10.1029/2002JC001594, 2003.

Amon, R.M.W.: The Role of Dissolved Organic Matter for the Organic Carbon Cycle. the Arctic Ocean, [in:] The organic carbon cycle in the Arctic Ocean, Stein, R., and Macdonald, R. W. (Eds.) Springer, Berlin, Heidelberg Chapter 4, 82-99, 2004.

Amon, R. M. W., Rinehart, A. J., Duan, S., Louchouarn, P., Prokushkin, A., Guggenberger, G., Bauch, D., Stedmon, C. A., Raymond, P. A., Holmes, R .M., McClelland, J. W., Peterson, B. J., Walker, S. A., Zhulidov, A. V.: Dissolved organic matter sources in large Arctic rivers, Geochimica et Cosmochimica Acta, 94, 217–237, doi: 10.1016/j.gca.2012.07.015, 2012.

Anderson and Amon: DOM in the Arctic Ocean. [in:] Biogeochemistry of Marine Dissolved Organic Matter, D. A. Hansell, D. A., and Carlson, C. A. (eds), 609–633, 2015.

Arrigo K. and C. Brown: Impact of chromophoric dissolved organic matter on UV inhibition of primary productivity in the sea. Marine Ecology Progress Series, 140, 207-2016, 1996.

Arrigo, K. R., van Dijken, G., and Pabi, S.: Impact of a shrinking Arctic ice cover on marine primary production, Geophys. Res. Lett., 35(19), doi:10.1029/2008GL035028, 2008.

Belzile C., Roesler, C. S., Christensen, J. P., Shakhova, N., and Semiletov, I.: Fluorescence measured using the WETStar DOM fluorometer as a proxy for dissolved matter absorption, Estuar. Coast. Shelf Sci., 67(3), 441–449, 2006.

Bélanger, S., Cizmeli, S. A., Ehn, J., Matsuoka, A., Doxaran, D., Hooker, S., and Babin, M.: Light absorption and partitioning in Arctic Ocean surface waters: Impact of multiyear ice melting, Biogeosciences, 10, 6433-6452, doi:10.5194/bg-10-6433-2013, 2013.

Brym, A., Paerl, H. W., Montgomery, M. T., Handsel, L. T., Ziervogel, K., and Osburn, C. L.: Optical and chemical characterization of base-extracted particulate organic matter in coastal marine environments, Marine Chemistry, 162, 96-113. doi: 10.1016/j.marchem.2014.03.006, 2014.

Catalá, T. S., Álvarez-Salgado, X. A., Otero, J., Iuculano, F., Companys, B., Horstkotte, B., Romera-Castillo, C., Nieto-Cid, M., Latasa, M., Morán, X. A. G., Gasol, J. M., Marrasé, C., Stedmon, C. A. and Reche, I.: Drivers of fluorescent dissolved organic matter in the global epipelagic ocean. Limnol. Oceanogr., 61(3), 1101–1119. doi:10.1002/lno.10281, 2016.

916 Coble, P. G.: Characterization of marine and terrestrial DOM in seawater using excitation–
917 emission matrix spectroscopy, Mar. Chem., 51(4), 325–346, 1996.
918 Coble, P. G.: Marine optical biogeochemistry: The chemistry of ocean color, Chem. Rev.,
919 107(2), 402-418, doi:10.1021/cr050350+, 2007.
920 Cullen, J. J.: The Deep Chlorophyll Maximum: Comparing Vertical Profiles of Chlorophyll a,
921 Canadian Journal of Fisheries and Aquatic Sciences, 39(5), 791–803, 1982.
922 Dalpadado, P., Arrigo, K.R., Hjøllo, S.S., Rey, F., Ingvaldsen, R.B., Sperfeld, E., van Dijken,
923 G.L., Stige, L.C., Olsen, A. and Ottersen, G. Productivity in the Barents Sea-response to
924 recent climate variability. PloS one, 9(5), p.e95273, 2014.
925 Erickson III, D.J., Sulzberger, B., Zepp, R.G. and Austin, A.T.: Effects of stratospheric ozone
926 depletion, solar UV radiation, and climate change on biogeochemical cycling:
927 interactions and feedbacks, Photochemical and Photobiological Sciences, 14(1),127–
928 148, 2015.
929 Fichot C. G. and Benner, R.: A novel method to estimate DOC concentrations from CDOM
930 absorption coefficients in coastal waters, Geophys. Res. Lett., 38, L03610,
931 doi:10.1029/2010GL046152, 2011.
932 Fichot C. G. and Benner, R.: The spectral slope coefficient of chromophoric dissolved organic
933 matter (S275–295) as a tracer of terrigenous dissolved organic carbon in river–
934 influenced ocean margins, Limnology and Oceanography, 57, doi:
935 10.4319/lo.2012.57.5.1453, 2012.
936 Fichot, C. G., K. Kaiser, S. B. Hooker, R. M. W. Amon, M. Babi, S. Bélanger, S. A. Walker,
937 and R. Benner. Pan-Arctic distributions of continental runoff in the Arctic Ocean. ,
938 Scientific Reports, 3: 1053, DOI: 10.1038/srep01053, 2013.
939 Findlay, H.S., Gibson, G., Kędra, M., Morata, N., Orchowska, M., Pavlov, A.K., Reigstad,
940 M., Silyakova, A., Tremblay, J.É., Walczowski, W., and Weydmann, A.: Responses in
941 Arctic marine carbon cycle processes: conceptual scenarios and implications for
942 ecosystem function. Polar Research, 34(1), 24252, 2015.
943 Granskog, M.A., Macdonald, R.W., Mundy, C. J., Barber, D.G.: Distribution, characteristics
944 and potential impacts of chromophoric dissolved organic matter (CDOM) in the Hudson
945 Strait and the Hudson Bay, Canada, Cont. Shelf Res., 27(15), doi:
946 10.1016/j.csr.2007.05.001, 2007.
947 Granskog, M. A., Stedmon, C. A., Dodd, P. A., Amon, R. M., Pavlov, A. K., Steur, L., and
948 Hansen, E.: Characteristics of colored dissolved organic matter (CDOM) in the Arctic
949 outflow in the Fram Strait: Assessing the changes and fate of terrigenous CDOM in the
950 Arctic Ocean, J. Geophys. Res., 117, C12021, doi:10.1029/2012JC008075, 2012.
951 Granskog, M. A., Nomura, D., Müller, S., Krell, A., Toyota, T., & Hattori, H.: Evidence for
952 significant protein-like dissolved organic matter accumulation in Sea of Okhotsk sea
953 ice. *Annals of Glaciology*, *56*(69), 1–8. https://doi.org/10.3189/2015AoG69A002,
954 2015a.
955 Granskog, M. A., Pavlov, A. K.,Sagan, S., Kowalczuk, P., Raczkowska, A., and Stedmon, C.
956 A.: Effect of sea–ice melt on inherent optical properties and vertical distribution of solar
957 radiant heating in Arctic surface waters, J. Geophys. Res., Oceans, 120, 7028–7039,
958 doi:10.1002/ 2015JC011087, 2015b.
959 Gonçalves–Araujo, R, Stedmon, C. A., Heim, B., Dubinenkov, I., Kraberg, A., Moiseev, D.,
960 and Bracher, A.: From Fresh to Marine Waters: Characterization and Fate of Dissolved
961 Organic Matter in the Lena River Delta Region, Siberia, Front. Mar.Sci., 2(108), doi:
962 10.3389/fmars.2015.00108, 2015.

Gonçalves–Araujo, R., Granskog, M. A., Bracher, A., Azetsu–Scott, K., Dodd, P. A., and Stedmon, C. A.: Using fluorescent dissolved organic matter to trace and distinguish the origin of Arctic surface waters. Scientific Reports, 6, 1–12. doi:10.1038/srep33978, 2016.

~~Guéguen, C., Cuss, C. W., Cassels, C. J., and Carmack, E. C.: Absorption and fluorescence of dissolved organic matter in the waters of the Canadian Arctic Archipelago, Baffin Bay and the Labrador Sea, J. Geophys. Res. Oceans, 119(3), 2034–2047, doi:10.1002/2013JC009173, 2014.~~

Hancke, K., Hovland, E. K., Volent, Z., Pettersen, R., Johnsen, G., Moline, M., and Sakshaug, E.:Optical properties of CDOM across the Polar Front in the Barents Sea: Origin, distribution and significance, Journal of Marine Systems, 130, 219–227, 2014.

Harvey, G. R., Boran, D. A., Chesal, L. A., and Tokar, J. M.: The structure of marine fulvic and humic acids, Marine Chemistry, 12, 119–132, 1983.

Hill, V.: Impacts of chromophoric dissolved organic material on surface ocean heating in the Chukchi Sea, J. Geophys. Res., Oceans 113, C07024, doi:10.1029/2007JC004119, 2008.

~~Hur, J., Williams, M. A., and Schlautman, M. A.: Evaluating spectroscopic and chromatographic techniques to resolve dissolved organic matter via end member mixing analysis, Chemosphere, 63, 387–402, 2006.~~

Jørgensen, L., Stedmon, C. A., T. Kragh, T., Markager, S., Middelboe, M., and Søndergaard, M.: Global trends in the fluorescence characteristics and distribution of marine dissolved organic matter, Marine Chemistry, 126. 139–148, 2011.

Jørgensen, L., Stedmon, C. A., Granskog, M. A. & Middelboe, M. Tracing the long-term microbial production of recalcitrant fluorescent dissolved organic matter in seawater. Geophys. Res. Lett. 41, 2481–2488, 2014.

Kitidis, V., Stubbins, A.P., Uher, G., Goddard, R.C.U., Law, C.S. and Woodward, E.M.S.: Variability of chromophoric organic matter in surface waters of the Atlantic Ocean, Deep Sea Research Part II: Topical Studies in Oceanography, 53(14), 1666–1684, 2006.

Kieber, D.J., Peake, B.M., Scully, N.M.: Reactive oxygen species in aquatic ecosystems. In: Helbling, E.W., Zagarese, H. (Eds.), UV Effects in Aquatic Organisms. Royal Society of Chemistry, Cambridge, pp. 251– 288, 2003.

Kowalczuk, P., Stedmon, C. A., and Markager, S.: Modelling absorption by CDOM in the Baltic Sea from season, salinity and chlorophyll, Marine Chemistry, 101, 1–11. .2006.

Kowalczuk P., Zabłocka, M., Sagan, S., and Kuliński, K.: Fluorescence measured in situ as a proxy of CDOM absorption and DOC concentration in the Baltic Sea, Oceanologia, 52(3), 431–471, 2010.

Kowalczuk P., Tilstone, G. H., Zabłocka, M., Röttgers, R., and Thomas, R.: Composition of Dissolved Organic Matter along an Atlantic Meridional Transect from fluorescence spectroscopy and Parallel Factor Analysis, Marine Chemistry, 157, 170–184, 2013.

Kowalczuk, P., Meler, J., Kauko, H., Pavlov, A. K., Zabłocka, M., Peeken, I., Dybwad, C., Castellani, G., and Granskog, M. A.: Bio–optical properties of Arctic drift ice and surface waters north of Svalbard from winter to spring. Journal of Geophysical Research–Oceans, 122(6), 4634–466, 2017.

Loeng, H.: Features of the physical oceanographic conditions of the Barents Sea, Polar Res., 10, 5–18. 1991.

Loginova, A. N., Thomsen, S., and Engel, A.: Chromophoric and fluorescent dissolved organic matter in and above the oxygen minimum zone off Peru, J. Geophys. Res. Oceans, 121, 7973–7990, doi:10.1002/2016JC011906, 2016.

Lund-Hansen, L. C., Markager, S., Hancke, K., Stratmann, T., Rysgaard, S., Ramløv, H., and Sorrell, B. K.: Effects of sea-ice light attenuation and CDOM absorption in the water below the Eurasian sector of central Arctic Ocean (>88°N), Polar Res. 34(1), 23978, doi: 10.3402/polar.v34.23978, 2015.

Mann, P. J., Spencer, R. G. M., Hernes, P. J., Six, J., Aiken, G. R., Tank, S. E., McClelland, J. W., Butler, K. D., Dyda, R. Y., and Holmes, R. M.: Pan–Arctic Trends in Terrestrial Dissolved Organic Matter from Optical Measurements, Frontiers in Earth Science, 4(25), doi:10.3389/feart.2016.00025, 2016.

Matsuoka A., Hill, V., Huot, Y., Babin, M., and Bricaud, A.: Seasonal variability in the light absorption properties of western Arctic waters: Parameterization of the individual components of absorption for ocean color applications, J. Geophys. Res., Oceans, 116, C02007, doi:10.1029/2009JC005594, 2011.

Matsuoka, A., Bricaud, A., Benner, R., Para, J., Sempéré, R., Prieur, L., Bélanger, S., and Babin, M.: Tracing the transport of colored dissolved organic matter in water masses of the Southern Beaufort Sea: relationship with hydrographic characteristics, Biogeosciences, 9, 925–940, 2012.

Matsuoka, A., Hooker, S. B., Bricaud, A., Gentili, B., and Babin, M.: Estimating absorption coefficients of colored dissolved organic matter (CDOM) using a semi–analytical algorithm for southern Beaufort Sea waters: application to deriving concentrations of dissolved organic carbon from space, Biogeosciences, 10, 917–927, 2013.

Matsuoka, A., Boss, E., Babin, M., Karp–Boss, L., Hafezd, M., Chekalyuk, A., Proctore, C. W., Werdell, P. J., Bricaud, A.: Pan–Arctic optical characteristics of colored dissolved organic matter: Tracing dissolved organic carbon in changing Arctic waters using satellite ocean color data, Remote Sensing of Environment, 200, 89–101, 2017.

Massicotte, P., Asmala, E., Stedmon C. A., and Markager, S.: Global distribution of dissolved organic matter along the aquatic continuum: Across rivers, lakes and oceans, Science of the Total Environment, 609, 180–191, doi:10.1016/j.scitotenv.2017.07.076, 2017.

Meier, W. N., et al.: Arctic sea ice in transformation: A review of recent observed changes and impacts on biology and human activity, Rev. Geophys., *52*, 185–217, doi:10.1002/2013RG000431, 2014.

Meler, J., Kowalczuk, P., Ostrowska, M., Ficek, D., Zabłocka, M., and Zdun, A.: Parameterization of the light absorption properties of chromophoric dissolved organic matter in the Baltic Sea and Pomeranian lakes, Ocean Sci., 12, 1013–1032, https://doi.org/10.5194/os-12-1013-2016, 2016.

Mopper, K., Kieber, D.J.: Photochemistry and the cycling of carbon, sulfur, nitrogen and phosphorus. In: Hansell, D.A., Carlson, C.A. (Eds.), Biogeochemistry of Marine Dissolved Organic Matter. Academic Press, New York, pp. 455– 507, 2002.

Murphy. K. R., Stedmon, C. A., Waite, T. D.,and Ruiz, G. M.: Distinguishing between terrestrial and autochthonous organic matter sources in marine environments using fluorescence spectroscopy, Marine Chemistry, 108, 40–58, 2008.

Murphy, K. R., Stedmon, C. A., Graeber, D., and Bro, R.: Fluorescence spectroscopy and multi–way techniques. PARAFAC, Analytical Methods, 5, 6557, doi:10.1039/c3ay41160e, 2013.

Murphy, K. R., Stedmon, C. A., Wenig, P., and Bro, R.: OpenFluor–an online spectral library of auto–fluorescence by organic compounds in the environment, Analytical Methods, 6, 658–661, doi:10.1039/C3AY41935E, 2014.

Nelson, N. B. and Siegel, D. A.:The Global Distribution and Dynamics of Chromophoric Dissolved Organic Matter, Annual Review of Marine Science, 5, 447–476, doi:10.1146/annurev-marine-120710-100751, 2013.

Nilsen F., Skogseth, R., Vaardal–Lunde, J., Inall, M.: A Simple Shelf Circulation Model: Intrusion of Atlantic Water on the West Spitsbergen Shelf, American Meteorological Society, doi:10.1175/JPO-D-15-0058.1, 2015.

Nima, C., Frette, Ø., Hamre, B., Erga, S.R., Chen, Y.-C., Zhao, L., Sørensen, K., Norli, M., Stamnes, K., Stamnes, J.J.: Absorption properties of high-latitude Norwegian coastal water: the impact of CDOM and particulate matter, Estuar. Coast. Shelf Sci., 178, 158—167, http://dx.doi.org/10.1016/j.ecss.2016.05.012, 2016.

Obernosterer, I. and Benner, R.: Competition between biological and photochemical processes in the mineralization of dissolved organic carbon, Limnol. Oceanogr., 49, 117–124, 2004.

Olsen, E., Aanes, S., Mehl, S., Holst, J.C., Aglen, A. and Gjøsæter, H. Cod, haddock, saithe, herring, and capelin in the Barents Sea and adjacent waters: a review of the biological value of the area. ICES Journal of Marine Science, 67(1), pp.87-101, 2009.

~~Organelli E., Bricaud A., Antoine D., and Matsuoka A.,: Seasonal dynamics of light absorption by chromophoric dissolved organic matter (CDOM) in the NW Mediterranean Sea (BOUSSOLE site), Deep Sea Research I, 91, 72–85, doi: http://dx.doi.org/10.1016/j.dsr.2014.05.003, 2014.~~

Osburn, C.L., Retamal, L. and Vincent, W.F. Photoreactivity of chromophoric dissolved organic matter transported by the Mackenzie River to the Beaufort Sea, Marine Chemistry, 115(1), 10–20, 2009.

Para, J., Charriere, B., Matsuoka, A., Miller, W. L., Rontani, J. F., and Sempéré, R.: UV/PAR radiation and DOM properties in surface coastal waters of the Canadian shelf of the Beaufort Sea during summer 2009, Biogeosciences, 10, 2761–2774, 2013.

Pavlov, A.K., Silyakova, A., Granskog, M.A., Bellerby, R.G., Engel, A., Schulz, K.G. and Brussaard, C.P.: Marine CDOM accumulation during a coastal Arctic mesocosm experiment: No response to elevated pCO2 levels, Journal of Geophysical Research: Biogeosciences, 119(6), 1216-1230, doi:10.1002/2013JG002587, 2014.

Pavlov, A. K., Granskog, M. A., Stedmon, C. A., Ivanov, B. V., Hudson, S. R., and Falk–Petersen, S.: Contrasting optical properties of surface waters across the Fram Strait and its potential biological implications, J. Mar. Syst., 143, 62–72, doi:10.1016/j.jmarsys.2014.11.001, 2015.

Pavlov, A. K., Stedmon, C. A., Semushin, A. V., Martma, T., Ivanov, B. V., Kowalczuk, P., and Granskog, M. A.: Linkages between the circulation and distribution of dissolved organic matter in the White Sea, Arctic Ocean, Continental Shelf Research, 119, 1–13, doi:10.1016/j.csr.2016.03.004, 2016.

Pavlov, A.K., Taskjelle, T., Kauko, H.M., Hamre, B., Hudson, S.R., Assmy, P., Duarte, P., Fernández-Méndez, M., Mundy, C.J. and Granskog, M.A.: Altered inherent optical properties and estimates of the underwater light field during an Arctic under ice bloom of Phaeocystis pouchetii, J. Geophys. R.: Oceans, 122, 4939–4961, doi: 10.1002/2016JC012471, 2017.

Pegau,W. S.: Inherent optical properties of the central Arctic surface waters, J.Geophys. Res., 107(C10), 8035, doi:10.1029/2000JC000382, 2002.

Polyakov, I.V., Pnyushkov, A.V., Alkire, M.B., Ashik, I.M., Baumann, T.M., Carmack, E.C., Goszczko, I., Guthrie, J., Ivanov, V.V., Kanzow, T. and Krishfield, R.: Greater role for Atlantic inflows on sea–ice loss in the Eurasian Basin of the Arctic Ocean, Science, 356(6335), 285–291, 2017.

Prowse, T., Bring, A., Mård, J., Carmack, E.,Holland, MInstanes, A., Vihma, T., and Wrona, F. J.: Arctic Freshwater Synthesis: Summary of key emerging issues, Journal of Geophysical Research: Biogeosciences, 120(10), 1887–1893, doi:10.1002/2015JG003128, 2015.

Retelletti-Brogi, S., S-Y. Ha, K. Kim, M. Derrien, Y.K. Lee, and J. Hur,: Optical and molecular characterization of dissolved organic matter (DOM) in the Arctic ice core and the underlying seawater (Cambridge Bay, Canada): Implication for increased autochthonous DOM during ice melting. Science of the Total Environment 627, 802–811, 2018.

Roesler, C. S. and Barnard A. H.: Optical proxy for phytoplankton biomass in the absence of photophysiology: Rethinking the absorption line height, Methods Oceanogr, 7, 79–94. doi:10.1016/j.mio.2013.12.003, 2013.

Romera-Castillo, C., Sarmento, H., Álvarez-Salgado, X.A., Gasol, J.M., Marrasé, C.: Production of chromophoric dissolved organic matter by marine phytoplankton, Limnol. Oceanogr, 55 (1), 446–454, 2010.

Rudels, B., Friedrich, H.J., and Quadfasel, D.: The arctic circumpolar boundary current, Deep–Sea Res., II 46, 1023– 1062, 1999.

Rudels, B., Fahrbach, E., Meincke, J., Bude´us, G., Eriksson,P.: The East Greenland Current and its contribution to the Denmark Strait Overflow. ICES J. Mar. Sci. 59,1133– 1154, 2002.

Rudels, B, Björk, G, Nilsson, J, Winsor, P, Lake, I & Nohr, C.: The interaction between waters from the Arctic Ocean and the Nordic Seas north of Fram Strait and along the East Greenland Current: results from the Arctic Ocean–02 Oden expedition, Journal of Marine Systems, 55(1–2), 1–30. doi:10.1016/j.jmarsys.2004.06.008, 2005.

Sagan, S., Kowalczuk, P., Makarewicz, A., Meler, J., Borzycka, K., Zabłocka, M., Konik, M., and Zdun, A..: Bio–optical properties of West Spitsbergen Shelf waters, 2017, *in preparation*

Schlichtholz, P. and Houssais, M.–N.: An investigation of the dynamics of the East Greenland Current in Fram Strait based on a simple analytical model, Journal of Physical Oceanography, 29, 2240–2265, 1999a.

Schlichtholz, P. and Houssais, M.–N.: An inverse modeling study in Fram Strait. Part II: Water mass distribution and transports, Deep–Sea Research, II, 46, 11367–1168, 1999b.

Schlichtholz, P. and Houssais, M.–N.: An overview of the q-S correlations in Fram Strait based n the MIZEX 84 data, Oceanologia, 44 (2), 243–272, 2002.

Sharp, J.H.: Analytical methods for total DOM pools, in: Hansell, D.A. et al. (Ed.), Biogeochemistry of marine dissolved organic matter,35–58, In: Hansell, D.A.; Carlson, C.A. (Ed.),Biogeochemistry of marine dissolved organic matter, Academic Press: San Diego, XXII, 774, 2002.

Skogen, M.D., Budgell, W.P. and Rey, F. Interannual variability in Nordic seas primary production. ICES Journal of Marine Science, 64(5), 889-898, 2007.

Spencer, R. G. M., Butler, K. D., and Aiken, G. R.:Dissolved organic carbon and chromophoric dissolved organic matter properties of rivers in the USA, J. Geophys. Res., 117, G03001, doi:10.1029/2011JG001928, 2012.

Spencer, R. G. M., Mann, P. J., Dittmar, T., Eglinton, T. I., McIntyre, C., Holmes, R. M., Zimov, N., and Stubbins, A.: Detecting the signature of permafrost thaw in Arctic rivers. Geophys. Res. Lett., 42, doi:10.1002/2015GL063498, 2015.

Stedmon C. and Markager, S.: The optics of chromophoric dissolved organic matter (CDOM) in the Greenland Sea: An algorithm for differentiation between marine and terrestrially derived organic matter, Limnol. Oceanogr., 46(8), 2087–2, 2001.

Stedmon C. A. and Nelson, N. B.: The Optical Properties of DOM in the Ocean. in: Biogeochemistry of Marine Dissolved Organic Matter, D. A. Hansell, D. A., and Carlson, C. A. (eds), 480–508, 2015.

Stedmon, C. A., Markager, S., and Kaas. H.: Optical properties and signatures of chromophoric dissolved organic matter (CDOM) in Danish coastal waters, Estuarine, Coastal and Shelf Science, 51, 267–278, 2000.

Stedmon C. A., Markager S., and Bro, R.: Tracing dissolved organic matter in aquatic environments using a new approach to fluorescence spectroscopy, Marine Chemistry, 82(3–4), 239–254. Available from: 10.1016/S0304-4203(03)00072-0093, 2003.

Stedmon, C. A., Amon, R. M. W., Rinehart, A. J., and Walker, S. A.: The supply and characteristics of colored dissolved organic matter (CDOM) in the Arctic Ocean: Pan Arctic trends and differences, Marine Chemistry, 124, 108–118, 2011.

Stedmon C. A., Granskog, M.A., and Dodd, P. A.: An approach to estimate the freshwater contribution from glacial melt and precipitation in East Greenland shelf waters using colored dissolved organic matter (CDOM). J. Geophys. Res.: Oceans, 120 (2), 1107-1117, doi.org/10.1002/2014JC010501, 2015.

Stein, R. and Macdonald, R.W., Organic carbon budget: Arctic Ocean vs. global ocean: in: The organic carbon cycle in the Arctic Ocean, 315–322, Springer, Berlin Heidelberg, 2004.

Sternal, B., Szczucinski, W., Forwick, M., Zajączkowski, M., Lorenc, S., and Przytarska, J.: Postglacial variability in near–bottom current speed on the Continental shelf off south–west Spitsbergen, J. Quaternary Sci., 29, 767–777, 2014.

Stramska, M., Stramski, D., Hapter, R., Kaczmarek S., and Stoń, J.: Bio–optical relationships and ocean color algorithms for the north polar region of the Atlantic, J. Geophys. Res., 108(C5), 3143, doi:10.1029/2001JC001195, 2003.

Strickland J. D. H. and Parsons, T. R.: A practical handbook of seawater analysis, Second Edition, Bulletin 167, Fisheries Research Board of Canada, Ottawa, 1972.

Swift, J. H. and Aagaard, K.: Seasonal transitions and water mass formation in the Iceland and Greenland seas, Deep–Sea Res., 28A: 1107–1129, 1981.

Walczowski W.: Atlantic Water in the Nordic Seas, Springer, Heidelberg, New York, London,300, 2014.

Walczowski W., Beszczynska–Möller, A., Wieczorek, P., Merchel, M., and Grynczel, A.: Oceanographic observations in the Nordic Sea and Fram Strait in 2016 under the IOPAN long–term monitoring program AREX, Oceanologia, 59(2), 187–194, doi:10.1016/j.oceano.2016.12.003, 2017.

Walker, S. A., R. M. W. Amon, and C. A. Stedmon: Variations in high-latitude riverine fluorescent dissolved organic matter: A comparison of large Arctic rivers, Journal of

Geophysical Research Biogeoscience, 118, 1689–1702, doi:10.1002/2013JG002320, 2013.

Weishaar, J.L., Aiken, G.R., Bergamaschi, B.A., Fram, M.S., Fujii, R., Mopper, K.: Evaluation of specific ultraviolet absorbance as an indicator of the chemical composition and reactivity of dissolved organic matter, Environ. Sci. Technol., 37, 4702–4708, 2003.

Whitehead, K. and Vernet, M.: Influence of mycosporine–like amino acids (MAAs) on UV absorption by particulate and dissolved organic matter in La Jolla Bay, Limnology and Oceanography, 45(8), 1788–1796, 2000.

Yamashita, Y., Hashihama, F., Saito, H., Fukuda, H., and Ogawa, H.: Factors controlling the geographical distribution of fluorescent dissolved organic matter in the surface waters of the Pacific Ocean. Limnology and Oceanography, 62 (6), 2360-2374, doi: 10.1002/lno.10570, 2017.

Zaneveld, J. R. V., Kitchen, J. C., and Moore C.: The scattering error correction of reflecting–tube absorption meters, Proc. SPIE Soc. Opt. Eng., 2258, 44–55, 1994.

Zepp, R.G.: Solar ultraviolet radiation and aquatic biogeochemical cycles. In: Helbling, E.W., Zagarese, H. (Eds.), UV Effects in Aquatic Organisms and Ecosystems, vol. 1. The Royal Society of Chemistry, Cambridge UK, pp. 137– 184, 2003.

Supplementary information

The water identification was based on Rudels at al. (2005) with the modifications ~~marked~~ noted in Table S1. In general we assumed that water characterized by density, potential temperature and salinity found south of 74N parallel could not be regard as PSW or PSWw due strong influence of high temperature on density.

Table S1. Water masses definition by Rudels et al. (2005) with modifications and remarks.

	Rudels at al. (2005)			Modifications			
Water Masses	Symbol	Θ [°C]	σ_θ [kg*m^{-3}]	S	Lat [N]	D [m]	Remarks
Atlantic Water	AW	>2	27.7<σ_θ≤27.97				
	AW	>0	27.97<σ_θ, $\sigma_{0.5}$≤30.44				
	AW	>0	≤27.7	>34.9			This part was separated from PSWw on the basis of high salinity >34.9. It covers the Atlantic domain where low density is caused by high temperatures
Polar Surface Water	PSW	≤0	≤27.7		>74		Assumption that PSW does not occur south of 74 N
Polar Surface Water warm	PSWw	>0	≤27.7	≤34.9	>74	≤50	Assumption that PSW does not occur south of 74 N, and surface water occur in first 50 m
Arctic Atlantic Water	AAW	0 < x≤2	27.7<σ_θ≤27.97				
Deep water	DW(AIW)	≤0	27.97<σ_θ, $\sigma_{0.5}$≤30.44				All waters classified ~~to~~ as AIW in AREX cruises occur close to the bottom.

Table S1: The results of T test with variables grouped by year and water masses. Table results of t-test that measure significance in differences in mean value. The difference between variable averages in selected layer are significant if significance level p<0.05. NS - not significant, S – signifycant differences.

Variable	Year	Water masses	t-value	df	p	significance
$a_{CDOM}(350)$	2013	AW vs. PSW	0.077730	44	0.938395	NS
		AW vs. PSWw	-1.55385	74	0.124487	NS
		PSW vs. PSWw	-0.484689	34	0.631005	NS
	2014	AW vs. PSW	1.057659	176	0.291660	NS
		AW vs. PSWw	-0.057183	200	0.954456	NS
		AW vs.AAW	-0.084527	176	0.932733	NS
		AW vs. IW/DW	-1.31413	183	0.190446	NS
		PSW vs. PSWw	-1.20685	30	0.236920	NS
		PSW vs. AAW	-1.16764	6	0.287250	NS

		PSW vs. IW/DW	-1.31478	13	0.211308	NS
		PSWw vs. AAW	-0.068131	30	0.946133	NS
		PSWw vs. IW/DW	-1.11398	37	0.272473	NS
		AAW vs. IW/DW	-0.511292	13	0.617720	NS
	2015	AW vs. PSW	**-4.44626**	**160**	**0.000016**	S
		AW vs. PSWw	**-4.06548**	**227**	**0.000066**	S
		AW vs. AAW	**-4.78185**	**163**	**0.000004**	S
		AW vs. IW/DW	**3.248989**	**173**	**0.001392**	S
		PSW vs. PSWw	**2.620125**	**77**	**0.010584**	S
		PSW vs. AAW	0.295868	13	0.772004	NS
		PSW vs. IW/DW	**4.306062**	**23**	**0.000263**	S
		PSWw vs. AAW	**-2.64463**	**80**	**0.009840**	S
		PSWw vs. IW/DW	**4.851875**	**90**	**0.000005**	S
		AAW vs. IW/DW	**5.090324**	**26**	**0.000026**	S
$S_{300-600}$	2013	AW vs. PSW	0.524860	44	0.602315	NS
		AW vs. PSWw	1.118054	74	0.267160	NS
		PSW vs. PSWw	0.064696	34	0.948795	NS
	2014	AW vs. PSW	-0.405673	176	0.685476	NS
		AW vs. PSWw	0.874175	200	0.383071	NS
		AW vs. AAW	0.240337	176	0.810348	NS
		AW vs. IW/DW	1.881482	183	0.061494	NS/close
		PSW vs. PSWw	0.811732	30	0.423340	NS
		PSW vs. AAW	0.713604	6	0.502273	NS
		PSW vs. IW/DW	1.561149	13	0.142494	NS
		PSWw vs. AAW	-0.123383	30	0.902627	NS
		PSWw vs. IW/DW	1.316258	37	0.196184	NS
		AAW vs. IW/DW	1.058590	13	0.309061	NS
	2015	AW vs. PSW	0.455974	160	0.649027	NS
		AW vs. PSWw	1.928425	227	0.055050	NS/close
		AW vs. AAW	**2.012286**	**163**	**0.045837**	S
		AW vs. IW/DW	**-2.89410**	**173**	**0.004292**	S
		PSW vs. PSWw	0.193909	77	0.846757	NS
		PSW vs. AAW	0.752780	13	0.464996	NS
		PSW vs. IW/DW	-1.49834	23	0.147646	NS
		PSWw vs. AAW	0.900161	80	0.370736	NS
		PSWw vs. IW/DW	**-3.14968**	**90**	**0.002219**	S
		AAW vs. IW/DW	**-2.86486**	**26**	**0.008150**	S

Table S3: The results of T test with variables grouped by year and water masses. Table list results of t-test that measure significance in differences in mean value. The difference between variable averages in selected layer are significant if significance level $p<0.05$. NS - not significant, S – signify cant differences.

Variable	Water mass	Year	t-value	df	p	significance
$a_{CDOM}(350)$	AW	2013 vs. 2014	**13.20111**	**215**	**0.000000**	S
		2013 vs. 2015	**11.62407**	**197**	**0.000000**	S
		2014 vs. 2015	**-5.97262**	**328**	**0.000000**	S
	PSW	2013 vs. 2014	**6.162425**	**5**	**0.001638**	S
		2013 vs. 2015	0.254644	7	0.806317	NS
		2014 vs. 2015	**-3.16292**	**8**	**0.013336**	S
	PSWw	2013 vs. 2014	**5.540343**	**59**	**0.000001**	S
		2013 vs. 2015	**5.685240**	**104**	**0.000000**	S
		2014 vs. 2015	**-5.42899**	**99**	**0.000000**	S

	AAW	2014 vs. 2015	**-3.05781**	**11**	**0.010894**	S
	IW/DW	2014 vs. 2015	1.086729	28	0.286424	NS
$S_{300-600}$	AW	2013 vs. 2014	**-5.34852**	**215**	**0.000000**	S
		2013 vs. 2015	**-4.23678**	**197**	**0.000035**	S
		2014 vs. 2015	**6.410876**	**328**	**0.000000**	S
	PSW	2013 vs. 2014	-1.99294	5	0.102863	NS
		2013 vs. 2015	-0.817157	7	0.440760	NS
		2014 vs. 2015	1.788011	8	0.111578	NS
	PSWw	2013 vs. 2014	**-3.98031**	**59**	**0.000191**	S
		2013 vs. 2015	**-2.50249**	**104**	**0.013890**	S
		2014 vs. 2015	**3.544709**	**99**	**0.000602**	S
	AAW	2014 vs. 2015	**3.045325**	**11**	**0.011140**	S
	IW/DW	2014 vs. 2015	-1.30430	28	0.202751	NS

Significant difference between averaged $a_{CDOM}(350)$ values in classified water masses were observed only in 2015 except of PSW vs. AAW with a low number of samples. Similarly, significantly different average slope values were observed in 2015 for four sets of water masses pairs. The interannual differences in averages values of $a_{CDOM}(350)$ were insignificant ($p>0.05$) in PSW for 2013 and 2015 and in IW/DW in 2014 and 2015. All other pairs of interannual differences for distinct water masses were significant. In case of S300-600 average values interannual differences were significant in all AW, PSWw and AAW. In the other hand PSW and IW/DW average values with a low number of samples were insignificant interannually.

The example of excitation–emission matrix (EEM) from AREX expedition with marked ex/em region for three channels of Wet Star Wet Lab CDOM fluorometer is presented (Figure S1). Coble (1996) specific peak areas: the humic–like 'A' region at 260 nm excitation (ex)/380–460 nm emission (em); terrestrial fulvic 'C' region at 350 nm ex/420–480 nm em; marine humic–like 'M' region at 312 nm ex/380–420 nm em; and the tryptophan–like or protein–like 'T' region at 275 nm ex/340 nm em were marked on Figure S1. This allowed for association of channels with different excitation/emission characteristics with specific peak areas as given in Coble (1996): Channel 1 (CH1), ex./em. 310/450 nm, represents marine ultraviolet humic–like peak C and marine humic–like peak M; Channel 2 (CH2), ex./em. 280/450 nm, represents UVC terrestrial humic–like peak A; and Channel 3 (CH3), ex./em. 280/350 nm, represents the protein–like tryptophane peak T (Figure S1).

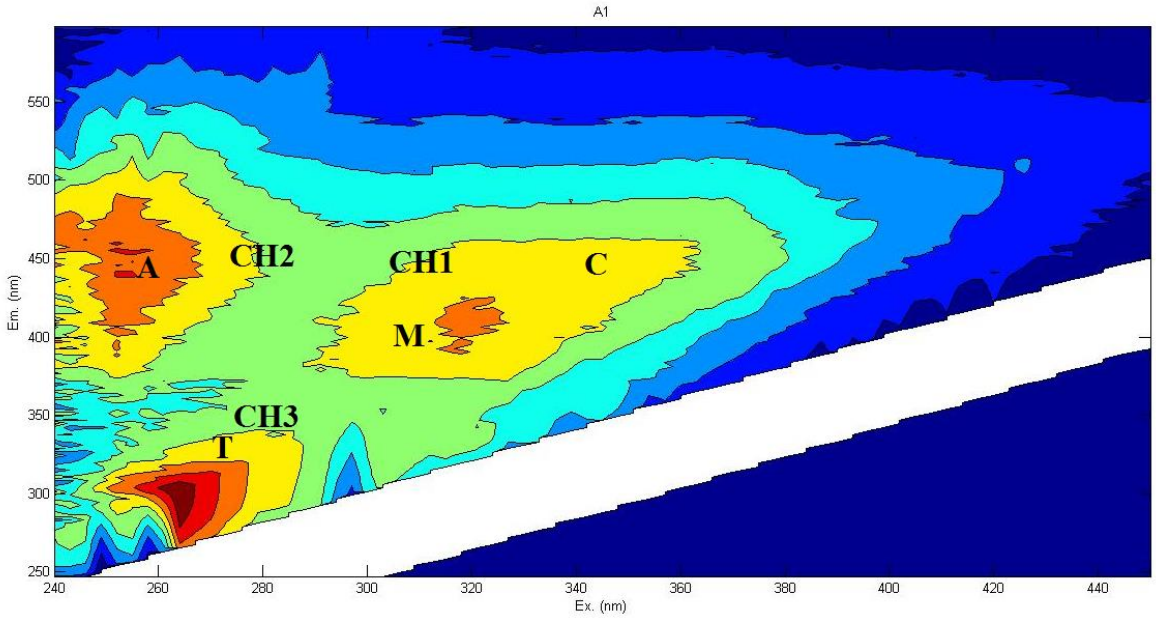

Figure S1: Typical example of excitation–emission matrix (EEM) from AREX expedition with marked ex/em region for three channels of Wet Star Wet Lab CDOM fluorometer (Channel 1 (CH1), ex./em. 310/450 nm, Channel 2 (CH2), ex./em. 280/450 nm,; Channel 3 (CH3), ex./em. 280/350 nm) together with Coble's specific EEM regions which characterize different sources of FDOM (the humic–like 'A' region at 260 nm excitation (ex)/380–460 nm emission (em); terrestrial fulvic 'C' region at 350 nm ex/420–480 nm em; marine humic–like 'M' region at 312 nm ex/380–420 nm em; and the tryptophan–like or protein–like 'T' region at 275 nm ex/340 nm em.).

The distribution of fluorescence intensity of the terrestrial humic–like FDOM (I_{CH2}), ~~protein–like FDOM (I_{CH3})~~ and $SUVA_{254}$ (ratio $a_{CDOM}254$ and DOC) in the TS diagram was shown in Figure S2. The highest terrestrial humic-like FDOM values were observed in PSW and part of PSWw in depth range 15-50 m. The lowest I_{CH2} values were found in surface layer of PSWw and there was a large variability in AW (Figure S2a). ~~In case of protein–like FDOM the highest values were observed in PSW, PSWw mid depth (15-50m,what can be associated with chlorophyll a maximum) and in part of AW which was separated form PSWw (upper part: T>0, $\sigma_\theta \leq 27.7$, S>34.9). The lowest protein–like FDOM values were observed in AW (2 lower parts) and in PSWw where $\sigma_\theta \leq 26.5$ (Figure S2b).~~ There was a large variability and no consistent trends in distribution of $SUVA_{254}$ values in different water masses in the study area, as shown in the TS diagram (Figure S2c).

a)

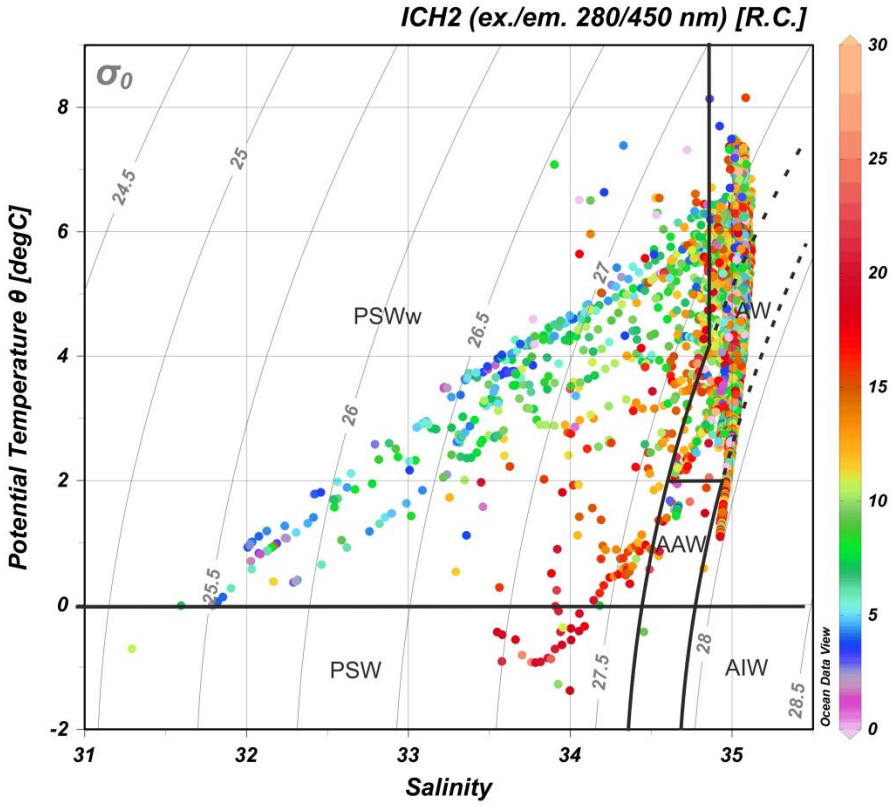
ICH2 (ex./em. 280/450 nm) [R.C.]
σ0
Potential Temperature θ [degC]
Salinity
PSWw
PSW
AAW
AW
AIW
24.5
25
25.5
26
26.5
27
27.5
28
28.5
Ocean Data View

~~b)~~

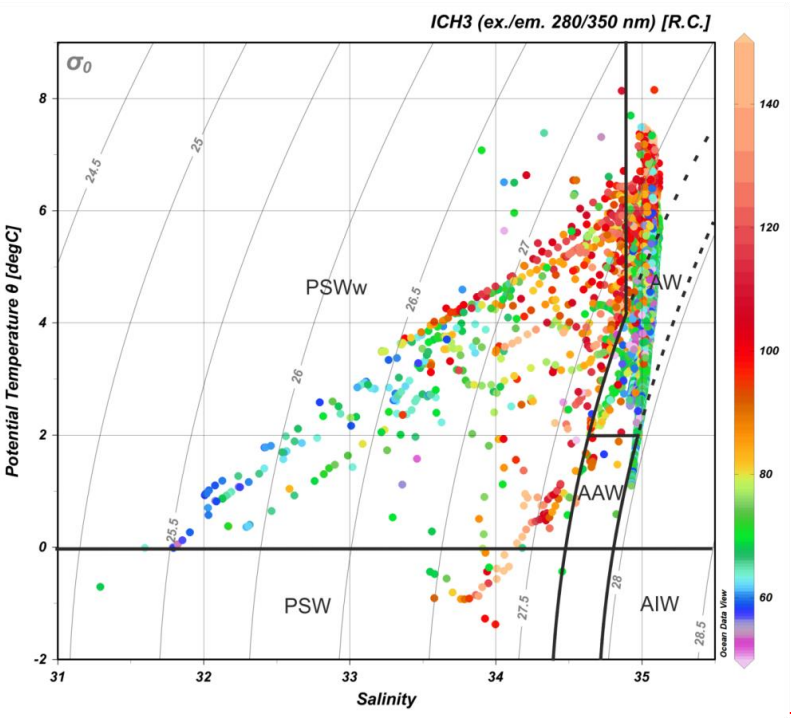
ICH3 (ex./em. 280/350 nm) [R.C.]
σ0
Potential Temperature θ [degC]
Salinity
PSWw
PSW
AAW
AW
AIW
24.5
25
25.5
26
26.5
27
27.5
28
28.5
Ocean Data View

be)

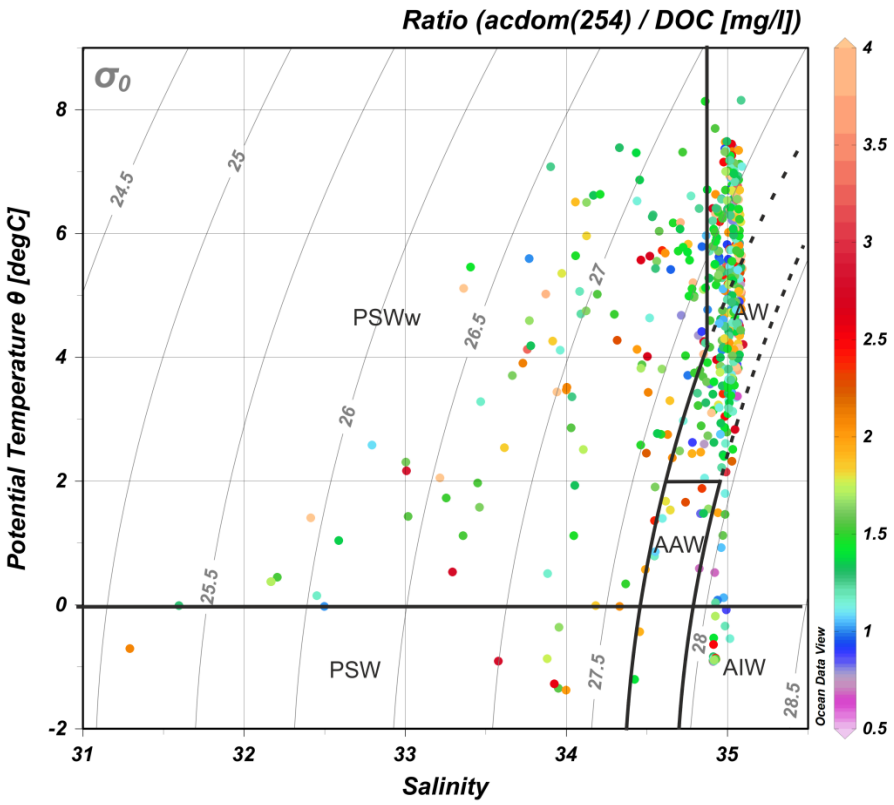

Figure S2: TS diagram of water mass distribution on the study 2013–2015. A) color represents terrestrial humic–like fraction fluorescence intensity I_{CH2}, (ex./em. 280/450 nm, [R.C.]). ~~B) color represents protein like fraction fluorescence intensity I_{CH3}, (ex./em. 280/350 nm, [R.C.]).~~ B~~C~~) color bar represents values of carbon specific CDOM absorption coefficient at 254 nm, $SUVA_{254}$ [m^2 gC^{-1}]. The lower number of points in c) resulted from fewer number of discrete water samples for determination of CDOM. Water masses: AW (Atlantic Water), AAW (Arctic Atlantic Water), AIW (Arctic Intermediate Water), PSW (Polar Surface Water), PSWw (Polar Surface Water warm). Three areas noted as AW follow the three sets of conditions that define AW (see Table S1).

We presented the relationship between absorption coefficient at 676 and stimulated chlorophyll a fluorescence in 2014 and 2015 in the selected water masses to prove that measurements were not biased by instrument offset . The stability of chlorophyll *a* intensity output was assessed by regressing the measured fluorescence intensity values against calibrated values of total absorption coefficient non–water at 676 nm, $a_{tot-w}(676)$ in selected water masses. Value of the $a_{tot-w}(676)$ is a good proxy of the chlorophyll *a* concentration (Roesler and Barnard, 2013). There was very good linear relationship between I_{FChla} and a_{tot-}

$_w$(676) in selected water masses in 2014 and 2015 with no visible offset in I_{FChla}, values in both years ensuring negligible time drift in MicroFlu–Chl output (Figure S3). The difference in the in the I_{FChla}, and a_{tot-w}(676) vertical distribution near the ocean surface in AW, shown on Figure 4, could in part be explained by a decrease in the fluorescence quantum yield by phytoplankton photoinhibition resulting from the stronger irradiance near the surface (Cullen, 1982).

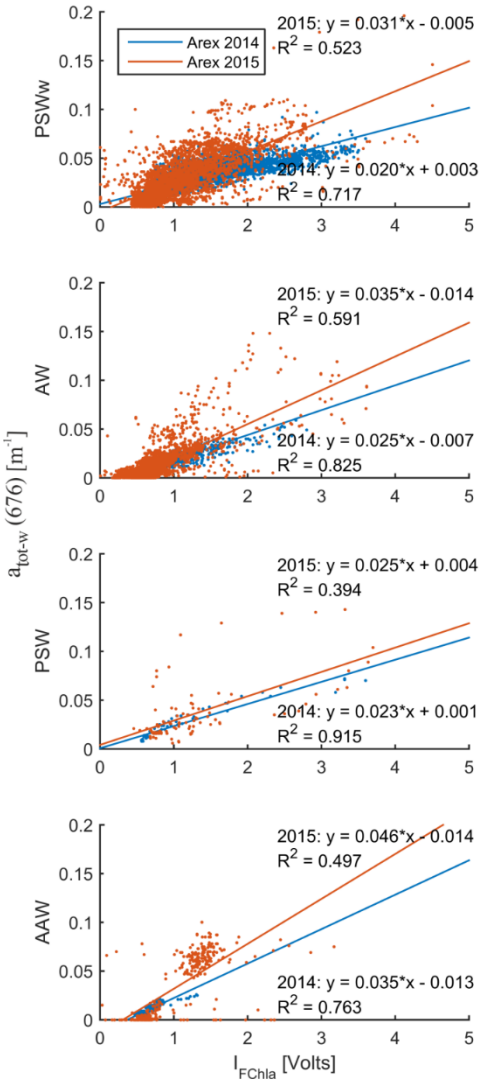

Figure S3: Relationship between total absorption coefficient non–water at 676 nm (a_{tot-w}(676) and stimulated chlorophyll a fluorescence (I_{FChla}) in different water masses in 2014 and 2015.

1293 According to Roesler and Barnard (2013) chlorophyll a concentration can be very well
1294 approximated by $a_{tot-w}(676)$. The very good correlation between I_{FChla} and $a_{tot-w}(676)$ in
1295 selected water masses shown on Figure S3, as well together with very good correlation
1296 between I_{CH3} and I_{FChla} suggested a direct dependence between I_{CH3} and $a_{tot-w}(676)$. There was
1297 a significant correlation between I_{CH3} and $a_{tot-w}(676)$ as summarized on the Figure S4. This
1298 was another evidence confirming strong contribution of phytoplankton dynamics to spatial
1299 and temporal variability of FDOM protein–like fraction in Nordic Seas.

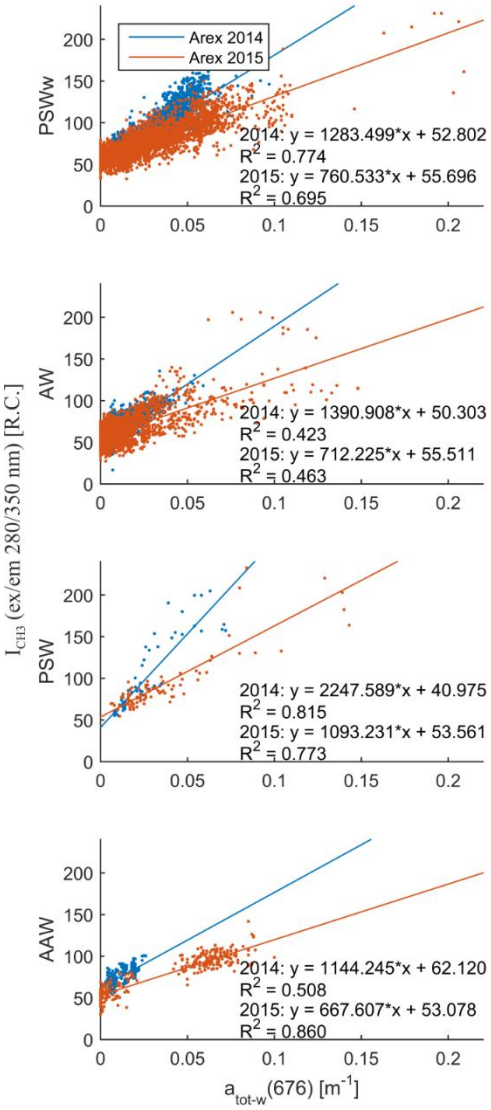

1300
1301 Figure S4: Relationship between fluorescence intensity of the protein–like component
1302 (I_{CH3}) and particulate absorption coefficient at 676 ($a_{tot-w}(676)$) in different
1303 water masses in 2014 and 2015.